# A Low-Cost Approach to Estimate the Crucial Biomechanical Parameters of Manual Wheelchair Propulsion Technique

Rabail Khowaja
Rehabilitation Sciences
McGill University, Montreal
August 2021

*A thesis submitted to McGill University in partial fulfillment of the requirements of the degree of Master of Science in Rehabilitation*

## Table of Contents

# List of Figures

# List of Tables

# Abstract

**Introduction:** A manual wheelchair (MWC) is an essential assistive device that enhances locomotion for individuals with restricted mobility. Unfortunately, 30% to 70% of total MWC users experience upper extremity pain due to repetitive propulsion. One fundamental aspect of MWC propulsion is a stroke pattern, of which one pattern is the semicircular (SC) pattern in which the hands return below the pushrim after a stroke. This pattern is favoured by MWC users, since it may help to decrease the prevalence of shoulder pain. To reduce the prevalence of upper extremity pain and injury for MWC users, research has identified critical changes in some of the specific parameters of MWC propulsion. In our lab, we have developed a low-cost virtual reality simulator that consists of a hardware interface that enables users to control a virtual MWC displayed on a screen, and which also provides force feedback. The present study measures push time, cycle time, velocity, and the contact angle of MWC propulsion, so users also can improve their stroke pattern.

**Objective:** To determine the accuracy and precision of the MWC simulator for measuring the crucial biomechanical parameters of the MWC propulsion technique of young-health individuals when compared to a gold standard system.

**Methods:** We recruited 12 healthy individuals through personal contacts. Participants propelled the MWC in a straight-line and an ecological scenario in the VR simulator. During the straight-line scenario, participants propelled MWC at each of eight increasing stroke cadences—in synchronization with metronome beats—using two different propulsion patterns (SC and arcing (ARC)). Then, the participants propelled the MWC in an ecological scenario: an outdoor sidewalk scene that included side slopes, straight slopes, static obstacles, and a street crossing. Push time,

cycle time, contact angle, and velocity were recorded simultaneously by the MWC simulator and the instrumented wheels (the SMARTWheel system) installed on the MWC. To analyze the collected data, we first calibrated the contact angle and velocity measured by the simulator by performing a regression analysis using the same variables measured by the SMARTWheel system. In the straight-line scenario, we compared the measurements of push time, cycle time, contact angle, and velocity by the simulator and the SMARTWheel by using a Bland-Altman analysis, which was done separately for each propulsion pattern (ARC and SC). Furthermore, we compared the effects of target cadence, propulsion pattern, and instrument measurements by using a mixed-model analysis. For the ecological scenario, in which propulsion pattern and cadence were unconstrained, we compared the measurements of cycle time, push time, contact angle, and velocity by the simulator and SMARTWheel by using Bland-Altman and mixed-model analyses.

**Results:** The measurements of the simulator and SMARTWheel were not influenced by the propulsion pattern (ARC and SC) or targeted cadence. All the measured variables in the straight-line scenario and ecological scenario were accurate but not precise. Among all the variables of interest, a good precision was achieved only for the measurement of cycle time during the straight-line scenario. For that measurement, the precision corresponded to 10% and 14% of the change due to training for propulsion with the ARC and SC patterns, respectively, with a 95% certainty.

**Discussion:** The wheelchair propulsion variables measured during the straight-line and ecological scenarios were accurate, but, unfortunately, a targeted precision was not attained. However, the precision of the simulator measurements could be enhanced potentially by taking repeated measurements of the same condition. This study demonstrates that important MWC propulsion parameters can be measured accurately by a simulator during straight-line movements. Therefore, the simulator could be used to train users to optimize their propulsion techniques by providing feedback on the critical parameters of wheelchair propulsion during straight-line movements. Future studies could be performed to improve the simulator further to measure other crucial parameters of manual wheelchair propulsion, such as mean force or power, which could add to the utility of the simulator.

# Résumé

**Introduction:** Un fauteuil roulant manuel (FRM) est un dispositif d'assistance essentiel qui améliore la locomotion des personnes à mobilité réduite. Malheureusement, 30 à 70 % de l'ensemble des utilisateurs de FRM ressentent des douleurs aux membres supérieurs en raison de l'aspect répétitif du mouvement de propulsion. Un aspect fondamental de la propulsion de la FRM est le patron de propulsion. Le patron semi-circulaire, où la main revient sous la main courante après une poussé, est privilégié car il peut réduire la prévalence de la douleur à l'épaule. Pour réduire la prévalence des douleurs et des blessures aux membres supérieurs chez les utilisateurs de FRM, la recherche a identifié des changements critiques dans des paramètres spécifiques de propulsion. Dans notre laboratoire, nous avons développé un simulateur de réalité virtuelle (RV) à faible coût, composé d'une interface matérielle permettant aux utilisateurs de contrôler un FRM virtuel affiché sur un écran tout en fournissant un retour de force. Nous souhaitons ajouter des informations sur le temps et la durée de cycle de poussée, la cadence, la vélocité et l'angle de contact de la propulsion en FRM, afin que les utilisateurs puissent également améliorer leur patron de propulsion.

**Objectif:** Déterminer la précision du simulateur FRM dans la mesure des paramètres biomécaniques cruciaux de la technique de propulsion, en comparaison avec un système de référence (SMARTWheel) chez de jeunes adultes en bonne santé.

Méthodes: Douze individus en bonne santé ont été recrutés par le biais de contacts personnels. Les participants ont propulsé le FRM en ligne droite et dans un scénario écologique, dans le simulateur RV. Pendant le scénario en ligne droite, les participants ont propulsé à chacune de huit cadences croissantes, en utilisant deux patrons de propulsion différents (semi-circulaire et arqué) en

synchronisation avec le rythme d'un métronome. Ensuite, les participants ont propulsé le FRM dans un scénario écologique : une scène de trottoir extérieur comprenant des pentes latérales, des pentes droites, des obstacles statiques et un croisement de rues. La cadence, l'angle de contact et la vitesse ont été enregistrés simultanément par le simulateur de la FRM et par les roues instrumentées SMARTWheel, installées sur la FRM. Pour analyser les données recueillies, nous avons d'abord calibré l'angle de contact et la vitesse mesurés par le simulateur, par régression avec les mêmes variables mesurées par le système SMARTWheel. Dans le scénario en ligne droite, nous avons comparé les mesures de cadence, d'angle de contact et de vitesse par le simulateur et le SMARTWheel, avec une analyse de Bland-Altman ; ceci a été fait séparément pour chaque patron de propulsion (arqué et semi-circulaire). En outre, nous avons comparé les effets de la cadence cible et du modèle de propulsion sur la précision des mesures du simulateur par une analyse de modèle mixte. Pour le scénario écologique, où le modèle de propulsion et la cadence n'étaient pas contraints, nous avons comparé les mesures de cadence, d'angle de contact et de vitesse par le simulateur et le SMARTWheel à l'aide d'analyses de Bland-Altman et de modèles mixtes.

**Résultats:** Pour le scénario en ligne droite, l'analyse de modèle mixte n'a montré aucun effet significatif du patroon de propulsion sur la précision de la mesure du temps de poussée, du temps de cycle, de la cadence et de l'angle de contact ; cependant, il y avait un effet significatif pour la mesure de la vitesse. De plus, le niveau de concordance entre l'instrument standard (SMARTWheel) et le simulateur FRM, comme le montrent les analyses Bland-Altman, était excellent pour toutes les variables mesurées. Pour le scénario écologique, une analyse de modèle mixte a montré une différence significative entre les instruments pour la mesure du temps de poussée, de la vélocité et de l'angle de contact, mais pas pour le temps de cycle et la cadence. De plus, le niveau de concordance était bon pour le temps de cycle, la cadence et la vélocité, mais pas pour le temps de poussée et l'angle de contact.

**Discussion:** La précision des variables de propulsion du fauteuil roulant mesurées pendant le scénario en ligne droite était bonne, contrairement aux mesures effectuées pendant le scénario écologique. Cela peut s'expliquer par le fait que dans le scénario écologique, les participants ont parfois propulsé une roue vers l'avant et une autre vers l'arrière, pour contourner un obstacle. Ils ont pu également augmenter leur vitesse pour franchir des pentes et utiliser des combinaisons de patrons de propulsion (arqués et semi-circulaires). De plus, pour les scénarios en ligne droite, nous avons calculé les valeurs moyennes des variables biomécaniques sur 10 cycles de propulsion ou plus avant de comparer les données de SMARTWheel et du simulateur; alors que des poussées uniques ont été comparées dans le scénario écologique. Cette étude démontre que d'importants paramètres de propulsion en FRM peuvent être mesurés avec précision par le simulateur lors de mouvements en ligne droite. Le simulateur pourrait donc être utilisé pour former les utilisateurs à l'optimisation de leurs techniques de propulsion, en fournissant un retour d'information sur les paramètres critiques de la propulsion du fauteuil roulant, lors de mouvements en ligne droite. Des études futures peuvent être menées pour améliorer d’avantage le simulateur, afin de mesurer d'autres paramètres cruciaux de la propulsion manuelle du fauteuil roulant, tels que la force moyenne et la puissance, ce qui pourrait accroître l'utilité du simulateur.

# Acknowledgements

Undoubtedly, the reward of the successful completion of this research project goes to my worthy supervisor, Dr. Philippe Archambault. I cannot be more grateful to him for giving me the precision opportunity of carrying out this research project under his supervision. Throughout my academic years, he was helpful and supportive. He guided me at every single step towards the completion of the project as well as encouraged me to enhance my research skills by participating in different seminars.

I am thankful to my co-supervisor, Dr. Felix Chenier, for providing valuable time to this project. Whenever I needed technical help, he was always there to guide me and add informative comments for improvements.

I would also like appreciate to my supervisory committee: Dr. Rachid Aissaoui and Dr. Krista best, for always being there to provide their expert advice and comments.

Thank you to the entire community of my School, including students and faculty, for providing me help and guidance whenever I need it.

I cannot end this acknowledgement without thanking two pillars of my life: my father, Haider Ali and my mother, Rashida. I am grateful to them for being in my life and encouraging me mentally, emotionally, and financially throughout every step of life and particularly this master's degree. In the end, thanks to my family and friends for my making this journey joyful.

# Preface and Contributions of author

All the contents of the present thesis are original material written by Rabail Khowaja under the guidance of Dr. Philippe Archambault.

This thesis includes one manuscript on the wheelchair simulator for estimating crucial biomechanical parameters of the manual wheelchair propulsion technique. The procedure was designed by Rabail Khowaja, with support of Philippe Archambault and Felix Chenier. Data analysis was carried out by Rabail Khowaja with assistance from Philippe Archambault, Shaheen Ghayourmanesh (programming) and Sam Leitkams.

# Abbreviations

AMD: Assistive mobility devices

ARC: Arcing

DLOP: Double loop of propulsion

FoV: Field of vision

HMD: Head mounted display

MiWe: McGill immersive wheelchair

MWC: Manual wheelchair

QOL: Quality of life

SC: Semicircular

SCI: Spinal cord injury

SLOP: Single loop of propulsion

SoP: Sense of presence

VR: Virtual reality

# Chapter 01: Introduction and Background

## Rationale and Objective

Around 81% of people with spinal cord injury (SCI) use a manual wheelchair (MWC) to accomplish their quotidian activities (Post, van Asbeck, van Dijk, & Schrijvers, 1997). Previously, instruments such as instrumented wheels (SMARTWheels) and 3D kinematic measurements systems have been used for measuring MWC propulsion biomechanics. However, these systems have limitations that constrain their usage. For instance, kinematic measurements systems are expensive and can be used only in a lab setting. SMARTWheels also are expensive and are no longer manufactured. Instead, inertial measurement units (IMU) can be used to measure stroke number and cadence (Ojeda & Ding, 2014). For use in a clinical or home setting, it would be important to have a low-cost system able to measure the crucial variables of MWC propulsion accurately and precisely. *Accuracy* is defined as the closeness of a measured value to a standard value, and *precision* refers to the closeness of repeated measured values. Therefore, this study has been designed to present such a system, which can estimate the essential parameters of MWC propulsion, and that could be used outside of a lab setting at a much-reduced cost, compared to existing systems. In this study, we obtained the values of push time, cycle time, contact angle, and the velocity of the MWC simulator, and we compared these values to a gold standard (SMARTWheels). The propulsion of a MWC with SC and ARC patterns at slow to fast speeds provides a wide range of push times, cycle times, velocities, and contact angles. Additionally, the study participants also propelled the MWC with their natural propulsion pattern in an ecological scenario. Together, these data provided a range of values for the variables of interest, and the varying speed and propulsion patterns that could affect the precision of the study measurements.

Ideally, the required precision for measuring biomechanical parameters related to MWC propulsion would be based on clinical guidelines. However, such guidelines do not currently exist. The current recommendations are solely to increase the contact angle and decrease cadence, and the optimal value or range is unknown.

The objective of this study was to assess the precision of the McGill immersive wheelchair (MiWe) simulator based on a 10% change in each variable due to training. Although the simulator was modified with the primary purpose of providing user feedback based on the MWC propulsion parameters, even so, with sufficient precision, the simulator should be able to detect a change in these parameters. A measurement precision equivalent to 10% is a good compromise between technical feasibility and potential clinical relevance.

# Comprehensive literature review

## 1.1 Influence of manual wheelchair on individuals with spinal cord injury

### 1.1.1 Spinal cord injury and its prevalence

SCI is a neurological disorder that causes irreversible impairments of motor, sensory, and autonomic functions below or at the level of a lesion (Marino et al., 2003). SCIs are widely categorized into traumatic and non-traumatic injuries, depending on the cause of the damage to the spinal cord structure. The most common causes of traumatic SCI are automobile crashes, falls, gunshots wound, and motorcycle crashes (Chen, Tang, Vogel, & DeVivo, 2013), whereas non-traumatic SCIs are caused by neoplasms, vascular disease, inflammatory disease, and stenosis (Citterio et al., 2004).

Around the world, every year, between 250,000 and 500,000 people suffer from SCIs ("Spinal cord injury," 2013). The highest traumatic SCI incidence rate in the world has been reported in the

USA (39 per million) and Canada (35 per million) (Cripps et al., 2011). The consequences of SCI are devastating, since they alter physical, psychological, and cognitive functions (deRoon-Cassini, de St. Aubin, Valvano, Hastings, & Horn, 2009; Murray et al., 2007); cause several secondary life-threatening diseases such as cardiovascular diseases (Bauman, Kahn, Grimm, & Spungen, 1999; Demirel, Demirel, Tükek, Erk, & Yilmaz, 2001; Myers, Lee, & Kiratli, 2007), obesity (Demirel et al., 2001), osteoporosis (Battaglino, Lazzari, Garshick, & Morse, 2012), and type 2 diabetes (Cragg et al., 2013; Lai et al., 2014); and pose an additional financial and emotional burden on family members, friends, and the community in general (Boschen, Tonack, & Gargaro, 2005; Post, Bloemen, & de Witte, 2005). For example, Kazmierczak and Lisinki have observed a significant reduction in the frequency of the physical activity of people with SCI, which leads to osteoporosis, bedsores, and articular contractions (Kaźmierczak & Lisiński, 2018; Totosy de Zepetnek, Pelletier, Hicks, & MacDonald, 2015). The most common reasons for inactivity in this population are environmental barriers and transportation difficulties (Kaźmierczak & Lisiński, 2018). On the other hand, Khazaeipour et al. found that psychological behaviours such as early rage, suicidal thoughts, and lack of confidence are common among people with SCI (Khazaeipour et al., 2014). Furthermore, Sachdeva et al. did carried out a systematic review on cognitive functions after SCI, finding that in most studies, the incidence of cognitive impairment of individuals with SCI was between 10% to 60% (Sachdeva, Gao, Chan, & Krassioukov, 2018).

Damage to the two-way connection between the brain and body via the spinal cord due to traumatic and neurological injury impairs functional ability and independent mobility (Marino et al., 2003). The extent of the impact on the ability to walk depends on the severity of the injury, so individuals with complete motor and sensory SCI have no chance of regaining their walking ability through physical training (Hubscher et al., 2018). Moreover, locomotion inability negatively affects quality of life (QOL) (Gutierrez et al., 2007). Thus, to improve the QOL of individuals with SCI, it is essential to identify a technique to rehabilitate their mobility. To achieve this improvement, assistive devices can play an important part.

### 1.1.2 The role of manual wheelchair in individuals' lives with spinal cord injury

An *assistive mobility device* (AMD) is defined as a device used by individuals with various limited walking abilities to help them with locomotion and the performance of daily activities. AMDs have been found to increase mobility and social participation, and improve activity for individuals with mobility impairments that might restrict them within their residential space (Salminen, Brandt, Samuelsson, Toytari, & Malmivaara, 2009). Indeed, a MWC is a crucial assistive mobility device that can ameliorate locomotion and the social participation of individuals with limited mobility.

Approximately 81% of individuals with SCI use a MWC for their routine activities (Post et al., 1997), and most have been found to be satisfied with their mobile device (Samuelsson & Wressle, 2008). Users have reported that their MWC facilitates access to work and leisure activities. Additionally, propelling a MWC is an exercise that may help to reduce the onset of secondary conditions such as cardiovascular disease, obesity, type 2 diabetes, and osteoporosis (Battaglino et al., 2012; Bauman et al., 1999; Cragg et al., 2013; Demirel et al., 2001; Lai et al., 2014), which result from a sedentary lifestyle that is prevalent in people confined to a MWC (Bauman et al., 1999; Cragg et al., 2013; Demirel et al., 2001; Lai et al., 2014). Thus, it is not surprising that the majority of individuals with SCI embrace their MWC as a lifetime companion (Post et al., 1997).

Within a year after an individual's SCI injury, a sudden shift from ambulation to MWC use often deteriorates their view of health, well-being, social participation, and life satisfaction or QOL (Riggins, Kankipati, Oyster, Cooper, & Boninger, 2011). However, gradual improvements in the QOL of individuals using a MWC have been observed over time (Westgren & Levi, 1998), possibly due to improvements in their MWC skills, social participation, and physical health, which have been found to be highly associated with QOL. Indeed, many natural environments are not MWC accessible due to their many obstacles, which can be overcome only by using certain MWC skills (Meyers, Anderson, Miller, Shipp, & Hoenig, 2002). These MWC skills include MWC folding/unfolding of foldable MWC, descending 15 cm curbs, ascending/descending at least three stairs, a bed-to-MWC transfer and back, turning 180 degrees, doing a wheelie, and holding a 30-degree wheelie. In addition, these MWC skills have been found to have a positive correlation with community reintegration and QOL (Hosseini, Oyster, Kirby, Harrington, & Boninger, 2012). A successful performance of MWC skills is essential for mobility, which can bring positive changes in social participation and an enhancement of self-satisfaction (Hosseini et al., 2012).

SCI is an infrequent but sudden incident in a person's life. In the most severe cases, it impairs an individual's ability to walk. For individuals with SCI and a walking impairment, a MWC is a great companion for performing daily activities with less support from caregivers. To optimally adopt to a MWC, SCI individuals must learn the critical MWC skills to enable them to socialize and re-integrate into the community. To optimize this re-integration, an instrument for measuring the biomechanics of acquired skills would be crucial.

## 1.2 Manual wheelchair propulsion and shoulder pain

### 1.2.1 Upper extremity pain in individuals with spinal cord injury

Individuals with SCI are always at risk of developing unforeseeable secondary conditions, which may aggravate their health conditions and ultimately affect their QOL and community participation (Bauman et al., 1999; Cragg et al., 2013). Moreover, these secondary conditions are the most common cause of rehospitalization (DeJong et al., 2013), increased morbidity, and mortality rates for individuals with SCI (Krause & Saunders, 2011). One of the frequently reported secondary conditions of MWC users is upper extremity pain (Richardson, Samaranayaka, Sullivan, & Derrett, 2019). Almost four decades ago, researchers and clinicians observed the prevalence of upper extremity pain in the SCI population who rely on a MWC as an indispensable means for mobility (Nichols, Norman, & Ennis, 1979).

For individuals with SCI, lower limb paralysis imposes considerable demands on the upper limb when executing everyday activities. As a result, upper limbs undergo repetitive and weight-bearing activities such as MWC propulsion, body transfer (Subbarao, Klopfstein, & Turpin, 1995), and body raising (Reyes, Gronley, Newsam, Mulroy, & Perry, 1995). Among these, MWC propulsion is the most frequently performed activity. On average, a MWC user hits the pushrim around 3,500 times per day (Boninger et al., 2003).

Unlike the hip joint, which is designed for stability and weight-bearing, the shoulder joint is rather flexible to enable a wide range of arm movement (Chung, 2019; Sawyers, 2018). However, an injury to the muscles or soft tissues at the shoulder joint can potentially cause an individual with SCI to develop pain or further injury at some point in their life. Unfortunately, 30% to 70% of total MWC users eventually experience shoulder pain (Dalyan, Cardenas, & Gerard, 1999; Samuelsson, Tropp, & Gerdle, 2004; Sie, Waters, Adkins, & Gellman, 1992). For these individuals, the onset of shoulder pain has a bimodal distribution, with peaks at 5 years and 13 years post-injury (Burnham, May, Nelson, Steadward, & Reid, 1993).

### 1.2.2 Causes of shoulder pain

The onset of shoulder joint disorder is not clearly understood, although the highly repetitive aspect of MWC propulsion may generate forces at the shoulder joint that tear rotor cuff muscles during propulsion. Morrow et al. have found that joint intersegmental forces and moments vary greatly at the shoulder joint during the performance of daily living activities and locomotion. The highest joint forces are developed during weight relief, ramp propulsion, and start-up propulsion (Morrow, Hurd, Kaufman, & An, 2010).

A review of the literature indicates various reasons for the prevalence of shoulder pain. Bayley et al. have observed that shoulder pain is reported mostly by individuals with chronic impingement syndrome (Bayley, Cochran, & Sledge, 1987). Burnham et al. also have found that muscle imbalance could be a factor in the development and perpetuation of the rotor cuff impingement syndrome in athletes who rely on MWC (Burnham et al., 1993). Moreover, Finley and Rodgers have found that bicipital tendonitis with impingement syndrome was the most common shoulder pathology in athletic and non-athletic MWC users, followed by instability (Finley & Rodgers, 2004).

### 1.2.3 Effects of shoulder pain on the life of individuals with spinal cord injury

The persisting pain of individuals with SCI affects QOL. Putzke et al. have shown that the pain that hinders the performance of day-to-day activities also decreases QOL (Putzke, Richards, Hicken, & DeVivo, 2002). Moreover, Gutierrez et al. have found that pain intensity is negatively proportional to the level of physical functioning and QOL, although participation in community activities was not influenced by pain (Gutierrez et al., 2007), since, regardless of having pain, individuals need to integrate into society to maintain their health and develop coping strategies. In contrast, Samuelsson et al. have found a lack of change in the activity and participation of individuals with shoulder pain (Samuelsson et al., 2004). These results of these last two studies may differ due to their use of different assessment tools.

In Canada, the life expectancy of individuals with SCI is lower than that of the average population, although it is increasing continuously. Therefore, it is crucial to improve their QOL, so they can live a satisfactory life. To improve the QOL and physical health of individuals with SCI, the crucial factor to consider is the reduction of the prevalence of shoulder pain (Gutierrez et al., 2007).

### 1.2.4 Treatments to alleviate shoulder pain

Advancements in science and technology have grown tremendously in almost every aspect of life. For example, several treatments have become available to reduce the prevalence of pain at the shoulder joint, which include physical therapy (Cratsenberg et al., 2015), medication (Blaine et al., 2008), massage (Diego et al., 2002), acupuncture and Trager (Jonas, 1998), surgery (Popowitz et al., 2003), and education in joint protection techniques (Paralyzed Veterans of America Consortium for Spinal Cord, 2005). All these interventions are part of the standard methods of care for individuals with SCI. A systematic review of the available exercise programs to mitigate shoulder pain in individuals with SCI shows that despite the differences in the time frames and interventions of the studies, exercise programs decreased participants scores on the MWC User Shoulder Pain Index (WUSPI). Also, the reduced WUSPI scores exceeded the minimal detectable changes, which showed that the positive changes in shoulder pain were clinically significant (Cratsenberg et al., 2015). However, these studies were aimed at measuring a decrease in the occurrence of shoulder pain rather than a reduction in the prevalence of pain. Also, the maximum follow-up period of these studies was six months, so it is not clear whether the changes due to exercise programs would be permanent or temporary.

Surgical procedures for torn rotor cuffs to reduce shoulder pain also have been performed on individuals with SCI, but due to their uncertain outcomes, they are considered only when other options are not available (Popowitz et al., 2003).

Unconventional therapies such as acupuncture and Trager also have gained attention over the decades as treatments for upper extremity pain (Jonas, 1998). According to the National Institute of Health Consensus Development Panel, acupuncture can be beneficial as an adjunct treatment for the management of myofascial and lower back pain and tendinitis ("NIH Consensus Conference. Acupuncture," 1998). Moreover, Dyson-Hudson et al. found that acupuncture and the Trager psychological treatment greatly help to abate shoulder pain (Dyson-Hudson, Shiflett, Kirshblum, Bowen, & Druin, 2001). However, these treatments do not improve the range of motion of the shoulder muscles. Also, in the Dyson-Hudson et al. study, the follow-up period for the treatments was just five weeks, which does not prove that these treatments have long-lasting effects beyond this time range. Thus, all the above-mentioned treatments were focused on decreasing the pain that already exists in the shoulder joint. Therefore, it is crucial to find an intervention that reduces the chance, or prolongs the development, of pain at the shoulder joint.

In summary, the majority of individuals who depend on MWC to perform their daily activities will likely experience shoulder pain. To reduce the prevalence of shoulder pain in individuals with SCI, it is pertinent to measure the critical variables of the MWC propulsion pattern.

## 1.3 Manual wheelchair propulsion pattern

The propulsion of MWC is characterized by a stroke pattern. A single stroke pattern can be divided into two phases: the push and the recovery phases as shown in Figure 1.1. During the *push phase*, the user’s hands contact the pushrims. This phase begins when the user grasps the pushrims near or behind top dead center, and it ends when the hands release the pushrims. This phase is followed by the recovery phase during which the user brings the hands back to initiate another cycle (Sanderson & Sommer, 1985). To decrease the prevalence of shoulder pain in individuals with SCI, the clinical practice guidelines have recommended the use of long and smooth pushes (Paralyzed Veterans of America Consortium for Spinal Cord, 2005).

Researchers have identified four different stroke patterns based on the trajectory of the user's hands in the recovery phase (Sanderson & Sommer, 1985). Sanderson and Sommer were the first to classify stroke patterns. They observed that the movements of the hands during the push phase were almost similar across subjects because, during this phase, the hands are in contact with the pushrims. However, during the recovery phase, two of their three participants' arm trajectories were similar to a circular motion in which the hands dropped below the pushrim during the recovery phase. They called this pattern *semicircular* (SC). In contrast, their third participant's arm motions were abrupt or pumping in nature, so they called this pattern *arching* (ARC). They also observed that the push time of the ARC pattern was shorter than the SC pattern (Sanderson & Sommer, 1985). Subsequently, Shimada et al. characterized the propulsion patterns of seven experienced MWC users, and found three different patterns by plotting the movement of the second metatarsal joint: SC, double loop over propulsion (DLOP), and single loop over propulsion (SLOP). The SC pattern was the same as that observed by Sanderson and Sommer. The DLOP and SLOP patterns were similar initially in that both the users raised their hands above the pushrim during the recovery phase. In the DLOP pattern, the hands then immediately crossed over and then dropped below the pushrim, whereas in the SLOP pattern, the hands remained above the pushrim to start the new push cycle. Finally, Boninger et al. recognized four propulsion patterns—SC, SLOP, DLOP, and ARC—in a relatively larger population of 38 individuals with paraplegia (Boninger et al., 2002). They found that SLOP was the most commonly used stroke pattern, followed by DLOP, SC, and ARC in that order. The SLOP pattern may be most commonly used because it involves an intuitive response of lifting the hands in the recovery phase of the MWC propulsion. Moreover, Boninger et al. concluded that 58% of the users in their study used the same propulsion pattern on both sides and at two different speeds (0.9m/s, 1.8m/s). On the other hand, in their study, Kwarciak et al. have inferred that a majority of users adopted DLOP followed by SLOP, ARC, and SC, although ARC and SC were equally common among users (Kwarciak, Turner, Guo, & Richter, 2012).

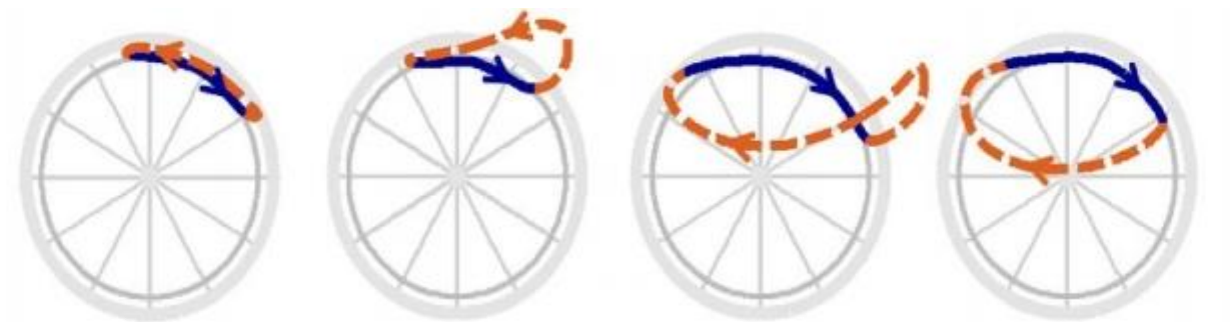

ARC SC DLOP SLOP

Figure 1.1: Four different patterns of MWC propulsion, the dashed line represents the recovery phase, and the solid line represents the push phase. AR, SL, DL, and SC stands for arcing, single loop, double loop, and semi-circular, respectively

A stroke pattern is a pivotal parameter for the propulsion of a MWC. SC, ARC, SLOP, and DLOP are four different propulsion patterns that have been observed in MWC users. It is important to identify a more efficient pattern of MWC propulsion.

## 1.4 Critical biomechanical parameters for safe manual wheelchair propulsion

Various kinetic and kinematic variables can be measured during MWC propulsion. However, to reduce the prevalence of upper extremity pain and injury in MWC users, it is essential to identify the critical parameters of MWC propulsion. The following sections describe these critical parameters.

### 1.4.1 Cadence

*Cadence*, one of the important biomechanical variables of MWC propulsion, is defined as the number of pushes per minute (pushes/min) or seconds. In the literature, *cadence* is sometimes termed push frequency or stroke frequency.

While studying the relationship between pushrim forces, weight, and median nerve function, Boninger et al. observed that the frequent loading of the upper limb during MWC propulsion and transfer causes median nerve damage that leads to carpal tunnel syndrome, which is a neurological cause of shoulder pain in MWC users (Boninger, Cooper, Baldwin, Shimada, & Koontz, 1999). In a subsequent study, Boninger et al. found that out of the four stroke patterns, subjects who adopted a SC pattern propelled their MWC at a lower cadence and spent a higher percentage of time in the push phase than in the recovery phase. The use of this strategy by MWC users may help to decrease the chance of repeated shoulder strain injury (Boninger et al., 2002).

#### 1.4.1.1 Cadence and stroke patterns

Boninger et al. calculated the cadence of MWC users at two different speeds (0.90 m/s and 1.8 m/s) during propulsion with four different stroke patterns as shown in Table 1.1. This table shows the lucid variations among the stroke patterns and that the SC pattern had the lowest cadence, while the ARC had the highest (Boninger et al., 2002). In contrast, Kwarciak et al. reported that the DLOP pattern had the lowest cadence and the ARC pattern had the highest cadence at the self-selected speed, as shown in Table 1.1. At the self-selected speed, MWC users using a DLOP pattern are slower in performing the complex hand movements during propulsion because they involve raising the hands above the pushrim, followed by crossing over and dropping below, whereas the SC pattern involves an elliptical movement that does not have any interruption (Kwarciak et al., 2012).

However, the higher cadence of the ARC pattern, as compared to the others, does not imply that this pattern should not be adopted for a particular environment. For example, Richter et al. found that for uphill propulsion, experienced MWC users use the ARC pattern to prevent the backward movement of the MWC (Richter, Rodriguez, Woods, & Axelson, 2007).

Table 1.1: Cadence for the propulsion patterns at two different speeds (Boninger et al., 2002; Kwarciak et al., 2012). Numbers indicate means and (standard deviation).

| **Propulsion patterns** | **Speed 1 (0.9 m/s)** | **Speed 2 (1.80 m/s)** | **Self-selected** |
|---|---|---|---|
| ARC | 1.13 (0.18) (pushes/min) | 1.56 (0.27) (pushes/min) | 0.93 (0.21) (pushes/min) |
| SC | 0.88 (0.08) (pushes/min) | 1.18 (0.11) (pushes/min) | 0.85 (0.11) (pushes/min) |
| SLOP | 1.03 (0.14) (pushes/min) | 1.39 (0.23) (pushes/min) | 0.86 (0.16) (pushes/min) |
| DLOP | 0.81 (0.13) (pushes/min) | 1.13 (0.11) (pushes/min) | 0.75 (0.11) (pushes/min) |

### 1.4.2 Contact angle

The *push phase* and *recovery phase* can be detected when a certain threshold value is exceeded and then drops below the threshold, respectively. The *contact angle* is the wheel angle when the user's hands are in contact with the pushrim during propulsion, when the push cycle is detected, and it is measured in degrees (Kwarciak et al., 2012) as shown in Figure 1.2.

The propulsion of a MWC is a repetitive activity requiring frequent loading of the upper limb. To avoid this frequent loading during MWC propulsion, it is crucial to follow the Clinical Practice Guidelines for the Preservation of Upper Limb Function Following SCI (Paralyzed Veterans of America Consortium for Spinal Cord, 2005). The long pushes can be achieved by maximizing the contact angle during the push phase of the stroke cycle. Increasing the push angle during the push phase lowers the peak force at the pushrim and makes pushes more efficient.


Figure 1.2: Contact Angle

#### 1.4.2.1 Contact angle and propulsion pattern

Kwarciak et al. conducted a study with experienced MWC users to determine the kinetic parameters of four different stroke patterns. At the self-selected speed, they found that the SC and DLOP patterns had significantly larger contact angles compared to the ARC pattern (Kwarciak et al., 2012). It can be inferred that the propulsion patterns in which the hands drop down the push rim (SC and DLOP) have higher contact angles than those in which the hands are raised above the pushrim. On the other hand, Boninger et al. determined the behaviour of the kinetic parameters of MWC propulsion among the propulsion patterns at two contact speeds (0.9m/s and 1.8m/s) (Boninger et al., 2002) as shown in Table 1.2. Their study found that the highest contact angle during propulsion occurred when using a SC pattern and the lowest contact angle occurred when using an ARC pattern.

Table 1.2: Contact angle with different propulsion patterns at self-selected, 0.9 m/s and 1.8 m/s (Boninger et al., 2002; Kwarciak et al., 2012)

| Propulsion patterns | Speed 1 (0.9 m/s) | Speed 2 (1.80m/s) | Self-selected |
|---|---|---|---|
| ARC | 94.4 (24.4) (°) | 101.9 (19.2) (°) | 74.5(12.9) (°) |
| SC | 114 (13.7) (°) | 133.6 (9.3) (°) | 86.7 (15.0) * (°) |
| SLOP | 91.7 (13.8) (°) | 108.1 (13.1) (°) | 77.7 (11.2) (°) |
| DLOP | 110.0 (13.0) (°) | 119.9 (11.6) (°) | 90.3 (13.1) ** (°) |

* Significantly different than ARC
** significantly different than SLOP

### 1.4.3 Peak force

*Peak force* is defined as the largest total or resultant force generated by a MWC user during propulsion when measured at the pushrim. To propel a MWC, users apply force at a point of force application (PFA) on the pushrim in the direction of motion. Boninger et al. concluded that peak force was directly associated with median nerve damage (Boninger et al., 1999). Additionally, Fronczak et al. reported that over time, a high peak force during MWC propulsion decreased the function of the median nerve (Fronczak, Boninger, Souza, & Cooper, 2003). Both of these studies caution that peak force should be reduced to decrease the chance of upper limb injuries. Therefore, measuring the forces applied by users on the pushrim would be useful for minimizing peak force.

To observe the behaviour of pushrim forces in users, Robertson et al. calculated the forces produced by experienced and non-experienced MWC users during propulsion (Robertson, Boninger, Cooper, & Shimada, 1996). They observed that experienced users applied forces with lower peak values compared to inexperienced users (Table 1.3), which may be the result of experienced users intuitively developing a more efficient style of MWC propulsion over time.

Table 1.3: Peak force and time to peak force in MWC users and non-MWC users propulsion (Robertson et al., 1996)

| Parameters | MWC users | Non MWC users |
|---|---|---|
| **Peak force (N)** | 94.6 (10.1) | 66.2 (14.4) |
| **Time to peak force(sec)** | 0.3(0.1) | 0.40(0.1) |

### 1.4.4 Power output

*Power output* is defined as the energy transferred or converted per unit time. Pellegrini et al. have suggested that power output is an important measure of MWC users' performance. Power output is the amount of external work per unit time that a user is required to produce to propel a MWC (Pellegrini et al., 2004). Thus, a higher power output is an indicator of better performance. Furthermore, Kwarciak et al. studied the power output of experienced and inexperienced users, and found that experienced users deliver more power output than inexperienced users, although the difference was insignificant (Kwarciak et al., 2012).

### 1.4.5 Relationship among biomechanics variables

The above-specified variables such as cadence, contact angle, peak force, and power output are not independent, since they are interrelated, which implies that changes in one variable instantaneously affects one or more other variables. Previously mentioned studies have suggested that to achieve long and smooth pushes during MWC propulsion the following are required: a decrease in cadence, a maximization of the contact angle, and a reduction in peak force (Boninger et al., 2002; Kwarciak et al., 2012; Paralyzed Veterans of America Consortium for Spinal Cord, 2005).

Degroot et al. studied the effects of verbal and visual training for MWC propulsion. In their study, they instructed their participants to decrease cadence. Their results indicated a significant increase in peak force immediately after training (DeGroot, Hollingsworth, Morgan, Morris, & Gray, 2009). Also, Requejo et al. studied the relationship between the contact angle and shoulder loading in paraplegic MWC users, and found a significant decrease in cadence and an increase in peak force when the users applied a greater contact angle (Requejo et al., 2015).

The parameters of MWC propulsion—specifically push frequency, contact angle, and power output—are crucial for identifying the characteristics of propulsion patterns. In the present study, we focus on determining the relationship between these variables, so this information can be used to help MWC users optimize their propulsion technique.

### 1.4.6 Effects of manual wheelchair training on propulsion biomechanics

Training is a common approach to improve any skill, and feedback can further assist trainees to acquire motor skills. Rice et al. assessed MWC propulsion on the ground after training with visual feedback of contact angle, cadence, and velocity on a dynamometer. They measured the cadence and contact angle of long-term MWC users at baseline and three months after training at a self-selected and predefined speed. After training, their participants increased their contact angle and decreased cadence at both speeds (Rice, Gagnon, Gallagher, & Boninger, 2010). Moreover, DeGroot et al. measured increases in push time and cycle time after three weeks of training on a computer-controlled MWC ergometer, which provided visual feedback on velocity (De Groot, Veeger, Hollander, & V. Van Der Woude, 2002). However, a VR-based MWC simulator that could simultaneously measure and provide feedback in real-time would further facilitate the acquisition of an effective propulsion technique. In a very recent study, Hui and Archambault utilized a VR-based MWC simulator to optimize their participants' cadence and contact angle, and observed a significant difference in the feedback group compared to the control group (Hui & Archambault, 2021).

## 1.5 An effective approach to train a naive manual wheelchair user by using a virtual reality simulator

Maneuvering a MWC is not an easy task, since it requires the coordination of motor skills, vision, balance, spatial awareness, and orientation (Pithon, Weiss, Richir, & Klinger, 2009). People with SCI who use a MWC often perform several tasks in various settings, such as home, school, work, etc. A difficulty with MWC propulsion not only leads to frustration, but also may decrease social participation (Smith, Sakakibara, & Miller, 2016). Virtual reality (VR) offers a safe and motivating environment to help individuals with disabilities familiarize themselves with new assistive technology (Mahajan, Dicianno, Cooper, & Ding, 2013). VR is a cutting-edge technology that has emerged from the integration of different fields such as electronic engineering, mechanical engineering, cybernetics, database design, real-time and distributed systems, simulation, computer graphics, human engineering, stereoscopy, human anatomy, and artificial intelligence. Through a human-computer interface, it enables interaction within virtual scenarios that represent a concrete environment of the real world (Zheng, Chan, & Gibson, 1998). With the advancement in technology, it has become convenient to deploy VR in medicine, aviation training, and military applications (Holden, 2005). In the last 20 years, VR has encompassed new domains such as disability, rehabilitation, and training, and it has proven to be a beneficial tool in various areas of therapy and rehabilitation (Holden, 2005).

Undoubtedly, VR-based simulators have made tremendous progress in the training of new skills in almost every area: science, physical activities, culture, and industry (Slater & Sanchez-Vives, 2016). Moreover, VR has successfully simulated driving of power and MWC (Alshaer, O'Hare, Archambault, Shirley, & Regenbrecht, 2020; Bigras, Kairy, & Archambault, 2019). VR-based MWC simulators have been created for various purposes, such as designing infrastructures that provide accessibility for MWC users, training for maneuvering MWCs, and creating a platform of exercise for persons with a disability (Harrison et al., 2000; Mahajan et al., 2013).

The most basic design of VR-based MWC simulators requires a visualization device and a sensorimotor interface. The most commonly used display devices for designing MWC simulators are the head mounted display (HMD) and desktop screens (Inman, Loge, Cram, & Peterson, 2011). To implement an optimal visualization device for a MWC simulator, sense of presence (SoP) is a critical evaluation criterion. SoP alludes to the feeling of being within a software-generated computer-based scenario, rather than just perceiving the VR simulator as a physical device (Witmer & Singer, 1998). Various factors such as *control*, *sensory*, *distraction*, and *realism* contribute to the subjective feelings of involvement and immersion, which are two essential parameters for understanding SoP. *Involvement* is the user's response to stimuli, and *immersion* is the feeling of presence in virtual scenarios. The *control* factor refers to the control that the user experiences in virtual scenarios. The more control a user has over the virtual world, the higher the SoP. *Sensory* factors deal with a user's ability to utilize their senses to perceive a virtual world. *Distraction* factors include the attentiveness of the user in a virtual scenario, regardless of activities happening in the surrounding, real environment. Finally, *realism* factors refer to the replication of the real-world environment (Witmer & Singer, 1998). Alshaer et al. compared MWC users' driving performance in a virtual environment (VE) with three different conditions of field of vision (FoV): narrow, wide, and stereoscopic narrow. They found that the wide FoV resulted in a better user driving performance, as compared to the other two FoVs in VE (Alshaer, Hoermann, & Regenbrecht, 2013). Alshaer et al. also demonstrated that the use of an HMD with a changing FoV and a user's avatar increased SoP in VR simulators (Alshaer, Regenbrecht, & O'Hare, 2017).

Using a subjective questionnaire, Archambault et al. measured a good level of SoP when using a desktop screen for visualization (Archambault, Tremblay, Cachecho, Routhier, & Boissy, 2012).

The second basic part of a VR simulator is a sensorimotor interface that enables users to interact with a virtual world. This interface varies based on the MWC used in the simulator—such as a joystick for power wheelchairs and pushrims for MWC—and the feedback provided such as visual, auditory, vestibular, and haptic, which deliver information to users from a virtual scenario (Inman et al., 2011).

MWC-based simulators are being used in different situations to improve the life of MWC users. For instance, O'Connor et al. investigated the use of a MWC simulator as a training tool to increase metabolic activities and motivate users to exercise every day. Their study found that 87% of their participants felt that the system would help them to work out harder and more regularly (O'Connor, Fitzgerald, Cooper, Thorman, & Boninger, 2001). By implementing haptic feedback, Blouin et al. successfully utilized a MWC simulator to modify their participants' propulsion patterns and to help them achieve more effective propulsion patterns (Blouin, Lalumière, Gagnon, Chénier, & Aissaoui, 2015).

A barrier in rehabilitation settings is often a lack of space, which is a challenge for teaching MWC users their required skills. In this situation, VR has proven to be a convenient training tool. VR has been used to evaluate and teach MWC skills by ensuring a safe and motivational environment. Additionally, it can enhance users' confidence by providing a controllable and repeatable environment for practicing MWC propulsion techniques (Cooper et al., 2005; Schultheis & Rizzo, 2001). For example, O'Connor et al. found that a video game-based VR system motivated MWC users to use VR for training (O'Connor et al., 2000).

VR-based MWC simulators have been adopted extensively in the field of rehabilitation and physical therapy to train MWC propulsion techniques and skills in engaging, safe, and varying environments.

## 1.6 Measuring the biomechanics of manual wheelchair propulsion

The studies described previously have shown the importance of biomechanics during MWC propulsion to the prevention of strain injuries in MWC users, such as shoulder injury and pain and carpal tunnel syndrome. Therefore, the accurate measurement of these variables is important. Currently, several systems are available for measuring the biomechanics of MWC propulsion, including motion tracking systems, instrumented wheels, and inertial measurement units.

### 1.6.1 Instrumented wheels

Since the 1990s, researchers have identified a need for instrumented wheels to measure the kinematics and kinetics of MWC propulsion. In 1989, the first article published on the SMARTWheel explained the design and the basic mathematics behind its force and torque calculations (R. A. Cooper & Cheda, 1989). In 2000, SMARTWheels were commercialized for use by research groups around the world. The SMARTWheel is a six degrees of freedom sensor that measures the forces and torque applied by a MWC user on the pushrim. The variables measured by the SMARTWheel during MWC propulsion are push time, cycle, push frequency contact angle, forces, and power output. Different study designs have used the SMARTWheel to investigate the biomechanics of MWC propulsion (Boninger, Baldwin, Cooper, Koontz, & Chan, 2000; Hurd, Morrow, Kaufman, & An, 2008; Robertson et al., 1996). Furthermore, in a recent study, Klerk et al. compared measurements of kinetic parameters of MWC propulsion obtained by a MWC ergometer they designed to measurements obtained by the SMARTWheel (Klerk, Vegter, Veeger, & Woude, 2020).

In the past few years, SMARTWheels have been used as the gold standard system for studying the biomechanics of MWC propulsion, although they are no longer being commercialized.

### 1.6.2 Wearable sensor system

Wearable sensor systems are used in research to enhance the usability and convenience of measuring biomechanical movement. A wearable sensor system usually is made up of inertial measurement units (IMUs). IMUs contain three triaxial sensors and software; the sensors include a gyroscope, accelerometer, and magnetometer. An accelerometer determines a change in acceleration, a gyroscope recognizes rotational velocity about an axis, and a magnetometer measures changes in the magnetic field relative to a reference. The software provides the results of the sensors to a user.

In different areas of research such as gait analysis, rehabilitation, and neurorehabilitation, IMUs have proven to be an efficient system for measuring biomechanical parameters. Mahmoud El-Gohar et al. compared shoulder and elbow joint angles measured using IMUs to those obtained with an optical tracking system (El-Gohary et al., 2011). They suggested that IMUs could be used to track upper limb movements. Additionally, Ojeda and Ding used IMUs to monitor stroke number and cadence during MWC propulsion, and compared these measurements with those of the SmartWheel. This study found that IMUs could be used to accurately measure the stroke number and push frequency (Ojeda & Ding, 2014). Furthermore, Karinharju et al. found a strong correlation between the push count measured on an Apple watch and direct observation (Karinharju Kati, Boughey, Tweedy, Clanchy, & Trost, 2021).

Instruments such as SMARTWheels, 3D kinematic measurements, and wearable sensors systems have been used widely for measuring the biomechanical variables of MWC propulsion. However, the available systems have limitations that constrain their usage. For instance, the optoelectronic motion capture system, similar to a SMARTWheel—the gold standard for measuring kinematic parameters—is expensive and requires a specific lab setting. Similarly, SMARTWheels are high-priced and are no longer manufactured, and IMUs can only measure the stroke number and push frequency. Thus, it is essential to have a system that could measure the crucial variables of MWC propulsion at a low cost.

### 1.6.3 Manual wheelchair simulators

In the literature, different MWC ergometers (an instrument that simulates MWC propulsion) have been categorized into four types: roller ergometer, treadmill ergometer, flywheel ergometer, and integrated ergometer (Klerk, Vegter, Veeger, et al., 2020). A personal wheelchair is fixed on a roller to design a roller ergometer. For treadmill-based ergometers, a MWC is placed on a treadmill and attached to its front to keep it in a straight position. For a flywheel ergometer, a MWC is linked to a flywheel system by a chain and sprocket. Finally, an integrated ergometer or simulator includes both the simulation of the MWC and the measurement of the MWC propulsion parameters capabilities (Klerk, Vegter, Goosey-Tolfrey, et al., 2020).

Among the four, the roller ergometer is found most commonly in the literature. Regarding its basic design, at least one roller should be available on which a personal MWC can be set up. The roller has inertia and resistance that can be calibrated to overcome the mass and rolling resistance yielded by the MWC-user combination (Klerk, Vegter, Veeger, et al., 2020). Table 1.4 shows the MWC ergometers used to measure the biomechanical variables of MWC propulsion. All the ergometers are based on a roller, include platforms, and can accommodate a user's personal MWC. A recent study, Klerk et al. measured the critical parameters of MWC propulsion with a roller ergometer (Klerk, Vegter, Veeger, et al., 2020).

VR-based MWC simulators have been designed with different aims: training for MWC maneuvering skills, providing an exercise platform for a person with a disability, and supplying an accessibility awareness tool (Smith et al., 2016). Niniss and Inoue used a VR-based MWC simulator to compare the driving skills of experienced and inexperienced MWC users (Niniss & Inoue, 2006)., and Inman et al. found that children with severe orthopedic disabilities could utilize VR simulators to acquire MWC driving skills (Inman et al., 2011).

The instrument used in the present study is the McGill immersive wheelchair (MiWe) simulator. This MWC simulator is a low-cost (approximately $1000) haptic VR platform designed to simulate MWC dynamics as experienced by users in the real world. It can be controlled by the user's MWC. The simulator is designed with 1) a steel frame that stabilizes the MWC and raises it 2 cm above the ground so the rear wheels can rotate freely and 2) two independently controlled motors along with optical incremental encoders fixed under each wheel, which provide force feedback to the wheels based on an interaction with the virtual environment through velocity data. Moreover, the motors are used in a feedback loop to simulate two types of forces: inertial (so the user feels acceleration and braking forces, including collisions) and gravitational (to feel the effects of slopes). The simulator also includes 3) an Arduino microcontroller, 4) a custom made program that enables the Arduino to communicate between sensors and simulator software to produce torque to the wheels, and 5) a 69 cm (27'') screen to display the "infinite sidewalk" VR scenario where users can practice in an outdoor sidewalk environment for a set amount of time. Two types of "infinite sidewalk" scenarios were developed for the MiWe simulator. First, the straight-line scenario was designed so users can practice propulsion—participants are retained in the center of the sidewalk in a straight line (turning motions have no effect). Second, the ecological scenario also includes various obstacles that users can encounter in a contemporary city environment—side slope on the right side, side slope on the left side, straight slope, fallen signs, and street crossings—which enable users to practice handling various obstacles while pushing a MWC.

The primary purpose of this system is to help individuals with mobility limitations acquire MWC manoeuvring and propulsion skills (Hui & Archambault, 2021). However, to help reduce the prevalence of upper extremity pain and injury in MWC users, it is essential to modify the critical parameters of MWC propulsion. Therefore, the MiWe was further enhanced to measure push time, cycle time, contact angle, and velocity.

Table 1.4: MWC ergometers for the measurement of kinetic parameters of MWC propulsion

| **Category Of ergometer** | **Wheelchair Type** | **Visualization Screen** | **Platform** | **Kinetics parameters measured** | **Reference** |
| --- | --- | --- | --- | --- | --- |
| Roller | Personal | No | Yes | Power output and speed | (Niesing, Eijskoot, Kranse, Denouden, & Storm, 1990) |
| Roller | Personal | No | Yes | Tangential force, speed, and power output | (Hutzler, Vanlandewijck, & Vlierberghe, 2000) |
| Roller | Personal | No | Yes | Power output and speed | (Stewart, Melton-Rogers, Morrison, & Figoni, 2000) |
| Roller | Personal | No | Yes | Power out, speed and 2D forces (horizontal and axial) | (Devillard et al., 2001) |
| Roller | Personal | No | Yes | Torque and speed | (DiGiovine, Cooper, & Boninger, 2001) |
| Roller | Standard | No | Yes | Power output and velocity | (Faupin, Gorce, & Thevenon, 2008) |

| | | | | | |
|---|---|---|---|---|---|
| Roller | Personal | No | Yes | Speed and distance | (Kurt, Geyik, Mutlu, Tatar, & Nart, 2008) |
| Roller | Personal | yes | Yes | 3d forces and torques measured on SMARTWheel | (Chénier, Bigras, & Aissaoui, 2014) |
| Roller | Personal | No | Yes | Push time, cycle time, contact angle, torque, power and slope | (Klerk, Vegter, Veeger, et al., 2020) |

### 1.6.4 Precision and accuracy

An important consideration in the assessment of the quality of an instrument is its accuracy and precision. Prior to providing feedback on MWC propulsion variables to naïve MWC users for training purposes, it is mandatory to validate the variables measured by a simulator against a known standard instrument.

The *accuracy of an instrument* refers to the closeness of its measured values to a standard value. The *lack of accuracy of an instrument* is also termed *bias* that is due to a systematic error in measurement. *Precision* refers to the proximity of repeated measured values to each other. Precision also is related to random error or noise in a measurement. Giavarina has suggested that by using the Bland-Altman plot, which is a plot of the difference of two measurements against a mean, accuracy can be assessed in method A relative to method B by determining whether the line of equality (zero) is within the confidence limit for the mean. This study also has suggested that an efficient way to utilize the Bland-Altman is to first determine the limits of the maximum acceptable differences by using a biological and analytical criterion, and then utilizing statistics to determine whether these limits were surpassed or not. To achieve the required precision, the maximum acceptable difference between the measurements taken by the two instruments should not fall outside the range of a 95% agreement between these two instruments (Giavarina, 2015).

In light of the above study, we used Bland-Altman plots to assess the accuracy and precision of the MiWe simulator against the measurements made by high-quality instrumented wheels. In other words, our objective was to determine the accuracy and precision of the MWC simulator for measuring the crucial biomechanical parameters of the MWC propulsion technique, as compared to a gold standard system (SMARTWheel), with respect to young-healthy individuals.

## 1.7 Hypothesis

The present study presents three hypotheses:

1) During straight-line propulsion, the precision of a simulator is not influenced by stroke pattern (SC or ARC) nor by push cadence.

2) During straight-line propulsion, the measurement error of push time, cycle time, velocity, and contact angle will be less than 10% of the reported change due to training, when compared to the gold standard method.

3) In an ecological scenario, no statistical difference will be found between a measurement by the simulator and a measurement by the SMARTWheel of push time, cycle time, cadence, velocity, and contact angle.

# Chapter 02: Manuscript 1

## A low-cost approach for estimating the crucial biomechanical parameters of a manual wheelchair propulsion technique

Rabail Khowaja[1,2]

Philippe S. Archambault[1,2]

[1]*Interdisciplinary Research Center in Rehabilitation (CRIR), Canada*

[1]*School of Physical and Occupational Therapy, McGill University, Canada*

Corresponding author

RK: rabail.khowaja@mail.mcgill.ca

Authors' emails

RK: rabail.khowaja@mail.mcgill.ca

PSA: philippe.archambault@mcgill.ca

This manuscript will be submitted for review in the *Disability and Rehabilitation: Assistive Technology* journal.

## 2.1 Introduction

Spinal cord injury (SCI) is a devastating neurological disorder that causes irreparable motor, sensory, and autonomic dysfunction at or below the level of the injury (Kirshblum et al., 2011). In Canada, around 85,556 persons are living with SCI (Noonan et al., 2012). The immobility of individuals who have sustained an SCI modifies their physical, psychological, and cognitive functioning (deRoon-Cassini et al., 2009; Murray et al., 2007). Moreover, this immobility puts an extensive financial and emotional burden on the individual, their family and friends, and society (Kirshblum et al., 2011).

Assistive devices are an important tool for improving an individual's impaired walking mobility (Salminen et al., 2009). Manual wheelchairs (MWC) are one of the commonly used mobility devices adopted by many individuals with SCI to enhance their locomotion and socialization (Post et al., 1997). Around 90% of SCI individuals with preserved upper limb movements rely on a MWC for mobility (Post et al., 1997).

The propulsion of a MWC constitutes an exercise that may reduce the chance of secondary conditions prevalent in SCI individuals, such as cardiovascular disease, obesity, type 2 diabetes, and osteoporosis (Battaglino et al., 2012; Bauman et al., 1999; Cragg et al., 2013; Demirel et al., 2001; Lai et al., 2014). However, upper extremity injury is eminently common among people who rely on a MWC for mobility. The literature has shown that 30% to 70% of total MWC users experience shoulder pain (Dalyan et al., 1999; Samuelsson et al., 2004; Sie et al., 1992), and the prevalence of median nerve injury in this population ranges from 49% to 73% (Gellman et al., 1988; Tun & Upton, 1988). This damage to the upper extremities may be caused by the repetitive movements required to propel a MWC. Moreover, the prolonged shoulder pain of MWC users decreases quality of life (QOL) and physical functioning (Gutierrez et al., 2007; Putzke et al., 2002).

The literature describes different interventions for reducing shoulder pain, such as physical therapy, medication, massage, acupuncture, surgery, home modifications, and MWC modifications (Cratsenberg et al., 2015; Jonas, 1998; Popowitz et al., 2003). All these treatments reduce the existing pain at the shoulder joint, although it also is critical to have an intervention that prevents the development of shoulder pain in the first place.

Studies have shown that stroke pattern is an important factor in MWC propulsion. Sanderson and Sommer were the first to characterize the propulsion of a MWC by *stroke pattern*, which is defined as the trajectory of the hands during the push stroke (Sanderson & Sommer, 1985). Building on these results, Boninger et al. observed four different propulsion patterns: semicircular, arcing, single loop, and double loop. The pattern in which the hands drop below the path of the pushrim after the push is called *semicircular* (SC). In the *arcing pattern* (ARC), the user's hands closely follow the pushrim after release. In the *single loop pattern* (SLOP), users lift their hands above the pushrim after release. The *double loop pattern* (DLOP) is similar to the SLOP, with the difference being that the hands cross over the pushrims and then drop below them (Boninger et al., 2002). These four patterns are illustrated in Figure 2.1.

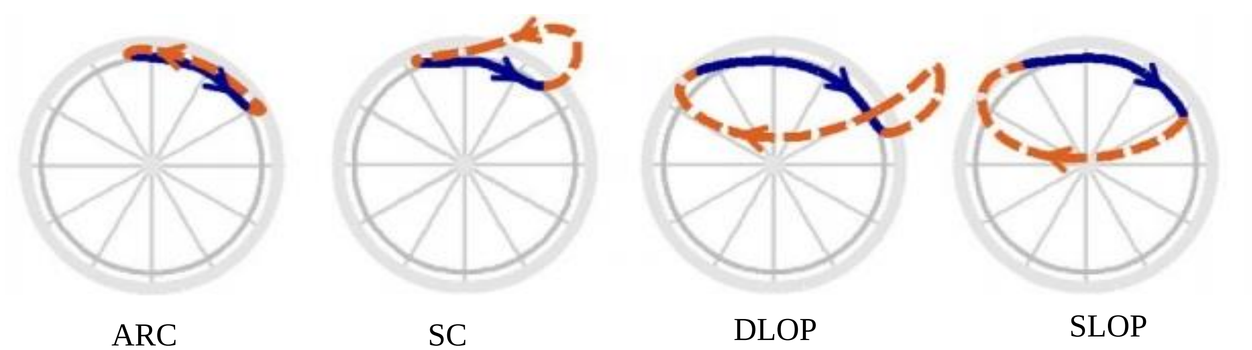


Figure 2.1: Four different patterns of MWC propulsion, the dashed line represents the recovery phase, and the solid line represents the push phase. ARC, SLOP, DLOP, and SC stands for ARC, single loop, double loop, and semi-circular, respectively.

Boninger et al. were the first to report an association between pushrim biomechanics and median nerve injury, which is related to the peak propulsion force and frequency of pushrim loading. (Boninger et al., 1999). Moreover, their study found that cadence, the magnitude of the force, and the stroke pattern may be related to upper extremity injury. To reduce the risks of injury, these researchers have suggested that peak force and cadence should be decreased (Boninger et al., 2002). As a result, the clinical practice guidelines for SCI recommends the use of long and smooth pushes to decrease the prevalence of shoulder pain in individuals with SCI (Paralyzed Veterans of America Consortium for Spinal Cord, 2005). The long pushes can be achieved by maximizing the contact angle during the push phase of the stroke cycle.

These recommended guidelines can be achieved naturally through the adoption of a SC propulsion pattern. Indeed, the SC pattern has been found to have low cadence, high push time to recovery time ratio, and less sudden changes in the hands direction of propulsion, compared to other propulsion patterns (Boninger et al., 2002). However, it also has been observed that the SC pattern is not intuitively adopted by new MWC users (Boninger et al., 2002). Virtual reality (VR) could be a potential solution for teaching MWC propulsion to naive MWC users by providing a safe, controlled and motivating environment (Mahajan et al., 2013). Recently, VR has made a remarkable impact in rehabilitation, disability, and training (Holden, 2005). For example, O’Connor et al. observed that a video game-based VR system motivated MWC users to use VR for training (O'Connor et al., 2000). Moreover, VR technology can properly simulate the driving of power wheelchair and propulsion of MWC (Arlati, Colombo, Ferrigno, Sacchetti, & Sacco, 2020).

In a lab setting, Klerk et al. carried out a critical analysis of stationary instruments that simulate MWC propulsion. They categorized the stationary ergometers into four types: 1) treadmills, 2) rollers, 3) flyover, and 4) integrated (Klerk, Vegter, Goosey-Tolfrey, et al., 2020). With respect to the treadmill-based ergometers, a MWC is placed on a treadmill and attached to its front to keep the MWC in a straight position. One advantage of using a treadmill is that it realistically displays the distance travelled by the user, although a treadmill moving at a fixed velocity does not allow rotation movements or accelerations. Figure 2.2a shows a treadmill-based ergometer (Klerk, Vegter, Goosey-Tolfrey, et al., 2020; Kwarciak et al., 2011). The most widely used ergometers are roller-based, with at least one roller on which a MWC is fixed. These vary from completely passive ergometers to advanced setups that include electric brakes or motors for individual rear wheels, which require a calibration of inertia and resistance of the system that may be difficult to perform (DiGiovine et al., 2001; Klerk, Vegter, Goosey-Tolfrey, et al., 2020).  Figure 2.3 shows a roller-based ergometer.

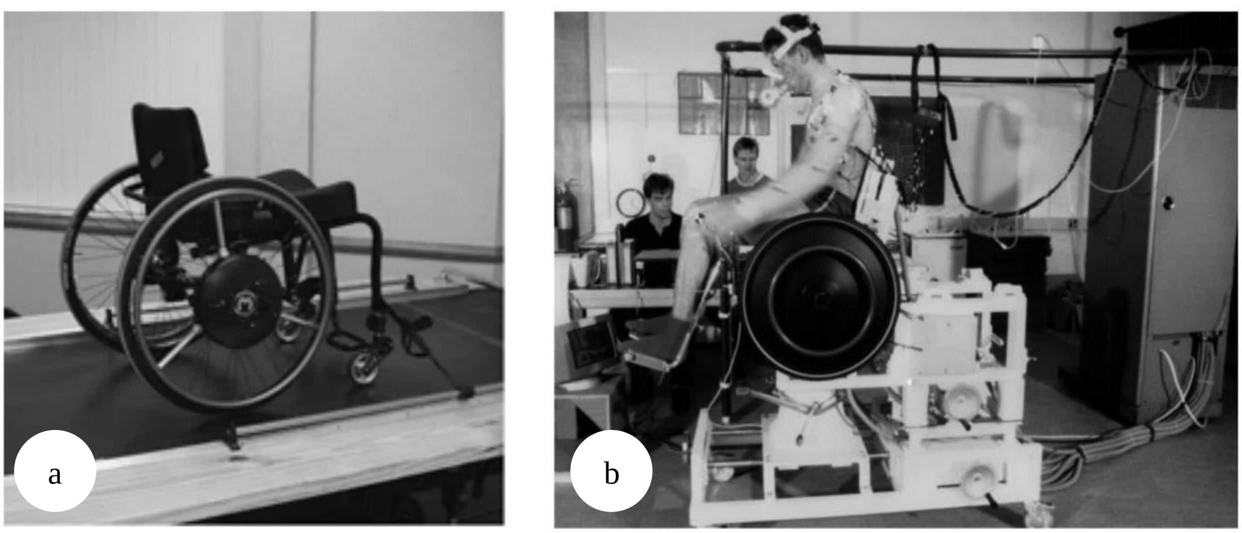

Figure 2.2: (a) Treadmill-based MWC ergometer (Kwarciak, Turner, Guo, & Richter, 2011) (b) Integrated manual wheelchair ergometer (R. Niesing et al., 1990)

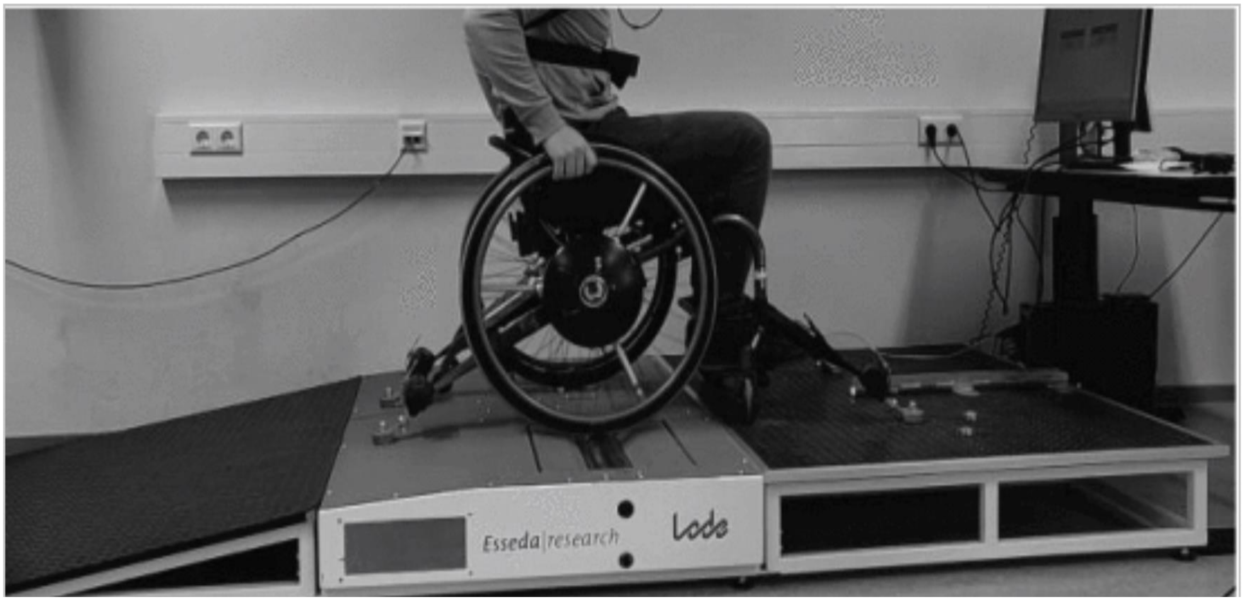

Figure 2.3: Roller-based MWC ergometer (Klerk, Vegter, Veeger, et al., 2020)

With respect to a flywheel ergometer, a MWC is linked to a flywheel system by a chain and sprocket. The main advantage is that this ergometer can be designed using commercial bicycle parts. However, the properties of a flywheel ergometer depend on the bicycle used in the design (Klerk, Vegter, Goosey-Tolfrey, et al., 2020).

Finally, an integrated ergometer or simulator provides both a simulation of the MWC and the measurement of the MWC propulsion parameters capabilities (Klerk, Vegter, Goosey-Tolfrey, et al., 2020) as shown in Figure 2.2b.

The ergometer and treadmill designs described above can be improved by adding visual feedback that represents a real-world simulated environment. These designs can provide a safe, encouraging, and controlled environment for enhancing MWC propulsion skills (Mahajan et al., 2013). VR-based MWC simulators have different aims: training for MWC maneuvering skills, creating an exercise platform for persons with a disability, and as an accessibility awareness tool (Smith et al., 2016). Niniss and Inoue used a VR-based MWC simulator to compare the driving skills of experienced and inexperienced MWC users (Niniss & Inoue, 2006). In addition, Inman et al. found that children with severe orthopedic disabilities could utilize VR simulators to acquire MWC driving skills (Inman et al., 2011).

The instrument used in the present study is the McGill immersive wheelchair (MiWe) simulator as shown in figure 2.4. The primary purpose of this system is to help individuals with mobility limitations acquire MWC manoeuvring and propulsion skills (Hui & Archambault, 2021). However, to help reduce the prevalence of upper extremity pain and injury in MWC users, it is essential to modify the critical parameters of MWC propulsion. Therefore, the MiWe was further enhanced to measure push time, cycle time, contact angle, and velocity.

Figure 2.4: A full view of the MiWe simulator.

Before feedback on MWC propulsion variables can be provided to new MWC users for training purposes, the simulator's measurements need to be validated by comparing them with the measurements of a known standard. Instruments such as instrumented wheels (SMARTWheels) (shown in Figure 2.5) and 3D kinematic measurements systems have been used to measure MWC propulsion biomechanics. However, these systems have limitations that constrain their usage. For instance, kinematic measurements systems are expensive and can be used only in a lab setting. SMARTWheels also are expensive and are no longer manufactured. Inertial measurement units (IMU) can be used to measure stroke numbers and cadence (Ojeda & Ding, 2014). For use in a clinical or home setting, it would be important to have a low-cost system to measure the crucial variables of MWC propulsion. Therefore, the present study has been designed to provide such a system for estimating the essential parameters of MWC propulsion, and for use outside of a lab setting at a much-reduced cost, compared to existing systems. In this study, we obtain the values of push time, cycle time, contact angle, and velocity by using the MWC simulator, and we compare these values against the gold standard of SMARTWheels.

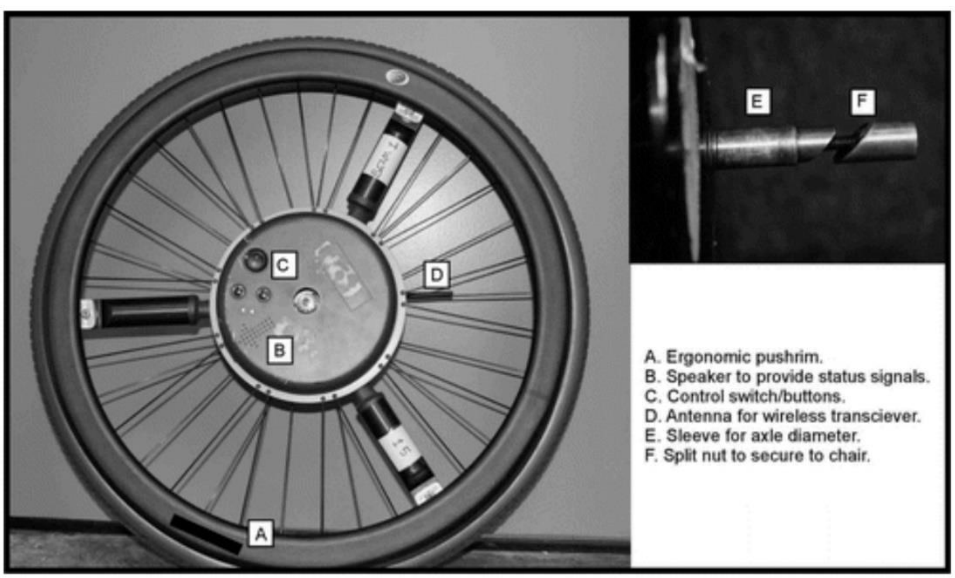


Figure 2.5: SMARTWheel system (Rory A. Cooper, 2009)

## 2.2 Objective

This study has been designed to determine the precision and accuracy of push time, cycle time, velocity, and contact angle as measured by the MiWe simulator (and to compare these measurements to the measurements of the SMARTWheels gold standard) that can be utilized outside a lab setting at a low cost, compared to existing measurement systems.

## 2.3 Hypothesis

The present study puts forward three hypotheses:

1) During straight-line propulsion, the precision of the simulator is not influenced by stroke pattern (SC or ARC) nor by push cadence.

2) During straight-line propulsion, the measurement error of push time, cycle time, velocity, and contact angle will be less than 10% of the reported change due to training, when compared to the gold standard method.

3) In an ecological scenario, no statistical differences will occur in the measurements of the simulator and the SMARTWheel with respect to push time, cycle time, cadence, velocity, and contact angle.

## 2.4 Methods

### 2.4.1 Participants

We recruited a total of 12 healthy individuals. We had planned to collect measurements from both young-healthy individuals and individuals with SCI, but due to the COVID-19 pandemic situation, data collection from the latter group was not possible. However, a future study could be carried out with participants with SCI to measure their MWC propulsion biomechanics. Table 2.1 shows the demographics of our participants. The inclusion criterion were ages between 18–45, no pain or injury in the upper extremities, and no impairments affecting the upper extremities. The participants provided their informed consent as approved by the ethics committee of the Centre for Interdisciplinary Research in Rehabilitation (CRIR, Canada). They were compensated for the reimbursement of their travel expenses and for investing their time in the study. The study was carried out over one month at the Advanced Technologies in Rehabilitation lab of the CRIR.

Table 2.1: Demographics of the participants

| **Participant** | **Age (year) Mean(std)** | **Height(cm) Mean(std)** | **Weight (kg) Mean(std)** | **BMI** |
|---|---|---|---|---|
| 01(F) | 42 | 160 | 85 | 33.2 |
| 02(F) | 28 | 169 | 50 | 17.5 |
| 03(F) | 24 | 159 | 58 | 22.9 |
| 04(F) | 34 | 178 | 67 | 21.1 |
| 05(F) | 24 | 155 | 62 | 25.8 |
| 06(F) | 27 | 153 | 59 | 25.2 |
| 07(F) | 22 | 153 | 51 | 21.8 |
| 08(F) | 26 | 171 | 64 | 21.9 |
| 09(M) | 31 | 180 | 82 | 25.3 |
| 10(M) | 19 | 183 | 77 | 23 |
| 11(M) | 28 | 175 | 71 | 23.2 |
| 12(M) | 28 | 176 | 76 | 24.5 |
| **12 (8F and 4M)** | 27.8(6.0) | 167.7(11.1) | 66.8(11.6) | 23.8 |

### 2.4.2 Sample Size

No prior data was available for calculating the sample size for the current study. We chose the sample size of 12 participants for reasons of feasibility, given the timeframe for the data collection. Likewise, we elected to have a total of 46 trials for each targeted cadence during each propulsion pattern (SC or ARC) in the straight-line scenarios, as well as 3 trials to overcome each of the 5 obstacles, so to limit the session duration to less than 60 minutes and to decrease the risks of participants developing fatigue during the experiment.

### 2.4.3 Experimental setup

#### 2.4.3.1 MiWe simulator

The MiWe simulator is a low-cost (approximately $1000) haptic VR platform designed to simulate MWC dynamics as experienced by users in the real world. It can be controlled by the user's MWC.

The simulator is designed with 1) a steel frame that stabilizes the MWC and raises it 2 cm above the ground so the rear wheels can freely rotate (Figure 2.6); 2) two independently controlled motors along with optical incremental encoders fixed under each wheel, which provide force feedback to the wheels based on the interaction with the virtual environment through velocity data; moreover, the motors are used in a feedback loop to simulate two types of forces: inertial (so the user feels the acceleration and braking forces, including collisions) and gravitational (to feel the effects of slopes); 3) an Arduino microcontroller; 4) a custom made program for the Arduino to communicate between the sensors and the simulator software to produce torque to the wheels; and 5) a 69 cm (27'') screen to display the VR scenario as shown in Figure 2.7.

When the wheels of the MWC rotate, the encoders measure the number of ticks passing in front of the sensor, during a sampling time of 25 ms, which provides a measurement of velocity.

The start of a push is recognized if the wheel rotates in the forward direction and exceeds a minimum threshold value of 10 ticks on the encoder per 25 ms sample, which corresponds to a change in wheel velocity of 104 deg/s. The push ends when the velocity value drops below the same threshold. The time difference between the start and end of a push is termed *push time* (in seconds). The *cycle time* is the time from a push start to the next push (in seconds). The angular velocity is multiplied by each sampling time to calculate the instantaneous angle, and then the instantaneous angles between the push start and push end are summed to find the *contact angle*. *Acceleration* is calculated as a change in velocity over time.

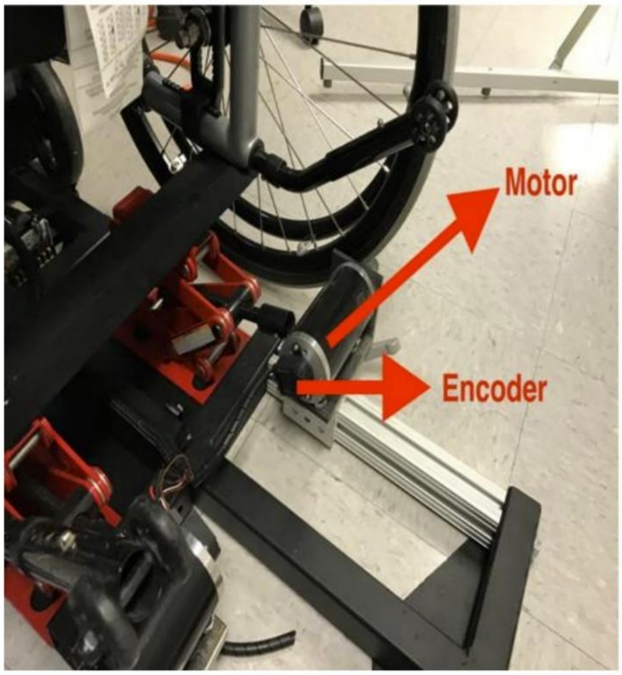


Figure 2.6: The placement of motors and encoders in the simulator

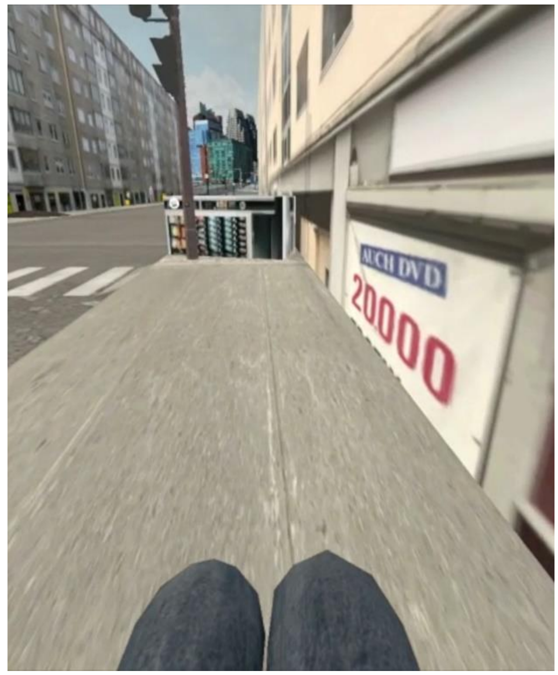


Figure 2.7: Virtual reality scenario

#### 2.4.3.2 SMARTWheels

Before installing the MWC on the simulator, the two rear wheels of the standard MWC, which were 62x105 cm, were equipped with 25" SMARTWheels. A MATLAB code was written to calculate push time, cycle time, velocity, and contact angle from the SMARTWheels data.

### 2.4.4 Data Collection

Data collection duration, including training, lasted from 45 to 60 minutes for each participant.

**Training**

Participants were seated in a standard MWC fitted on the simulator. They were trained for 15 minutes on propelling the MWC on the simulator. During this training period, they were shown a video of SC and ARC patterns on a computer screen. Next, a researcher provided verbal feedback to the participants on the propulsion of the MWC using the SC pattern and then the ARC pattern. Participants practiced each pattern at three cadences (slow, medium, and high) by matching a metronome beat. These two propulsion patterns were chosen because, among the four identified propulsion patterns, these provide the extreme values of the MWC propulsion parameters (Boninger et al., 2002). After this initial training, participants completed two tasks: a straight-line scenario and an ecological scenario.

**Straight-line scenario**

The straight-line scenario was designed to maintain the participants on the center of the sidewalk in a straight line (turning motions or an application of asymmetrical forces on both wheels had no effect). In this scenario, participants propelled the MWC using either the ARC or SC pattern at a pre-established cadence synchronized with metronome beats.

We selected two distinct ranges of cadences for the two patterns as shown in Table 2.2. Since the ARC technique requires hand contact with the pushrim for a short arc, it is not easy to achieve slow cadences (i.e., lower than 46 pushes/minute). In contrast, when using the SC pattern, the hands reach further back during the recovery phase, which makes it difficult to achieve fast cadences such as 100 or 120 pushes/minute.

Table 2.2: Target cadences and corresponding metronome frequencies

| **Patterns** | **Cadence (seconds)** | **BPM** |
|---|---|---|
| SC | 0.7 | 86 |
| SC | 0.8 | 75 |
| SC | 0.9 | 67 |
| SC | 1.0 | 60 |
| SC | 1.1 | 55 |
| SC | 1.2 | 50 |
| SC | 1.3 | 46 |
| SC | 1.4 | 43 |
| ARC | 0.5 | 120 |
| ARC | 0.6 | 100 |
| ARC | 0.7 | 86 |
| ARC | 0.8 | 75 |
| ARC | 0.9 | 67 |
| ARC | 1.0 | 60 |
| ARC | 1.1 | 55 |
| ARC | 1.2 | 50 |

Figure 2.8 shows the steps we followed for collecting data from the participants. In session 1, the participants propelled the MWC on a straight-line scenario that consisted of a total of 50 pushes for a given push pattern and cadence. The order of the required cadence and push pattern was randomized. Participants were given 30 sec breaks after every 4 trials. Upon completion of the straight-line scenario, they were given a 1 minute short break.

Our literature review showed that the SC pattern involves a high contact angle, low cadence, and high peak force. In contrast, the ARC pattern has a low contact angle, high cadence, and low peak force (Boninger et al., 2005; Boninger et al., 2002; Kwarciak et al., 2012). Additionally, in the ecological scenario, the participants also propelled the MWC with their natural propulsion pattern. Together, these data provided a range of values for the variables of interest.


Figure 2.6: Procedure for data collection

**Ecological scenario**

The ecological scenario included various obstacles that could be encountered in a contemporary city environment: side slope (left and right), straight slope, fallen signs, and street crossings as shown in Figure 2.9. Participants had to cross over side slopes and move up and down a straight slope. The street crossing was similar to an everyday street crossing scenario in which participants had to press a button that would start a timer of 15 sec (by pressing the spacebar on the keyboard) and then cross to the other side within that time limit. Finally, the fallen sign obstacle presented two fallen signs that the participants had to pass without striking. The motors provided realistic force feedback to mimic the acceleration effects of the slopes and collisions. Participants completed three trials, with each obstacle appearing once in a random order. During the ecological tasks, we asked the participants to propel the MWC using their natural pattern. However, if they used an ARC pattern during the straight-line segments (i.e., during the street crossing or in between obstacles), we reminded them to adopt a SC pattern, if needed. Each trial lasted approximately 2 minutes, followed by a 1 minute rest period to avoid fatigue.

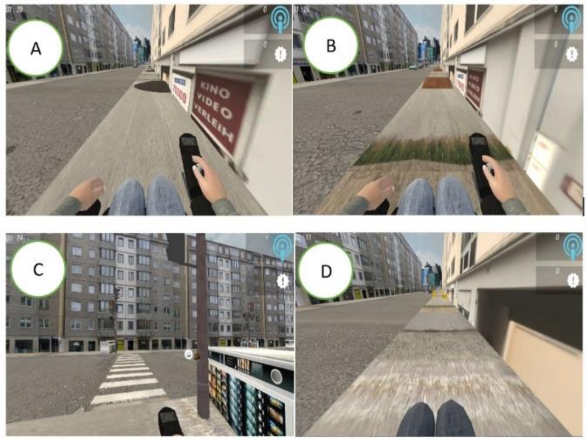

Figure 2.7: A, side slope; B, straight slope; C, street crossing; D, Fallen signs

### 2.4.5 Threshold for assessing the precision of the MiWe

Ideally, the required precision for measuring the biomechanical parameters related to MWC propulsion would be based on clinical guidelines. However, such guidelines do not currently exist, and current recommendations are only to increase the contact angle and decrease cadence, since the optimal value or range is unknown.

Table 2.3 shows 10% of the change in each variable due to training. A precision in measurements equivalent to 10% is a good compromise between what is technically feasible and potential clinical relevance. However, we were not able to find training values for propulsion velocity, since MWC users don’t train to improve their velocity and only require a minimal value to be able to perform tasks such as crossing a street. Therefore, the precision was set at 10% of minimal locomotion velocity for independent living that is 0.8m/s (i.e., 0.08 m/s).

Thus, we decided to base our precision requirements on the changes in parameters before and after training. For example, Rice et al. assessed MWC propulsion on the ground after training using visual feedback on the contact angle, cadence, and velocity on a dynamometer. These researchers measured the cadence and contact angle of long-term MWC users at baseline and three months after training at both a self-selected and predefined speed. After training, their participants increased the contact angle and decreased cadence at both speeds (Rice et al., 2010). Moreover, DeGroot et al. measured increases in push time and cycle time after three weeks of training on a computer-controlled MWC ergometer, which provided visual feedback on velocity (De Groot et al., 2002). The changes in biomechanical variables before and after training, obtained from these two studies, are summarized in Table 2.3. Both studies measured the contact angle, so the values obtained are provided, and the lowest value was used to investigate the highest precision of the simulator.

Table 2.3 Crucial biomechanical values before and after training. Values indicate mean (SD)

| References | Variables | Before training | After training | Change due to training | 10% of the difference |
|---|---|---|---|---|---|
| **(Rice et al., 2010)** | **Self-selected speed** | | | | |
| | Contact angle (Degrees) | 94.30 (18.9) | 109.70(12.6) | 15.40 | 1.54 |
| | **Targeted speed** | | | | |
| | Contact angle (Degrees) | 107.3(10.5) | 120.2(15.3) | 12.90 | **1.29** |
| **(De Groot et al., 2002)** | Cycle time(s) | 1.03(0.23) | 1.57(0.51) | 0.54 | 0.05 |
| | Push time (s) | 0.35(0.11) | 0.44(0.09) | 0.09 | 0.01 |
| (Abellan Van Kan et al., 2009) | Velocity(rad/sec) | NA | NA | 0.8 | 0.08 |

### 2.4.6 Data Processing

We synchronized the SMARTWheel and simulator data by using a cross-correlation analysis. We determined the delay between the two for each data record, where the correlation between cycle times was maximal.

To analyze the straight-line scenario data, each trial was first processed through a custom MATLAB code. From each of the trails, the steady push cycles were taken. If any of the instruments (SMARTWheel or simulator) recorded less than 10 good steady push cycles in any of the trials, that trial was excluded from further analysis. We removed individual pushes within a trial if they were *outliers*, which we defined as above and below three standard deviations of the targeted cadence as suggested by Kwarciak et al. (Kwarciak et al., 2012). We calculated all the variables of interest for each push cycle, and then averaged all the push cycles of the same trial.

To process the data from the ecological scenario, we created a MATLAB script to match the push cycles of the simulator and the SMARTWheel. To match the push cycle, for each push cycle in the right SMARTWheel, we determined the start and end of the push phase. We also found a matching cycle in the simulator. We defined *matching* as a push cycle on the simulator whose time range overlaps the push cycle on the SMARTWheel by at least 75%. If matching cycles were found, we retained the indices of the matching cycles. We performed a matching of the push cycles of the SMARTWheel and the simulator to compare the variables of the two systems. We carried out the synchronization of the SMARTWheel and the simulator data, since to navigate an obstacle during the ecological scenario, participants were sometimes using short cycles or propelling with the wheels in opposite directions; however, the simulator could not detect a cycle in the backward direction, which would have affected the results. Therefore, for the data analysis, we used only the matched push cycles. To decrease the outliers, we removed the trials with a cadence above 120 and below 43. These threshold values corresponded to the maximum and minimum target cadences in the straight-line scenarios (Table 2.2).

### 2.4.7 Data Analysis

We first scaled the simulator's spatial measures (contact angle and velocity) to the SMARTWheel measures using linear regression on the combined data from the straight-line scenario (all participants, propulsion patterns, and target cadences). Later, we also scaled the temporal variables (push time, cycle time) using the same strategy, since we observed bias in the simulator data as compared to the SMARTWheel data.

To address the three hypotheses of the present study, we performed Bland-Altman and mixed model analyses on push time, cycle time, velocity, and contact angle. We carried out the mixed model analysis on each variable of interest using the type of instrument (SMARTWheel or simulator), target cadence (50, 55, 60, 67, 75, and 86 strokes/minute) and stroke pattern (SC or ARC) as factors. We supported the first hypothesis if there was no interaction effect of stroke pattern and targeted cadence with the instruments.

To address the second hypothesis, we used a Bland-Altman analysis to determine the precision and accuracy (additional assessment) of the simulator to the SMARTWheel. The resultant graph is a scatter plot (Figure 2.10) in which the x-axis represents the average of the measurements from the simulator and SMARTWheel, and y represents the difference between the simulator and the SMARTWheel (Giavarina, 2015). We determined precision as the necessity for the two instruments to be in 95% limits of agreement (green solid lines in Figure 2.12), and we assessed the accuracy of the measured variables by determining whether the line of equality (zero) lies within the confidence limits (the red dotted line in Figure 2.12 and the green dotted lines represent the 95% confidence limits for the limits of agreement) of the mean (the solid red line in Figure 2.12) in the BA plot. We found support for the second hypothesis if the agreement between the measurements taken by the MiWe and the SMARTWheel was less than 10% of the reported changes due to training (the dotted black line in Figure 2.14).

Finally, to address the third hypothesis, we performed mixed model and Bland-Altman analyses. The Bland-Altman analyses were the same as hypothesis 2. The hypothesis was supported if an instrument effect was not present, and if the agreement between the measurements taken by the MiWe and the SMARTWheel were less than 10% of the reported changes due to training.

## 2.5 Results

Before performing a statistical analysis on the collected data to assess each of the three hypotheses, we performed a linear regression to calibrate the simulator with the SMARTWheel by using all the available data (from all participants, both patterns, and all target cadences) measured during the MWC propulsion in the straight-line scenario. We performed this regression for the two spatial variables only (contact angle and velocity) since we assumed that the time variables (push time and cycle time) would not require calibration. Figure 2.10 shows the fitted line of the contact angle during wheelchair propulsion in a straight-line scenario with the SMARTWheel (explanatory variable) on the x-axis and the simulator (dependent variable) on the y-axis. In addition, Figure 2.11 shows how calibration, calculated using all the available data, applies to each propulsion pattern.

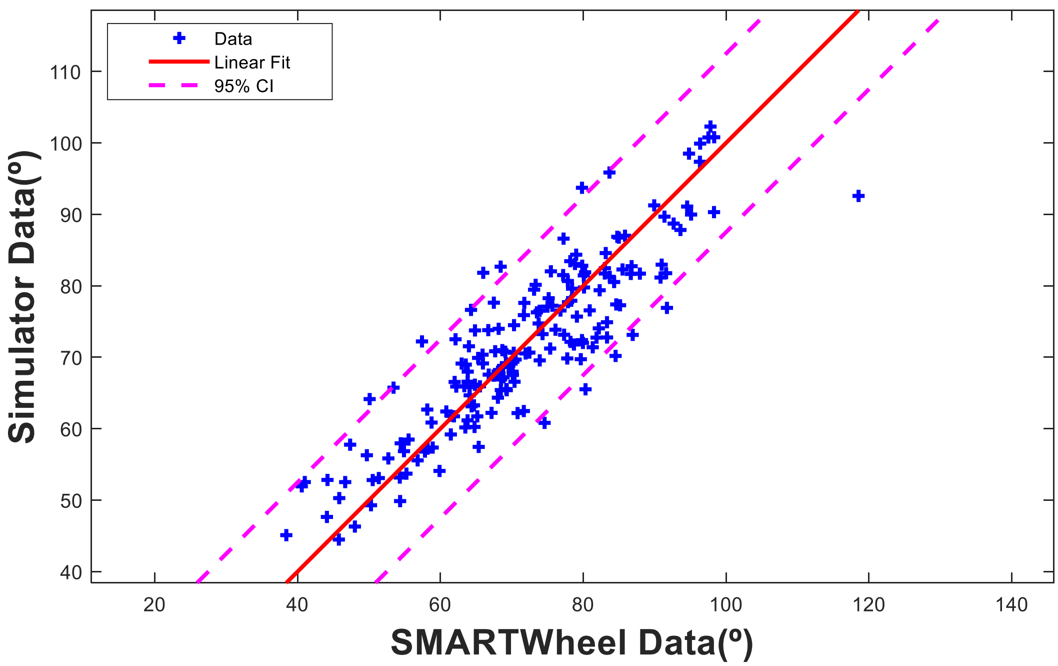

Figure 2.8: Fitted data of contact angle for arcing and semicircular pattern

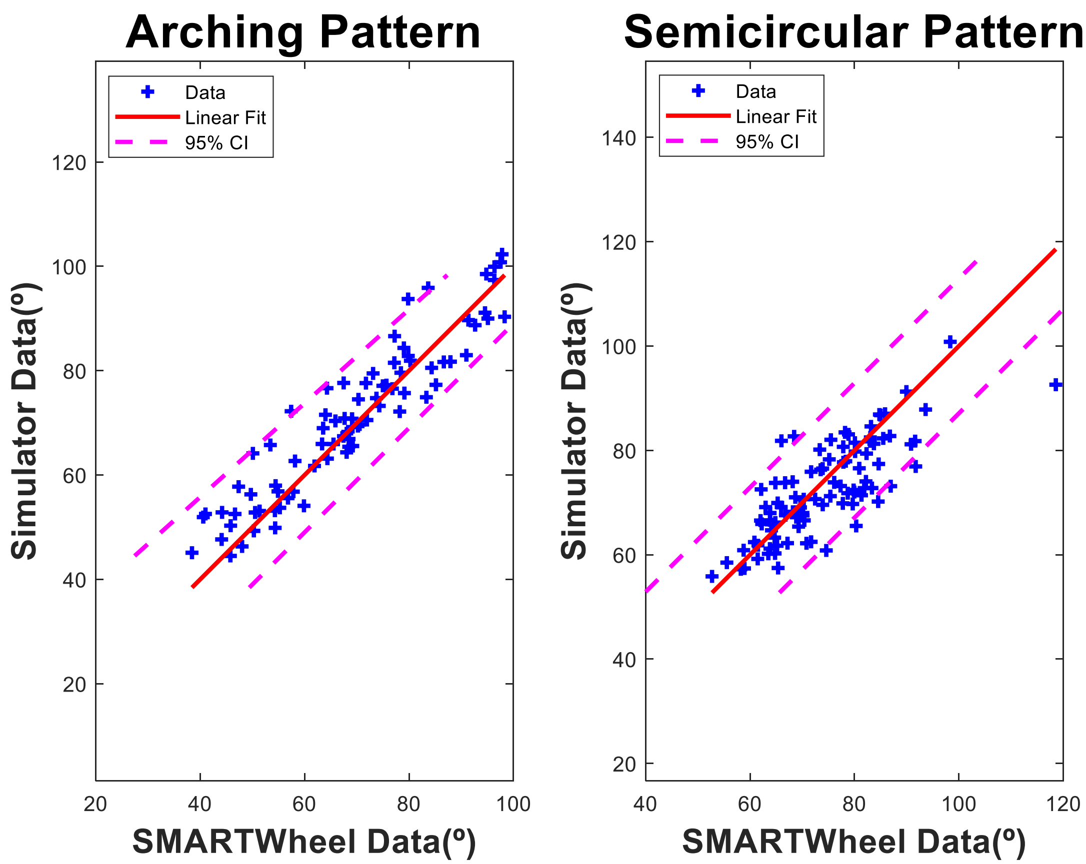


Figure 2.9: Fitted data of contact angle for arcing and semicircular pattern

### 2.5.1 Hypothesis 1

In the present study, the first hypothesis was put forward to determine whether the values measured by the MiWe simulator and the SMARTWheel were influenced by the stroke pattern (Arc or SC) and the targeted cadence, during the straight-line scenario. To that end, we performed mixed-model analyses comparing the effects of the instrument, stroke pattern, and target cadence on the measurement of each outcome. Table 2.4 shows the results of these analyses for all the measured parameters in the straight-line scenario. The main effects—P (pattern) and Tcad (targeted cadence)—for all the variables, except for cycle time in pattern and contact angle in target cadence, were significant with p-values lower than 0.001, which shows that the MWC propulsion parameters varied with both target cadence and pattern. This result was expected, since increasing or decreasing cadence will considerably vary the propulsion parameters.

To answer the first hypothesis, we examined the interaction between the stroke pattern and instrument and between the target cadence and instrument, i.e., P*Inst and Tcad*Inst, as shown in Table 2.4.

For all the outcome variables in the straight-line scenario, the p-values for P*Inst and Tcad*Inst were more than 0.05, which signifies that both patterns and target cadence did not significantly influence the measurements differently with respect to the two instruments. Therefore, we support the hypothesis that during the straight-line scenario, the MiWe measurements were not influenced by the stroke pattern (SC or ARC) or the targeted cadence.

Table 2.4: Results of the mixed model analysis for all the measured variables in the straight-line scenario.

| **Parameters** | **Straight-line Scenario** | | | |
|---|---|---|---|---|
| | **ARC and SC patterns** | | | |
| | **P** | **Tcad** | **P*Inst** | **TCad*Inst** |
| **Push time(sec)** | $F_{1,235}$=13.4, p=0.00 | $F_{1,235}$=56.0, p=0.00 | $F_{1,235}$=0, p=0.99 | $F_{5,235}$=1.9, p=0.10 |
| **Cycle time(sec)** | $F_{1,235}$=0.28, p=0.60 | $F_{1,235}$=1065.5, p=0.00 | $F_{1,235}$=0, p=0.87 | $F_{5,235}$=1.2, p=0.33 |
| **Velocity(rad/sec)** | $F_{1,235}$=323.84, p=0.00 | $F_{1,235}$=48.69, p=0.00 | $F_{1,235}$=1.9, p=0.17 | $F_{5,235}$=0.5, p=0.76 |
| **Contact Angle(º)** | $F_{1,235}$=384.86, p=0.00, | $F_{1,235}$=0.401, p=0.85 | $F_{1,235}$=5, p=0.03 | $F_{5,235}$=0.5, p=0.74 |

TCad: Target cadence factor; Inst: Instrument factor; P: Pattern

### 2.5.2 Hypothesis 2

For our second hypothesis, we aimed to determine whether measurement errors of the variables during the straight-line scenario were less than 10% of the reported changes due to training. To address this hypothesis, we used a Bland Altman analysis to assess the MiWe's precision and accuracy relative to the SMARTWheel.

We assessed the accuracy of the MiWe for all the variables in the SC and ARC patterns during straight-line scenario by determining whether the line of equality (zero) lies within the confidence limits of the mean in the BA plot, as illustrated in Figure 2.12 (push time for the SC pattern). This figure shows that the MiWe simulator did not accurately measure the push time for the SC pattern, since the line of equality was not within the confidence limits of the mean. This finding also was the case for push time for the ARC pattern. We observed that regarding the cycle time for the ARC pattern and the contact angle for the SC pattern, the line of equality was within the confidence limit of the mean. For contact angle for the ARC pattern, the line of equality was very close to the confidence limits of the mean. Moreover, for the cycle time for the SC pattern and the velocity for both patterns, the line of equality was a little far from the confidence limits of the mean. Since we observed a bias between the simulator and SMARTWheel measures of push time and cycle time, we decided to calibrate the simulator for the temporal variables as well. The presence of a bias can be explained by the different method used to measure the temporal variables, which is based on a force threshold for the SMARTWheel and a velocity threshold for the simulator. As shown in Figure 2.13, when using the calibrated simulator data, the line of equality for push time for the SC pattern is now within the confidence limits of the mean. The same finding was observed for the ARC pattern and for the cycle time in both patterns.

On the other hand, to access the precision of the MiWe simulator, the 10% threshold, which is the maximum acceptable difference between the variables measured by MiWe and SMARTWheel, was plotted to whether it contained the 95% limits of agreement between the two instruments as shown in Figure 2.14. This figure shows that regarding the push time for the SC pattern, the maximum acceptable difference did not fall outside the 95% limits of agreement between the MiWe and SMARTWheel, which also was the case for all the variables in both patterns. Moreover, the calibration of cycle time and push time data could not encompass 95% limits of agreement within maximum acceptable difference as shown in Figure 2.15. Table 2.5 shows the changes due to training, targeted precision, highest limit of the limits of agreement, and limits of agreement (LoA) due to training change for all the measured variables for both patterns in the straight-line scenario.

The LoA due to training change was obtained by dividing the measured highest limit of agreement of cycle time by the change in the variable due to training. With respect to the cycle time for the ARC and SC patterns, the LoA relative to training change was the lowest among all the variables. This finding signifies that the MiWe simulator was able to measure the 10% and 14% threshold change in the cycle time for the ARC and SC patterns, respectively, with a 95% certainty during the straight-line scenario. Moreover, the 95% LoA for the simulator measurement was very close to the required precision for the cycle time for both patterns.

With respect to the remaining variables, the LoA relative to training change was quite high, which suggests that the simulator was not able to measure the threshold change precisely for both patterns in the straight-line scenario.

Table 2.5: Percentage of change due to the training in the variables during the straight-line scenario

| Variables | Scenarios | Patterns | Change due to training | Targeted precision | Highest limit of 95 limits of agreement | LoA relative to training change |
|---|---|---|---|---|---|---|
| Push time(sec) | Straight-line | Arc | 0.09 | 0.009 | 0.084 | 93% |
| | | Semi | 0.09 | 0.009 | 0.095 | 106% |
| Cycle time (sec) | Straight-line | Arc | 0.54 | 0.054 | 0.053 | 10% |
| | | Semi | 0.54 | 0.054 | 0.076 | 14% |
| Velocity (rad/sec) | Straight-line | Arc | 0.8 | 0.08 | 0.802 | 100% |
| | | Semi | 0.8 | 0.08 | 0.766 | 96% |
| Contact angle($^o$) | Straight-line | Arc | 12.9 | 1.29 | 11.203 | 87% |
| | | Semi | 12.9 | 1.29 | 15.108 | 117% |

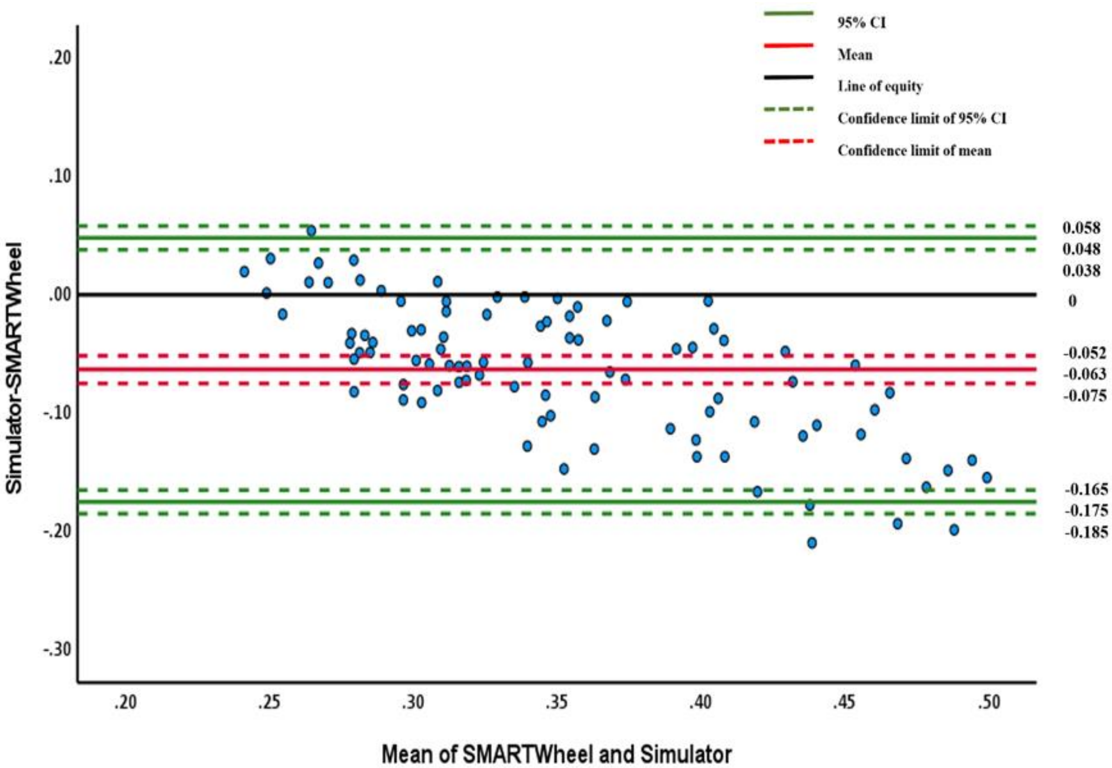


Figure 2.10: BA plot to assess accuracy of push time (sec) of semicircular pattern

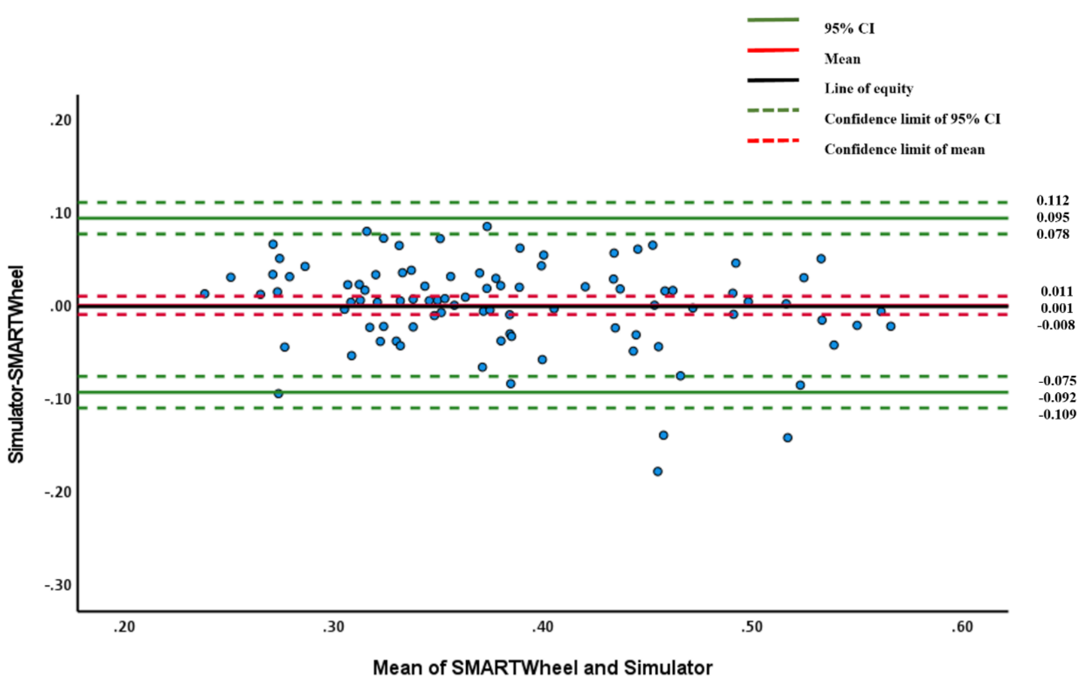


Figure 2.11: BA plot to assess accuracy of calibrated push time (sec) of semicircular pattern

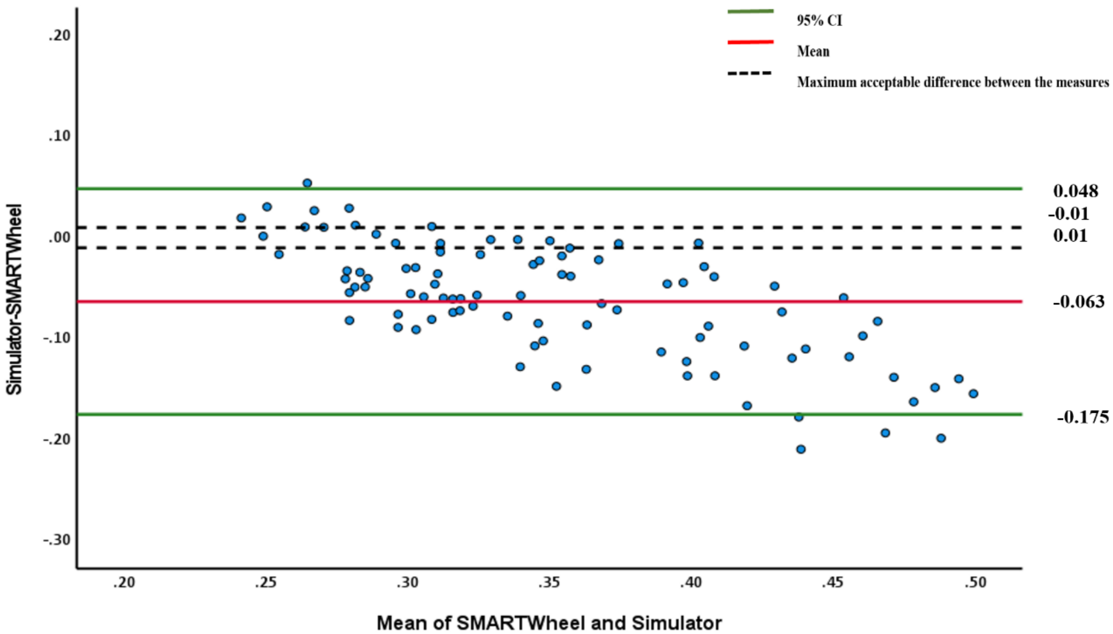


Figure 2.12: BA plot to assess precision of push time (sec) of semicircular pattern

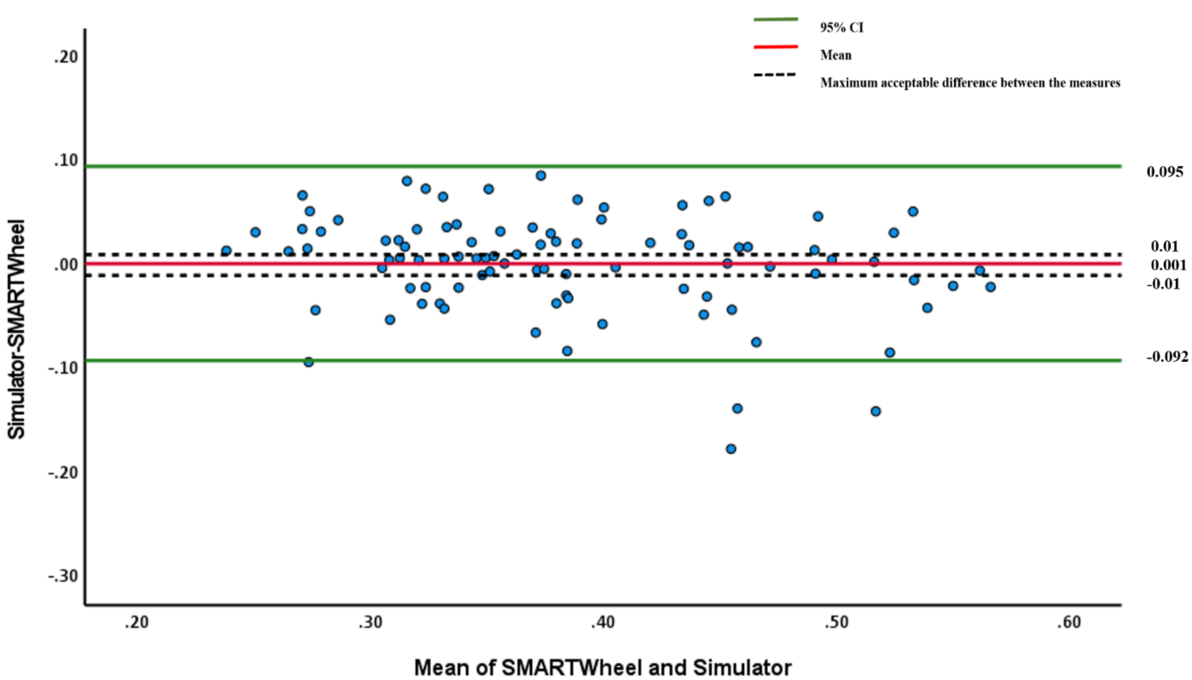


Figure 2.13: BA plot to assess precision of calibrated push time (sec) of semicircular pattern

### 2.5.3 Hypothesis 3

For hypothesis 3, we determined whether a difference existed between the variables measured by the MiWe and SMARTWheel in the ecological scenario, in which participants maneuvered around various obstacles. The results of the mixed model analysis for the ecological scenario in Table 2.6 show no significant difference for cycle time due to the instrument (Inst). However, a significant difference was found for push time, velocity, and the contact angle. In addition, Table 2.7 shows that the measurement errors for the variables in the ecological scenario were a lot greater than the 10% of change due to training.

Table 2.6: Results of mixed model analysis for all the measured variables during the ecological scenario

| **Parameters** | **Ecological Scenario** |
|---|---|
| | **No-specific pattern** |
| | **Inst** |
| **Push time(sec)** | $F_{1,1431}$=51**, p=0.00 |
| **Cycle time(sec)** | $F_{1,1404}$=0.0, p=0.94 |
| **Velocity(rad/sec)** | $F_{1,1421}$=5.2*, p=0.02 |
| **Contact Angle(º)** | $F_{1,1428}$=25.3**, p=0.00 |

* p<0.05
** p<0.01
Inst: Instrument factor

Table 2.7: Percentage of change due to the training in the variables during ecological scenario

| Variables | Scenarios | Change due to training | Targeted precision | Highest limit of 95 confidence interval | CI relative to training change |
|---|---|---|---|---|---|
| Push time(sec) | Ecological | 0.09 | 0.009 | 0.257 | 286% |
| Cycle time (sec) | Ecological | 0.54 | 0.054 | 0.295 | 55% |
| Velocity(rad/sec) | Ecological | 0.8 | 0.08 | 1.390 | 174% |
| Contact angle(º) | Ecological | 12.9 | 1.29 | 39.465 | 306% |

Figure 2.16 shows that the line of equality for push time was a little far from the confidence limits of the mean. Moreover, the lines of equality for cycle time, contact angle, and velocity were very close to the confidence limits of the mean. However, as shown in Figure 2.17, for all the outcome variables, the maximum acceptable difference between the variables measured by the MiWe and the SMARTWheel did not fall outside the 95% limits of agreement between the two instruments. This finding signifies that the MiWe simulator was not able to measure a 10% threshold change with a 95% certainty with respect to all the variables in the ecological scenario.

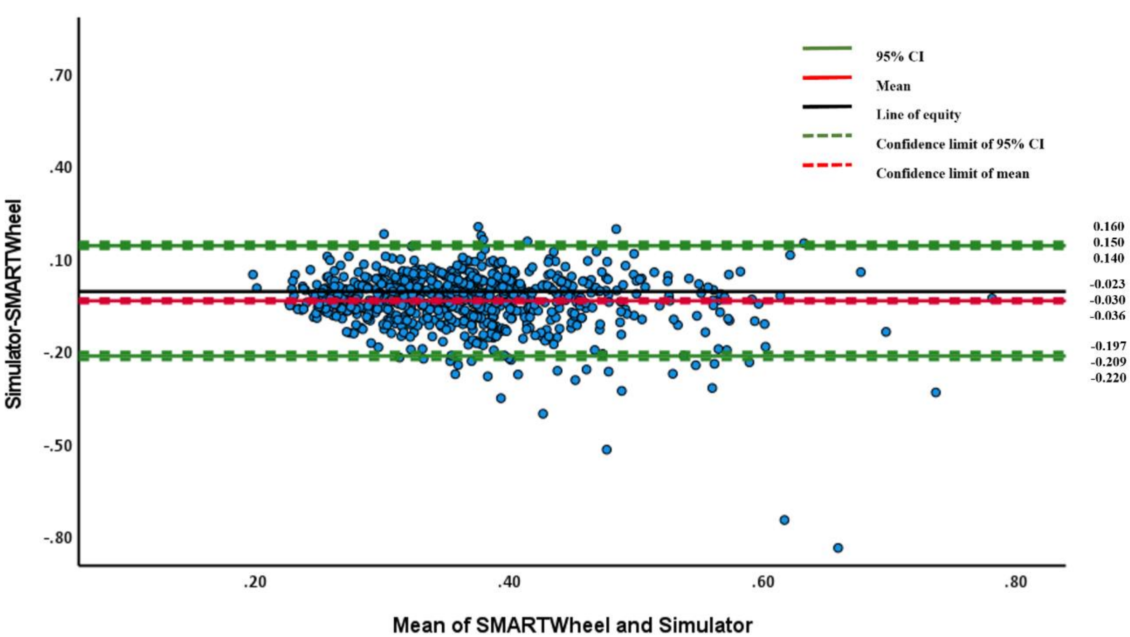


Figure 2.14: BA plot to access accuracy of push time (sec) during ecological scenario

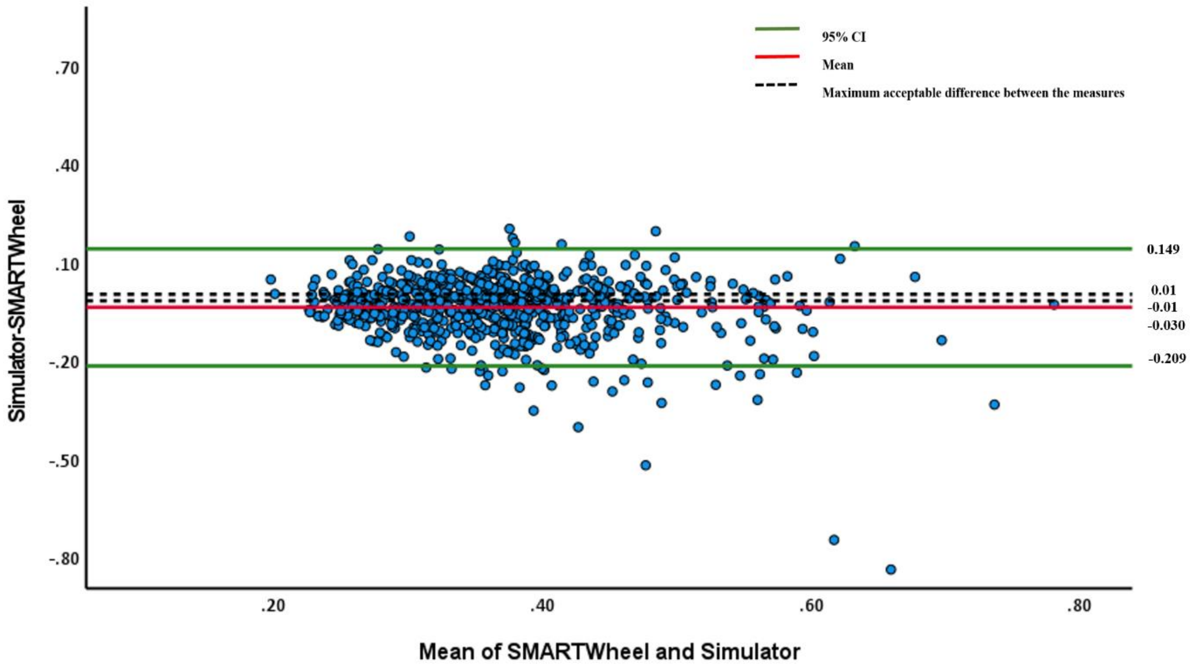


Figure 2.15: BA plot to access precision of push time (sec) during ecological scenario

## 2.6 Discussion

The main objective of the present study was to assess the MiWe simulator's precision for measuring the important biomechanical parameters of MWC propulsion. To that end, we compared the simulator's measurements to those obtained by a gold standard—an instrumented wheel (SMARTWheels). We gathered data using two scenarios: a straight-line scenario in which participants simply propelled a MWC forward, and an ecological scenario in which participants needed to circumvent various obstacles. In the former scenario, propulsion patterns and cadence were fixed, and MWC movement in a direction other than a straight line was blocked, whereas in the latter scenario, participants propelled a MWC in a VR environment without these constraints.

Our first hypothesis was that the precision of the MiWe simulator's measurement would neither depend on a stroke pattern (ARC or SC) nor a push cadence. We compared the effects of the instruments, stroke pattern, and target cadence using mixed model analyses. The MiWe simulator and SMARTWheel did not significantly differ with respect to their measurements of push time, cycle time, velocity, and contact angle for different stroke patterns and target cadences. These results support our first hypothesis.

Our second hypothesis was that during straight-line propulsion, the errors produced by the MiWe simulator's measurements of push time, cycle time, velocity, and contact angle would be less than 10% of the reported changes due to training. For this hypothesis, we calculated whether the mean difference between the instruments was less than 10%, and also determined the accuracy and precision of the simulator. The results indicated that the simulator was accurate for measuring the variables, since the line of equality was inside the confidence limits of the mean for push time and cycle time, close to mean limits for the contact angle, and a little far for velocity. However, the MiWe simulator was not precise regarding these measurements, except for the cycle time during propulsion with an ARC pattern as shown in Table 2.5. The precision of the simulator for each measured variable was determined if the 95% of the limits of the agreement would not fall outside the maximum acceptable difference between the two instruments. Thus, in general, the simulator was accurate but not precise regarding our variables of interest. The precision of the simulator's measurements could be improved potentially to some degree by performing repeated measurements, as long as the propulsion trials could be repeated by the participants using the same conditions (i.e., the same velocity and propulsion style). Taking an average of multiple measurements would provide a value closer to the "true" value of interest. In addition, replacing the simulator's sensors with those with a higher sampling rate (currently 25 milliseconds) might improve its precision for detecting pushes.

Our third hypothesis was that in the ecological scenario, no differences would exist between the simulator measurements and the SMARTWheel measurements with respect to push time, cycle time, velocity, and contact angle. Contrary to this hypothesis, we found significant differences in the measurements of push time, velocity and contact angle, but not for cycle time. Additionally, the errors on the measurements of the variables were higher than the target of 10%. In the ecological scenario, participants propelled a MWC around different obstacles using both ARC and SC patterns. During straight-line segments between the obstacles, the participants adopted long pushes. To navigate around the different barriers, they utilized short pushes, as well as turns, which sometimes necessitated moving one wheel forward and the other backward. The random choice of patterns and the presence of multiple turns help to explain the more variable data related to this scenario. Moreover, to evaluate the data collected for the straight-line scenario, we averaged the trials over many pushes, whereas this was not the case for the ecological scenario. However, the precision of the MiWe simulator in the ecological scenario could be improved by limiting the measurement of the biomechanical variables to the straight-line sections only, which would require additional programming to identify or detect a push cycle when a participant enters a straight-line, no obstacle section. The propulsion variables would then be calculated to obtain a precision and accuracy similar to the straight-line scenario.

Taken together, our results imply that the MiWe simulator did not precisely measure most of our variables of interest, although it did accurately measure the temporal variables. Nevertheless, the precision of its variable measurements could be enhanced by increasing the number of trials required to achieve the targeted precision.

Our study also confirmed that during the straight-line MWC propulsion, both with ARC and SC patterns, an increase in target cadence was associated with a decrease in push time, cycle time, and the contact angle, and with an increase in velocity. These results are consistent with the study conducted by Shamiada et al. and Boninger et al., which has suggested that with increasing speed, participants spend less time in the push phase, and cycle time and the contact angle also decrease. Similarly, we could compare the effects of a propulsion pattern on the biomechanical variables. At the same targeted cadence in a straight-line scenario, during propulsion with a SC pattern, push time, velocity, and contact angle were higher than during propulsion with an ARC pattern, which again confirms the study results in the literature (Boninger et al., 2002).

Although the SMARTWheel commonly is used to measure the kinetic parameters of MWC propulsion (Cowan, Boninger, Sawatzky, Mazoyer, & Cooper, 2008), they no longer are being manufactured, which is a big drawback. Another disadvantage of using SMARTWheels is that they must replace the regular wheels of a participant's MWC, whereas participants can use their own MWC with the simulator. Additionally, SMARTWheels do not always fit on all MWCs, which also limits their usage. Finally, the instrumented wheels enable the measurement of MWCs variables in a fixed MWC-user configuration, such as pushrim propulsion, whereas a MWC ergometer enables measurement in different configurations. MWC ergometers are lab-restricted instruments primarily developed to simulate MWC propulsion in a straight line (Yomtov, Derman, Cochran, & Brunski, 1978). However, a few recently designed ergometers can provide haptic feedback and can measure MWC propulsion parameters (Chénier et al., 2014; Klerk, Vegter, Veeger, et al., 2020).

One of the limitations of the MiWe simulator is that although it can provide biomechanical measurements during MWC propulsion in a VR scenario, these results may not be applicable to overground propulsion. However, Rice et al. trained participants in MWC propulsion by using an ergometer for three months and then measured any changes in their natural and overground MWC propulsion. They observed a significant difference in the cadence, contact angle, average force, and power between pre-training and after training (Rice et al., 2010). This finding clearly shows that training with an ergometer can transfer to overground propulsion. Since our simulator bears a resemblance to the ergometer, we expect that the results from the present study can be generalized to MWC overground propulsion. Another limitation is that increasing the speed of propulsion sometimes leads to simulator technical issues, for example, the failure of motor control and slippage between the wheel and the motor, which may have affected the data of the present study and increased variability. Furthermore, the sample size could not be calculated when planning the experiment. However, given that the confidence limits of the means and the 95% limit of agreement for all the outcomes were narrow (as shown in the dotted lines of the BA plot of push time in Figure 2.13), we are confident that the sample size was adequate for our study.

In summary, the enhancements of the MiWe simulator with respect to measuring the MWC propulsion variables of push time, cycle time, velocity, and contact angle were not completely successful. The simulator was quite accurate in both scenarios, but not precise for all the measured variables of the straight-line scenario, and less so for the ecological scenario. Thus, to provide feedback to users or clinicians regarding MWC propulsion during simulator training, it would be appropriate to do so only for straight-line segments without obstacles. It would be easy with our current setup to design a training scenario composed of sections with obstacles, interspersed with straight-line no obstacle segments. Then, feedback about propulsion would be given only for those straight-line-no-obstacle segments. Although at present the MiWe simulator project does not measure all critical variables, it provides some insights that suggest that accurate measurements of all critical variables, with some adjustments, could be possible with the low cost and simple design of the MiWe simulator. We believe that the MiWe simulator system could be further improved to measure with accuracy the other remaining critical variables of MWC propulsion.

# Chapter 03: Thesis summary and conclusion

Rehabilitation aims to ameliorate the quality of life (QOL) and independence of individuals with temporary or permanent disabilities. Thus, the rehabilitation field uses different approaches to improve the function, activity, and participation of people with disabilities that include, amongst others, exercise, training, and assistive devices (Cratsenberg et al., 2015; Jonas, 1998; Popowitz et al., 2003). Importantly, an assistive device sometimes requires specialized training to acclimate its users (Chiu & Man, 2004).

People with lower-limb paralysis after a SCI depend on a MWC for many of their daily life activities (Post et al., 1997). The literature has identified an association between MWC propulsion and the shoulder pain and injuries of MWC users (Morrow et al., 2010), which can be alleviated through rehabilitation. For example, Kemp et al. provided a 12-week training intervention for individuals with SCI. The training focused on enhancing the strength of shoulder muscles and on optimizing MWC propulsion patterns. At the end of the training, they found that shoulder pain had decreased, and that social participation and QOL had improved (Kemp et al., 2011). Thus, it is essential to train individuals with SCI with the most effective propulsion pattern to reduce shoulder pain and improve their QOL.

Previous studies have shown that upper extremity pain can be prevented by adopting an efficient propulsion pattern. The American clinical practice guidelines for the preservation of upper limb function following SCI have suggested that propulsion characteristics can be improved by lengthening and smoothing the pushes (Paralyzed Veterans of America Consortium for Spinal Cord, 2005). Moreover, an effective method for teaching a good propulsion pattern to a novice MWC user would be a VR-based MWC ergometer that simulates propulsion in a real environment, since it would reduce the user's fear of negative incidents and personal injuries (O'Connor et al., 2000).

In the past two decades, instrumented wheels have been used to calculate the biomechanical parameters of MWC propulsion, which, in turn, has helped to determine propulsion characteristics. However, SMARTWheels are quite expensive and are no longer available (Rory A. Cooper, 2009). Therefore, in the present project, the available MWC simulator (MiWe) was further enhanced to measure MWC propulsion variables—push time, cycle time, cadence, velocity, and contact angle.

In this study, we examined three hypotheses: 1) during straight-line propulsion, the precision of the simulator is not influenced by stroke pattern (SC or ARC) nor by push cadence; 2) during straight-line propulsion, the measurement error of push time, cycle time, velocity, and contact angle will be less than 10 % of the reported change due to training, when compared to a gold standard method; 3) in an ecological scenario, no statistical difference will exist between the measurements of the MiWe simulator and the SMARTWheel of push time, cycle time, cadence, velocity, and contact angle. Interestingly, we found our simulator measurements were not influenced by the propulsion pattern (ARC or SC) and targeted cadence. Although the variable measurements were not precise, they provided accurate values for all the variables of interest in the straight-line and ecological scenarios.

The MiWe simulator provides a safe, controlled environment for users to acquire MWC skills. To further enhance the simulator for training purposes, we measured some critical parameters of MWC propulsion related to kinematic variables to provide feedback to users. This feedback could be used to help users to acquire a good propulsion technique through a visual display of propulsion parameters in the form of numerical values, as well as a target to be reached, for example, "increase your average contact angle by 10°.” Indeed, it is relevant to contemplate the design of such a training paradigm. Currently, the MiWe simulator provides two types of scenarios: ecological and straight line. For novice MWC users, the straight-line scenario would be a good starting experience. Users would not need to avoid obstacles and could improve their propulsion technique by focusing on the feedback from the measured biomechanical variables. After achieving some proficiency, they could engage in a long scenario with various obstacles and tasks (ecological scenario). At times during this scenario, the user would encounter a straight-line section with no impediments and would receive feedback on their propulsion performance at the end of these segments. This scenario would help teach an optimal propulsion technique to MWC users in conditions similar to everyday life.

In a recent study conducted by Hui and Archambault, feedback on contact angle and cadence was provided to healthy adults during their propulsion activity with the MiWe simulator. Their study found a significant difference in contact angle and cadence of the group with feedback, compared to the control group that did not receive feedback (Hui & Archambault, 2021). Moreover, Blouin et al. successfully utilized a haptic biofeedback-based MWC simulator to modify the propulsion patterns of their participants and to achieve an effective propulsion pattern. The training focused on improving mechanical effective force (MEF) throughout the push phase. The MEF is the square of the ratio of the force applied tangentially to the total force (Blouin et al., 2015).

Usability and ease of use are important characteristics for the adoption of a technology in a clinical setting. Although many simulators are available for measuring wheelchair parameters, most of them are complex, bulky, and difficult to set up. Our MWC simulator is simple, lightweight, and inexpensive. Therefore, for clinical use, it would be easy to move and set up in any given clinical or rehabilitation setting with few constraints with respect to physical space requirements.

Additionally, the MiWe simulator requires little training to fix it to a user's MWC and for general usage.

**Future improvements**

To propel a MWC, users apply force at a point of force application (PFA) on the pushrim in the direction of motion. Boninger et al. have found that peak force is directly associated with median nerve damage (Boninger et al., 1999). Additionally, Fronczak et al. have reported that higher peak force during MWC propulsion decreased the function of the median nerve over time (Fronczak, Boninger, Souza, & Cooper, 2003). Both of these studies suggest reducing peak force to decrease the chance of upper limb injuries. Therefore, the measurement of forces applied by users on the pushrim would be useful since it could be provided as feedback to users to train them to adopt more efficient force patterns. In addition, *power output* is defined as the amount of energy transferred or converted per unit of time, which is the amount of external work per unit time that a user is required to produce to propel a MWC (Pellegrini et al., 2004). Pellegrini et al. also have suggested that power output is an important measure of the performance of MWC users—a higher power output indicates better user performance. Kwarciak et al. also found that experienced MWC users exhibited a higher power output than inexperienced MWC users (Kwarciak et al., 2012). Along with push time, cycle time, cadence, and contact angle, peak force and power output are important variables of MWC propulsion. In the future, our MiWe simulator could be further modified to measure these additional variables, although the best method for measuring propulsion force and power is still with instrumented wheels (SMARTWheels), but these are expensive, no longer manufactured, and must replace the wheels of a user's MWC. Devillard et al. have suggested another method that measures 2D propulsion force by force transducers attached to the frame of their wheelchair ergometer platform. Moreover, Feghoul et al. were able to estimate 2D forces and moments using inertial sensors for straight-line movements. We could use one of these approaches and either integrate force transducers in our MWC platform or use inertial sensors to measure propulsion force (Devillard et al., 2001; Feghoul, Chenier, & Aissaoui, 2019). Then, power output could be measured by multiplying force with velocity.

The precision of the MiWe simulator's measurements could be potentially improved to some degree by performing repeated measurements, as long as the propulsion trials were repeated by the participants using the same conditions (i.e., the same velocity and propulsion style). Taking the average of multiple measurements would provide a value closer to the "true" value of interest. In addition, replacing the sensors with a higher sampling rate (currently 25 milliseconds) could potentially improve the precision of the simulator to detect pushes.

This study contributes to the knowledge about a low-cost and simple method for measuring MWC propulsion parameters. Currently, most of the available MWC simulators are high-tech, expensive, and require a special lab setting. Thus, a future research project could be carried out to determine the effectiveness of the MiWe simulator for teaching a new propulsion pattern in a home or rehabilitation setting without the continuous assistance of a therapist.

As mentioned previously, we had planned to collect data from both young-healthy individuals and individuals with SCI, but due to the COVID-19 pandemic situation, data collection from the latter group was not possible. A future study could be repeated with SCI participants to measure their MWC propulsion biomechanics.

In summary, the simulator is a low-cost, simple, and convenient system for measuring the most critical parameters of wheelchair propulsion. Providing users with feedback on these measured variables would help to train them to achieve an optimal propulsion pattern.

# References


Abellan Van Kan, G., Rolland, Y., Andrieu, S., Bauer, J., Beauchet, O., Bonnefoy, M., . . . Vellas, B. (2009). Gait speed at usual pace as a predictor of adverse outcomes in community-dwelling older people an International Academy on Nutrition and Aging (IANA) Task Force. *The journal of nutrition, health & aging, 13*(10), 881-889. doi:10.1007/s12603-009-0246-z

Alshaer, A., Hoermann, S., & Regenbrecht, H. (2013, 26-29 Aug. 2013). *Influence of peripheral and stereoscopic vision on driving performance in a power wheelchair simulator system.* Paper presented at the 2013 International Conference on Virtual Rehabilitation (ICVR).

Alshaer, A., O'Hare, D., Archambault, P., Shirley, M., & Regenbrecht, H. (2020). How to Observe Users' Movements in Virtual Environments: Viewpoint Control in a Power Wheelchair Simulator. *Human Factors, 62*(4), 656-670. doi:10.1177/0018720819853682

Alshaer, A., Regenbrecht, H., & O'Hare, D. (2017). Immersion factors affecting perception and behaviour in a virtual reality power wheelchair simulator. *Applied Ergonomics, 58,* 1-12. doi:https://doi.org/10.1016/j.apergo.2016.05.003

Archambault, P., Tremblay, S., Cachecho, S., Routhier, F., & Boissy, P. (2012). Driving performance in a power wheelchair simulator. *Disability and rehabilitation. Assistive technology, 7*, 226-233. doi:10.3109/17483107.2011.625072

Arlati, S., Colombo, V., Ferrigno, G., Sacchetti, R., & Sacco, M. (2020). Virtual reality-based wheelchair simulators: A scoping review. *Assist Technol, 32*(6), 294-305. doi:10.1080/10400435.2018.1553079

Battaglino, R. A., Lazzari, A. A., Garshick, E., & Morse, L. R. (2012). Spinal cord injury-induced osteoporosis: pathogenesis and emerging therapies. *Current osteoporosis reports, 10*(4), 278-285. doi:10.1007/s11914-012-0117-0

Bauman, W., Kahn, N., Grimm, D., & Spungen, A. (1999). Risk factors for atherogenesis and cardiovascular autonomic function in persons with spinal cord injury. *Spinal Cord, 37*, 601-616. doi:10.1038/sj.sc.3100911

Bayley, J. C., Cochran, T. P., & Sledge, C. B. (1987). The weight-bearing shoulder. The impingement syndrome in paraplegics. *J Bone Joint Surg Am, 69*(5), 676-678.

Bigras, C., Kairy, D., & Archambault, P. S. (2019). Augmented feedback for powered wheelchair training in a virtual environment. *Journal of NeuroEngineering and Rehabilitation, 16*(1), 12. doi:10.1186/s12984-019-0482-3

Blaine, T., Moskowitz, R., Udell, J., Skyhar, M., Levin, R., Friedlander, J., . . . Altman, R. (2008). Treatment of Persistent Shoulder Pain with Sodium Hyaluronate: A Randomized, Controlled Trial: A Multicenter Study. *JBJS, 90*(5).

Blouin, M., Lalumière, M., Gagnon, D. H., Chénier, F., & Aissaoui, R. (2015). Characterization of the immediate effect of a training session on a manual wheelchair simulator with haptic biofeedback: towards more effective propulsion. *IEEE Trans Neural Syst Rehabil Eng, 23*(1), 104-115. doi:10.1109/tnsre.2014.2330837

Boninger, M. L., Baldwin, M., Cooper, R. A., Koontz, A., & Chan, L. (2000). Manual wheelchair pushrim biomechanics and axle position. *Archives of Physical Medicine and Rehabilitation, 81*(5), 608-613. doi:https://doi.org/10.1016/S0003-9993(00)90043-1

Boninger, M. L., Cooper, R. A., Baldwin, M. A., Shimada, S. D., & Koontz, A. (1999). Wheelchair pushrim kinetics: body weight and median nerve function. *Arch Phys Med Rehabil, 80*(8), 910-915. doi:10.1016/s0003-9993(99)90082-5

Boninger, M. L., Dicianno, B. E., Cooper, R. A., Towers, J. D., Koontz, A. M., & Souza, A. L. (2003). Shoulder magnetic resonance imaging abnormalities, wheelchair propulsion, and gender<sup>1</sup>. *Archives of Physical Medicine and Rehabilitation, 84*(11), 1615-1620. doi:10.1053/S0003-9993(03)00282-X

Boninger, M. L., Koontz, A. M., Sisto, S. A., Dyson-Hudson, T. A., Chang, M., Price, R., & Cooper, R. A. (2005). Pushrim biomechanics and injury prevention in spinal cord injury: recommendations based on CULP-SCI investigations. *J Rehabil Res Dev, 42*(3 Suppl 1), 9-19. doi:10.1682/jrrd.2004.08.0103

Boninger, M. L., Souza, A. L., Cooper, R. A., Fitzgerald, S. G., Koontz, A. M., & Fay, B. T. (2002). Propulsion patterns and pushrim biomechanics in manual wheelchair propulsion. *Archives of Physical Medicine and Rehabilitation, 83*(5), 718-723. doi:https://doi.org/10.1053/apmr.2002.32455

Boschen, K. A., Tonack, M., & Gargaro, J. (2005). The Impact of Being a Support Provider to a Person Living in the Community With a Spinal Cord Injury [Educational Publishing Foundation doi:10.1037/0090-5550.50.4.397]. Retrieved

Burnham, R. S., May, L., Nelson, E., Steadward, R., & Reid, D. C. (1993). Shoulder pain in wheelchair athletes: The role of muscle imbalance. *The American Journal of Sports Medicine, 21*(2), 238-242. doi:10.1177/036354659302100213

Chen, Y., Tang, Y., Vogel, L., & DeVivo, M. (2013). Causes of Spinal Cord Injury. *Topics in Spinal Cord Injury Rehabilitation, 19*(1), 1-8. doi:10.1310/sci1901-1

Chénier, F., Bigras, P., & Aissaoui, R. (2014). A New Wheelchair Ergometer Designed as an Admittance-Controlled Haptic Robot. *IEEE/ASME Transactions on Mechatronics, 19*(1), 321-328. doi:10.1109/TMECH.2012.2235079

Chiu, C. W. Y., & Man, D. W. K. (2004). The Effect of Training Older Adults with Stroke to Use Home-Based Assistive Devices. *OTJR: Occupation, Participation and Health, 24*(3), 113-120. doi:10.1177/153944920402400305

Chung, A. (2019, 13/05/2019). Hip anatomy, function and common problems.

Citterio, A., Franceschini, M., Spizzichino, L., Reggio, A., Rossi, B., & Stampacchia, G. (2004). Nontraumatic spinal cord injury: an Italian survey. *Arch Phys Med Rehabil, 85*(9), 1483-1487. doi:10.1016/j.apmr.2003.09.028

Cooper, Ding, D., Simpson, R., Fitzgerald, S. G., Spaeth, D. M., Guo, S., . . . Boninger, M. L. (2005). Virtual reality and computer-enhanced training applied to wheeled mobility: an overview of work in Pittsburgh. *Assist Technol, 17*(2), 159-170. doi:10.1080/10400435.2005.10132105

Cooper, R. A. (2009). SMARTWheel: From Concept to Clinical Practice. *Prosthetics and Orthotics International, 33*(3), 198-209. doi:10.1080/03093640903082126

Cooper, R. A., & Cheda, A. (1989, 9-12 Nov. 1989). *Measurement of racing wheelchair propulsion torque.* Paper presented at the Images of the Twenty-First Century. Proceedings of the Annual International Engineering in Medicine and Biology Society.

Cowan, R. E., Boninger, M. L., Sawatzky, B. J., Mazoyer, B. D., & Cooper, R. A. (2008). Preliminary Outcomes of the SmartWheel Users' Group Database: A Proposed Framework for Clinicians to Objectively Evaluate Manual Wheelchair Propulsion. *Archives of*

*Physical Medicine and Rehabilitation, 89*(2), 260-268. doi:https://doi.org/10.1016/j.apmr.2007.08.141

Cragg, J. J., Noonan, V. K., Dvorak, M., Krassioukov, A., Mancini, G. B., & Borisoff, J. F. (2013). Spinal cord injury and type 2 diabetes: results from a population health survey. *Neurology, 81*(21), 1864-1868. doi:10.1212/01.wnl.0000436074.98534.6e

Cratsenberg, K. A., Deitrick, C. E., Harrington, T. K., Kopecky, N. R., Matthews, B. D., Ott, L. M., & Coeytaux, R. R. (2015). Effectiveness of Exercise Programs for Management of Shoulder Pain in Manual Wheelchair Users With Spinal Cord Injury. *J Neurol Phys Ther, 39*(4), 197-203. doi:10.1097/npt.0000000000000103

Cripps, R. A., Lee, B. B., Wing, P., Weerts, E., Mackay, J., & Brown, D. (2011). A global map for traumatic spinal cord injury epidemiology: towards a living data repository for injury prevention. *Spinal Cord, 49*(4), 493-501. doi:10.1038/sc.2010.146

Dalyan, M., Cardenas, D. D., & Gerard, B. (1999). Upper extremity pain after spinal cord injury. *Spinal Cord, 37*(3), 191-195. doi:10.1038/sj.sc.3100802

De Groot, S., Veeger, D., Hollander, A. P., & V. Van Der Woude, L. H. (2002). Wheelchair propulsion technique and mechanical efficiency after 3 wk of practice. *Medicine & Science in Sports & Exercise, 34*(5).

DeGroot, K. K., Hollingsworth, H. H., Morgan, K. A., Morris, C. L., & Gray, D. B. (2009). The influence of verbal training and visual feedback on manual wheelchair propulsion. *Disabil Rehabil Assist Technol, 4*(2), 86-94. doi:10.1080/17483100802613685

DeJong, G., Tian, W., Hsieh, C. H., Junn, C., Karam, C., Ballard, P. H., . . . Backus, D. (2013). Rehospitalization in the first year of traumatic spinal cord injury after discharge from medical rehabilitation. *Arch Phys Med Rehabil, 94*(4 Suppl), S87-97. doi:10.1016/j.apmr.2012.10.037

Demirel, Ş., Demirel, G., Tükek, T., Erk, O., & Yilmaz, H. (2001). Risk factors for coronary heart disease in patients with spinal cord injury in Turkey. *Spinal Cord, 39*(3), 134-138. doi:10.1038/sj.sc.3101135

deRoon-Cassini, T. A., de St. Aubin, E., Valvano, A., Hastings, J., & Horn, P. (2009). Psychological well-being after spinal cord injury: Perception of loss and meaning making. *Rehabilitation Psychology, 54*(3), 306-314. doi:10.1037/a0016545

Devillard, X., Calmels, P., Sauvignet, B., Belli, A., Denis, C., Simard, C., & Gautheron, V. (2001). Validation of a new ergometer adapted to all types of manual wheelchair. *European Journal of Applied Physiology, 85*(5), 479-485. doi:10.1007/s004210100407

Diego, M. A., Field, T., Hernandez-Reif, M., Hart, S., Brucker, B., Field, T., & Burman, I. (2002). SPINAL CORD PATIENTS BENEFIT FROM MASSAGE THERAPY. *International Journal of Neuroscience, 112*(2), 133-142. doi:10.1080/00207450212023

DiGiovine, C. P., Cooper, R. A., & Boninger, M. L. (2001). Dynamic calibration of a wheelchair dynamometer. *J Rehabil Res Dev, 38*(1), 41-55.

Dyson-Hudson, T. A., Shiflett, S. C., Kirshblum, S. C., Bowen, J. E., & Druin, E. L. (2001). Acupuncture and trager psychophysical integration in the treatment of wheelchair user's shoulder pain in individuals with spinal cord injury. *Archives of Physical Medicine and Rehabilitation, 82*(8), 1038-1046. doi:https://doi.org/10.1053/apmr.2001.24888

El-Gohary, M., Holmstrom, L., Huisinga, J., King, E., McNames, J., & Horak, F. (2011, 30 Aug.-3 Sept. 2011). *Upper limb joint angle tracking with inertial sensors.* Paper presented at the 2011 Annual International Conference of the IEEE Engineering in Medicine and Biology Society.

Faupin, A., Gorce, P., & Thevenon, A. (2008). A wheelchair ergometer adaptable to the rear-wheel camber. *International Journal of Industrial Ergonomics, 38*(7), 601-607. doi:https://doi.org/10.1016/j.ergon.2008.01.008

Feghoul, A., Chenier, F., & Aissaoui, R. (2019). *Prédiction des forces et du moment de réaction sur la main courante lors de la propulsion manuelle en fauteuil roulant en utilisant des capteurs inertiels.* Paper presented at the 3e Quebec Congress in Adaptation-Rehabiliation Research, Montreal

Finley, M. A., & Rodgers, M. M. (2004). Prevalence and identification of shoulder pathology in athletic and nonathletic wheelchair users with shoulder pain: A pilot study. *J Rehabil Res Dev, 41*(3b), 395-402. doi:10.1682/jrrd.2003.02.0022

Fronczak, K. J., Boninger, M. L., Souza, A. L., & Cooper, R. A. (2003). *WHEELCHAIR PROPULSION BIOMECHANICS, WEIGHT, AND MEDIAN NERVE DAMAGE: A LONGITUDINAL STUDY*. Paper presented at the RESNA 26th International Annual Confence, Atlanta, Georgia.

Gellman, H., Chandler, D. R., Petrasek, J., Sie, I., Adkins, R., & Waters, R. L. (1988). Carpal tunnel syndrome in paraplegic patients. *The Journal of bone and joint surgery. American volume, 70*(4), 517-519.

Giavarina, D. (2015). Understanding Bland Altman analysis. *Biochemia medica, 25*(2), 141-151. doi:10.11613/BM.2015.015

Gutierrez, D. D., Thompson, L., Kemp, B., Mulroy, S. J., Physical Therapy Clinical Research, N., Rehabilitation, R., & Training Center on Aging-Related Changes in Impairment for Persons Living with Physical, D. (2007). The relationship of shoulder pain intensity to quality of life, physical activity, and community participation in persons with paraplegia. *The Journal of Spinal Cord Medicine, 30*(3), 251-255. doi:10.1080/10790268.2007.11753933

Harrison, C., Dall, P. M., Grant, M., Granat, M. H., Maver, T. W., & Conway, B. (2000). *Development of a wheelchair virtual reality platform for use in evaluating wheelchair access.* Paper presented at the Proceedings of the Third International Conference on Disability, Virtual Reality and Associated Technologies, Alghero, Sardinia, Italy.

Holden, M. K. (2005). Virtual environments for motor rehabilitation: review. *Cyberpsychol Behav, 8*(3), 187-211; discussion 212-189. doi:10.1089/cpb.2005.8.187

Hosseini, S. M., Oyster, M. L., Kirby, R. L., Harrington, A. L., & Boninger, M. L. (2012). Manual wheelchair skills capacity predicts quality of life and community integration in persons with spinal cord injury. *Arch Phys Med Rehabil, 93*(12), 2237-2243. doi:10.1016/j.apmr.2012.05.021

Hubscher, C. H., Herrity, A. N., Williams, C. S., Montgomery, L. R., Willhite, A. M., Angeli, C. A., & Harkema, S. J. (2018). Improvements in bladder, bowel and sexual outcomes following task-specific locomotor training in human spinal cord injury. *PLOS ONE, 13*(1), e0190998. doi:10.1371/journal.pone.0190998

Hui, Y., & Archambault, S. P. (2021). Augmented Feedback for Manual Wheelchair Propulsion Technique Training in a Virtual Reality Simulator. *Journal of NeuroEngineering and Rehabilitation*. doi:10.21203/rs.3.rs-86713/v1

Hurd, W. J., Morrow, M. M., Kaufman, K. R., & An, K.-N. (2008). Biomechanic Evaluation of Upper-Extremity Symmetry During Manual Wheelchair Propulsion Over Varied Terrain. *Archives of Physical Medicine and Rehabilitation, 89*(10), 1996-2002. doi:https://doi.org/10.1016/j.apmr.2008.03.020

Hutzler, Y., Vanlandewijck, Y., & Vlierberghe, M. V. (2000). Anaerobic Performance of Older Female and Male Wheelchair Basketball Players on a Mobile Wheelchair Ergometer %J Adapted Physical Activity Quarterly. *17*(4), 450. doi:10.1123/apaq.17.4.450

Inman, D. P., Loge, K., Cram, A., & Peterson, M. (2011). Learning to Drive a Wheelchair in Virtual Reality. *Journal of Special Education Technology, 26*(3), 21-34. doi:10.1177/016264341102600303

Jonas, W. B. (1998). Alternative medicine--learning from the past, examining the present, advancing to the future. *Jama, 280*(18), 1616-1618. doi:10.1001/jama.280.18.1616

Karinharju Kati, S. K., Boughey, A. M., Tweedy, S. M., Clanchy, K. M., & Trost, S. G. (2021). Validity of the Apple Watch® for monitoring push counts in people using manual wheelchairs. *Journal of Spinal Cord Medicine, The, 44*(2), 212-220.

Kaźmierczak, K., & Lisiński, P. (2018). Leisure time physical activity of people with chronic spinal cord injuries. *Clinical Neurology and Neurosurgery, 170*, 7-12. doi:https://doi.org/10.1016/j.clineuro.2018.04.013

Kemp, B. J., Bateham, A. L., Mulroy, S. J., Thompson, L., Adkins, R. H., & Kahan, J. S. (2011). Effects of reduction in shoulder pain on quality of life and community activities among people living long-term with SCI paraplegia: a randomized control trial. *The journal of spinal cord medicine, 34*(3), 278-284. doi:10.1179/107902611X12972448729486

Khazaeipour, Z., Norouzi-Javidan, A., Kaveh, M., Khanzadeh Mehrabani, F., Kazazi, E., & Emami-Razavi, S.-H. (2014). Psychosocial outcomes following spinal cord injury in Iran. *The Journal of Spinal Cord Medicine, 37*(3), 338-345. doi:10.1179/2045772313Y.0000000174

Kirshblum, S. C., Burns, S. P., Biering-Sorensen, F., Donovan, W., Graves, D. E., Jha, A., . . . Waring, W. (2011). International standards for neurological classification of spinal cord injury (revised 2011). *The Journal of Spinal Cord Medicine, 34*(6), 535-546. doi:10.1179/204577211X13207446293695

Klerk, R. d., Vegter, R. J. K., Goosey-Tolfrey, V. L., Mason, B. S., Lenton, J. P., Veeger, D. H. E. J., & Woude, L. H. V. v. d. (2020). Measuring Handrim Wheelchair Propulsion in the Lab: A Critical Analysis of Stationary Ergometers. *IEEE Rev Biomed Eng, 13*, 199-211. doi:10.1109/RBME.2019.2942763

Klerk, R. d., Vegter, R. J. K., Veeger, H. E. J., & Woude, L. H. V. v. d. (2020). Technical Note: A Novel Servo-Driven Dual-Roller Handrim Wheelchair Ergometer. *IEEE Transactions on Neural Systems and Rehabilitation Engineering, 28*(4), 953-960. doi:10.1109/TNSRE.2020.2965281

Krause, J. S., & Saunders, L. L. (2011). Health, secondary conditions, and life expectancy after spinal cord injury. *Arch Phys Med Rehabil, 92*(11), 1770-1775. doi:10.1016/j.apmr.2011.05.024

Kurt, M., Geyik, H., Mutlu, B., Tatar, Y., & Nart, E. J. A. M. e. A. (2008). Design, prototype and experimental evaluation of a wheelchair treadmill. *2*, 71-75.

Kwarciak, A. M., Turner, J. T., Guo, L., & Richter, W. M. (2011). Comparing handrim biomechanics for treadmill and overground wheelchair propulsion. *Spinal Cord, 49*(3), 457-462. doi:10.1038/sc.2010.149

Kwarciak, A. M., Turner, J. T., Guo, L., & Richter, W. M. (2012). The effects of four different stroke patterns on manual wheelchair propulsion and upper limb muscle strain. *Disabil Rehabil Assist Technol, 7*(6), 459-463. doi:10.3109/17483107.2011.650781

Lai, Y.-J., Lin, C.-L., Chang, Y.-J., Lin, M.-C., Lee, S.-T., Sung, F.-C., . . . Kao, C.-H. (2014). Spinal cord injury increases the risk of Type 2 diabetes: a population-based cohort study. *The Spine Journal, 14*(9), 1957-1964. doi:https://doi.org/10.1016/j.spinee.2013.12.011

Mahajan, H. P., Dicianno, B. E., Cooper, R. A., & Ding, D. (2013). Assessment of wheelchair driving performance in a virtual reality-based simulator. *The journal of spinal cord medicine, 36*(4), 322-332. doi:10.1179/2045772313y.0000000130

Marino, R. J., Barros, T., Biering-Sorensen, F., Burns, S. P., Donovan, W. H., Graves, D. E., . . . Priebe, M. (2003). International Standards For Neurological Classification Of Spinal Cord Injury. *The Journal of Spinal Cord Medicine, 26*(sup1), S50-S56. doi:10.1080/10790268.2003.11754575

Meyers, A. R., Anderson, J. J., Miller, D. R., Shipp, K., & Hoenig, H. (2002). Barriers, facilitators, and access for wheelchair users: substantive and methodologic lessons from a pilot study of environmental effects. *Soc Sci Med, 55*(8), 1435-1446. doi:10.1016/s0277-9536(01)00269-6

Morrow, M. M., Hurd, W. J., Kaufman, K. R., & An, K. N. (2010). Shoulder demands in manual wheelchair users across a spectrum of activities. *J Electromyogr Kinesiol, 20*(1), 61-67. doi:10.1016/j.jelekin.2009.02.001

Murray, R. F., Asghari, A., Egorov, D. D., Rutkowski, S. B., Siddall, P. J., Soden, R. J., & Ruff, R. (2007). Impact of spinal cord injury on self-perceived pre- and postmorbid cognitive, emotional and physical functioning. *Spinal Cord, 45*(6), 429-436. doi:10.1038/sj.sc.3102022

Myers, J., Lee, M., & Kiratli, J. (2007). Cardiovascular disease in spinal cord injury: an overview of prevalence, risk, evaluation, and management. *Am J Phys Med Rehabil, 86*(2), 142-152. doi:10.1097/PHM.0b013e31802f0247

Nichols, P. J., Norman, P. A., & Ennis, J. R. (1979). Wheelchair user's shoulder? Shoulder pain in patients with spinal cord lesions. *Scand J Rehabil Med, 11*(1), 29-32.

Niesing, R., Eijskoot, F., Kranse, R., den Ouden, A. H., Storm, J., Veeger, H. E. J., . . . Snijders, C. J. (1990). Computer-controlled wheelchair ergometer. *Medical and Biological Engineering and Computing, 28*(4), 329-338. doi:10.1007/BF02446151

Niesing, R. R., Eijskoot, F., Kranse, R., Denouden, A. H., & Storm, J. (1990). Computer-controlled wheelchair ergometer. *Medical and Biological Engineering and Computing, 28*(4), 329-338.

NIH Consensus Conference. Acupuncture. (1998). *JAMA, 280*(17), 1518-1524.

Niniss, H., & Inoue, T. (2006). Assessment of driving skills using Virtual Reality: Comparative survey on experts and unskilled users of electric wheelchairs. *Technology and Disability, 18*, 217-226. doi:10.3233/TAD-2006-18409

Noonan, V. K., Fingas, M., Farry, A., Baxter, D., Singh, A., Fehlings, M. G., & Dvorak, M. F. (2012). Incidence and Prevalence of Spinal Cord Injury in Canada: A National Perspective. *Neuroepidemiology, 38*(4), 219-226. doi:10.1159/000336014

O'Connor, T. J., Cooper, R. A., Fitzgerald, S. G., Dvorznak, M. J., Boninger, M. L., VanSickle, D. P., & Glass, L. (2000). Evaluation of a manual wheelchair interface to computer games. *Neurorehabil Neural Repair, 14*(1), 21-31. doi:10.1177/154596830001400103

O'Connor, T. J., Fitzgerald, S. G., Cooper, R. A., Thorman, T. A., & Boninger, M. L. (2001). Does computer game play aid in motivation of exercise and increase metabolic activity during wheelchair ergometry? *Med Eng Phys, 23*(4), 267-273. doi:10.1016/s1350-4533(01)00046-7

Ojeda, M., & Ding, D. (2014). Temporal parameters estimation for wheelchair propulsion using wearable sensors. *BioMed research international, 2014*, 645284-645284. doi:10.1155/2014/645284

Paralyzed Veterans of America Consortium for Spinal Cord, M. (2005). Preservation of upper limb function following spinal cord injury: a clinical practice guideline for health-care professionals. *The journal of spinal cord medicine, 28*(5), 434-470. doi:10.1080/10790268.2005.11753844

Pellegrini, N., Guillon, B., Prigent, H., Pellegrini, M., Orlikovski, D., Raphael, J. C., & Lofaso, F. (2004). Optimization of power wheelchair control for patients with severe Duchenne muscular dystrophy. *Neuromuscul Disord, 14*(5), 297-300. doi:10.1016/j.nmd.2004.02.005

Pithon, T., Weiss, T., Richir, S., & Klinger, E. (2009). Wheelchair simulators: A review. *Technology and Disability, 21*, 1-10. doi:10.3233/TAD-2009-0268

Popowitz, R. L., Zvijac, J. E., Uribe, J. W., Hechtman, K. S., Schürhoff, M. R., & Green, J. B. (2003). Rotator cuff repair in spinal cord injury patients. *Journal of Shoulder and Elbow Surgery, 12*(4), 327-332. doi:https://doi.org/10.1016/S1058-2746(03)00035-1

Post, M. W. M., Bloemen, J., & de Witte, L. P. (2005). Burden of support for partners of persons with spinal cord injuries. *Spinal Cord, 43*(5), 311-319. doi:10.1038/sj.sc.3101704

Post, M. W. M., van Asbeck, F. W. A., van Dijk, A. J., & Schrijvers, A. J. P. (1997). Services for spinal cord injured: availability and satisfaction. *Spinal Cord, 35*(2), 109-115. doi:10.1038/sj.sc.3100362

Putzke, J. D., Richards, J. S., Hicken, B. L., & DeVivo, M. J. (2002). Interference due to pain following spinal cord injury: important predictors and impact on quality of life. *Pain, 100*(3), 231-242. doi:https://doi.org/10.1016/S0304-3959(02)00069-6

Requejo, P. S., Mulroy, S. J., Ruparel, P., Hatchett, P. E., Haubert, L. L., Eberly, V. J., & Gronley, J. K. (2015). Relationship Between Hand Contact Angle and Shoulder Loading During Manual Wheelchair Propulsion by Individuals with Paraplegia. *Top Spinal Cord Inj Rehabil, 21*(4), 313-324. doi:10.1310/sci2104-313

Reyes, M. L., Gronley, J. K., Newsam, C. J., Mulroy, S. J., & Perry, J. (1995). Electromyographic analysis of shoulder muscles of men with low-level paraplegia during a weight relief raise. *Archives of Physical Medicine and Rehabilitation, 76*(5), 433-439. doi:https://doi.org/10.1016/S0003-9993(95)80572-9

Rice, Gagnon, Gallagher, & Boninger. (2010). Hand rim wheelchair propulsion training using biomechanical real-time visual feedback based on motor learning theory principles. *The journal of spinal cord medicine, 33*(1), 33-42. doi:10.1080/10790268.2010.11689672

Richardson, A., Samaranayaka, A., Sullivan, M., & Derrett, S. (2019). Secondary health conditions and disability among people with spinal cord injury: A prospective cohort study. *The Journal of Spinal Cord Medicine*, 1-10. doi:10.1080/10790268.2019.1581392

Richter, W., Rodriguez, R., Woods, K., & Axelson, P. (2007). Stroke Pattern and Handrim Biomechanics for Level and Uphill Wheelchair Propulsion at Self-Selected Speeds. *Archives of Physical Medicine and Rehabilitation, 88*, 81-87. doi:10.1016/j.apmr.2006.09.017

Riggins, M. S., Kankipati, P., Oyster, M. L., Cooper, R. A., & Boninger, M. L. (2011). The Relationship Between Quality of Life and Change in Mobility 1 Year Postinjury in Individuals With Spinal Cord Injury. *Archives of Physical Medicine and Rehabilitation, 92*(7), 1027-1033. doi:10.1016/j.apmr.2011.02.010

Robertson, R. N., Boninger, M. L., Cooper, R. A., & Shimada, S. D. (1996). Pushrim forces and joint kinetics during wheelchair propulsion. *Arch Phys Med Rehabil, 77*(9), 856-864.

Sachdeva, R., Gao, F., Chan, C. C. H., & Krassioukov, A. V. (2018). Cognitive function after spinal cord injury. *A systematic review, 91*(13), 611-621. doi:10.1212/wnl.0000000000006244

Salminen, A. L., Brandt, A., Samuelsson, K., Toytari, O., & Malmivaara, A. (2009). Mobility devices to promote activity and participation: a systematic review. *J Rehabil Med, 41*(9), 697-706. doi:10.2340/16501977-0427

Samuelsson, Tropp, H., & Gerdle, B. (2004). Shoulder pain and its consequences in paraplegic spinal cord-injured, wheelchair users. *Spinal Cord, 42*(1), 41-46. doi:10.1038/sj.sc.3101490

Samuelsson, & Wressle, E. (2008). User satisfaction with mobility assistive devices: an important element in the rehabilitation process. *Disabil Rehabil, 30*(7), 551-558. doi:10.1080/09638280701355777

Sanderson, D. J., & Sommer, H. J. (1985). Kinematic features of wheelchair propulsion. *Journal of Biomechanics, 18*(6), 423-429. doi:https://doi.org/10.1016/0021-9290(85)90277-5

Sawyers, T. (2018, september 13, 2018). Understanding the normal shoulder range of motion.

Schultheis, M., & Rizzo, A. (2001). The application of virtual reality technology in rehabilitation. *Rehabilitation Psychology, 46*, 296-311. doi:10.1037/0090-5550.46.3.296

Sie, I. H., Waters, R. L., Adkins, R. H., & Gellman, H. (1992). Upper extremity pain in the postrehabilitation spinal cord injured patient. *Arch Phys Med Rehabil, 73*(1), 44-48.

Slater, M., & Sanchez-Vives, M. V. (2016). Enhancing Our Lives with Immersive Virtual Reality. *Frontiers in Robotics and AI*.

Smith, E. M., Sakakibara, B. M., & Miller, W. C. (2016). A review of factors influencing participation in social and community activities for wheelchair users. *Disabil Rehabil Assist Technol, 11*(5), 361-374. doi:10.3109/17483107.2014.989420

Spinal cord injury. (2013, 13 Noveber 2013).

Stewart, M. W., Melton-Rogers, S. L., Morrison, S., & Figoni, S. F. (2000). The measurement properties of fitness measures and health status for persons with spinal cord injuries. *Archives of Physical Medicine and Rehabilitation, 81*(4), 394-400. doi:https://doi.org/10.1053/mr.2000.4417

Subbarao, J. V., Klopfstein, J., & Turpin, R. (1995). Prevalence and Impact of Wrist and Shoulder Pain in Patients with Spinal Cord Injury. *The Journal of Spinal Cord Medicine, 18*(1), 9-13. doi:10.1080/10790268.1995.11719374

Totosy de Zepetnek, J. O., Pelletier, C. A., Hicks, A. L., & MacDonald, M. J. (2015). Following the Physical Activity Guidelines for Adults With Spinal Cord Injury for 16 Weeks Does Not Improve Vascular Health: A Randomized Controlled Trial. *Archives of Physical Medicine and Rehabilitation, 96*(9), 1566-1575. doi:https://doi.org/10.1016/j.apmr.2015.05.019

Tun, C. G., & Upton, J. (1988). The paraplegic hand: electrodiagnostic studies and clinical findings. *J Hand Surg Am, 13*(5), 716-719. doi:10.1016/s0363-5023(88)80132-1

Westgren, N., & Levi, R. (1998). Quality of life and traumatic spinal cord injury. *Archives of Physical Medicine and Rehabilitation, 79*(11), 1433-1439. doi:https://doi.org/10.1016/S0003-9993(98)90240-4

Witmer, B. G., & Singer, M. J. (1998). Measuring presence in virtual environments: A presence questionnaire. *Presence: Teleoperators and Virtual Environments, 7*(3), 225-240. doi:10.1162/105474698565686

Yomtov, B., Derman, R. M., Cochran, G. V. B., & Brunski, J. (1978). A WHEELCHAIR ERGOMETER ADAPTABLE TO VARIOUS WHEELCHAIRS. In D. Jaron (Ed.), *Proceedings of the Sixth New England Bioengineering Conference* (pp. 97-99): Pergamon.

Zheng, J. M., Chan, K. W., & Gibson, I. (1998). Virtual reality. *IEEE Potentials, 17*(2), 20-23. doi:10.1109/45.666641

# Appendix

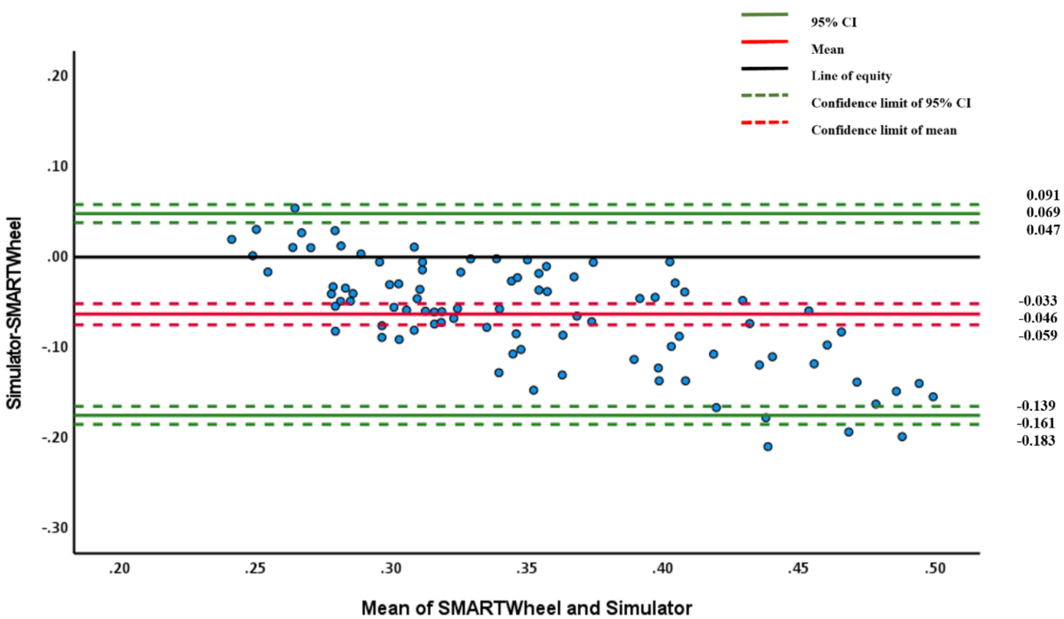


Figure: BA plot to assess accuracy of push time (sec) of arching pattern

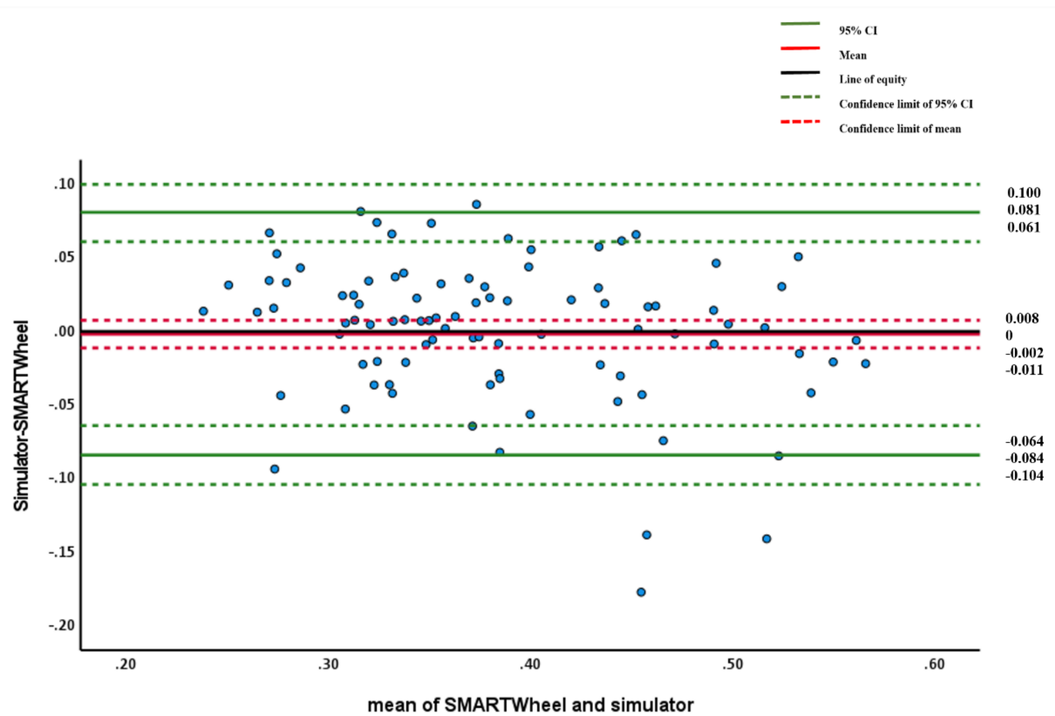


Figure: BA plot to assess accuracy of calibrated push time (sec) of arching pattern

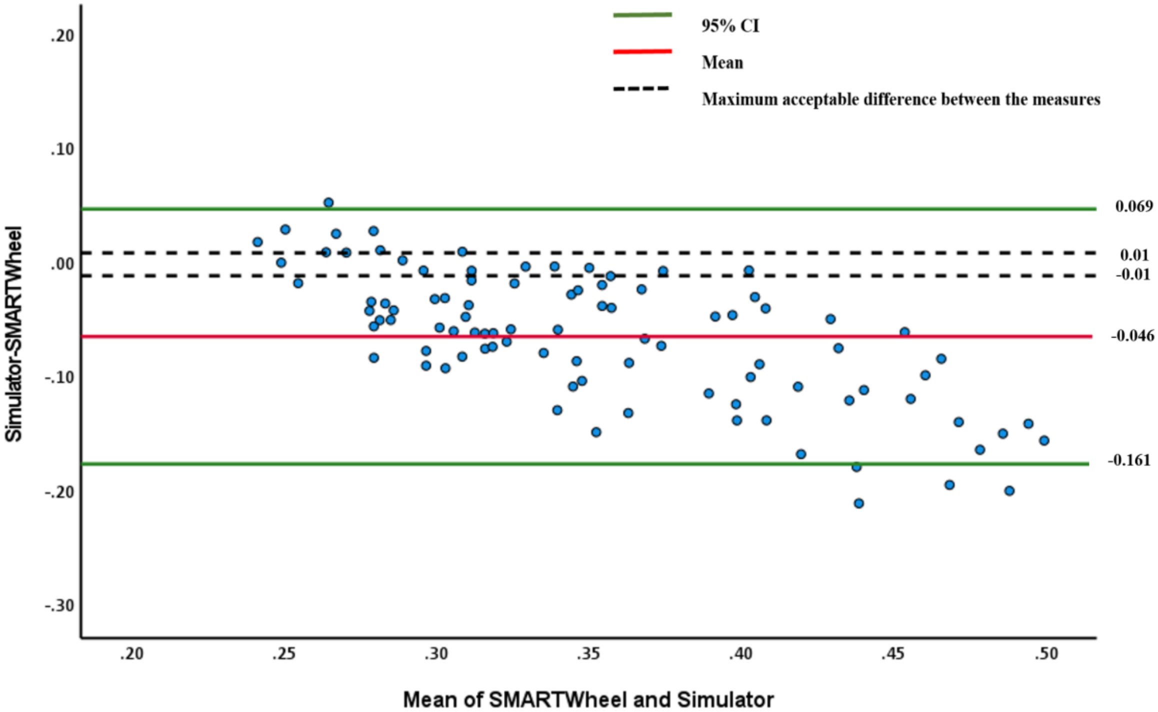


Figure: BA plot to assess precision of push time (sec) of arching pattern

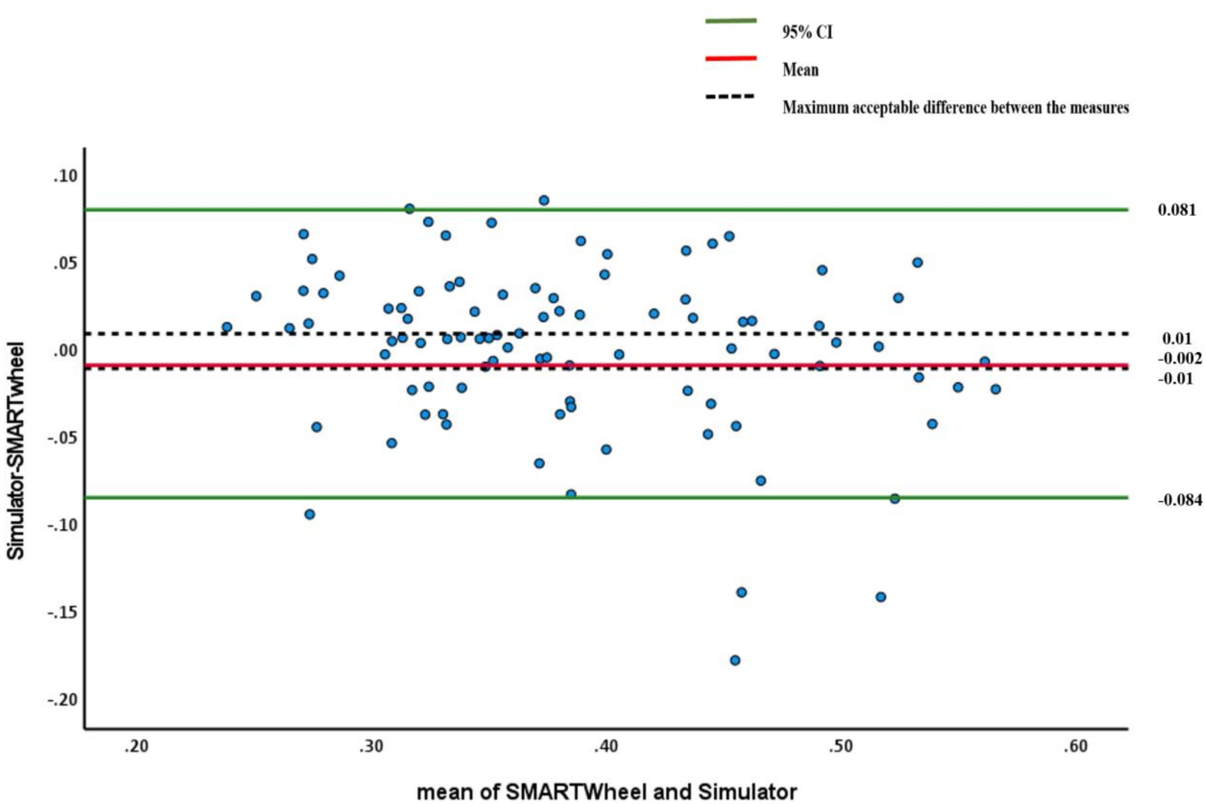


Figure: BA plot to assess precision of calibrated push time (sec) of arching pattern

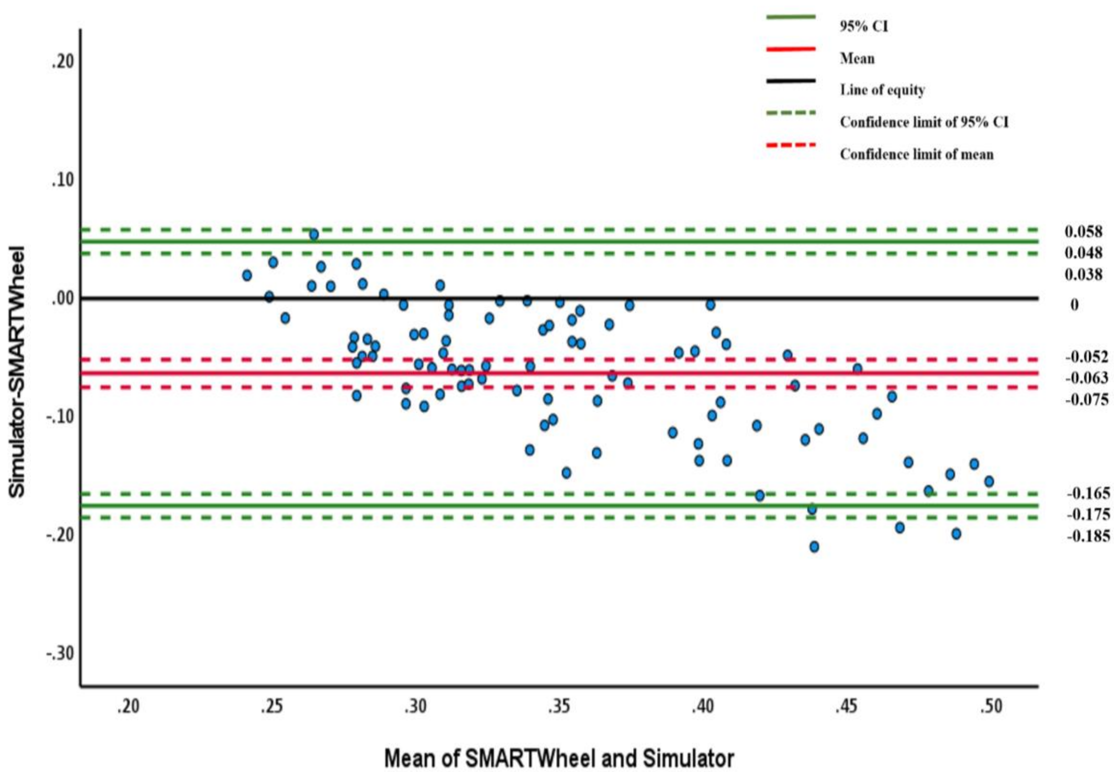


Figure: BA plot to assess accuracy of push time (sec) of semicircular pattern

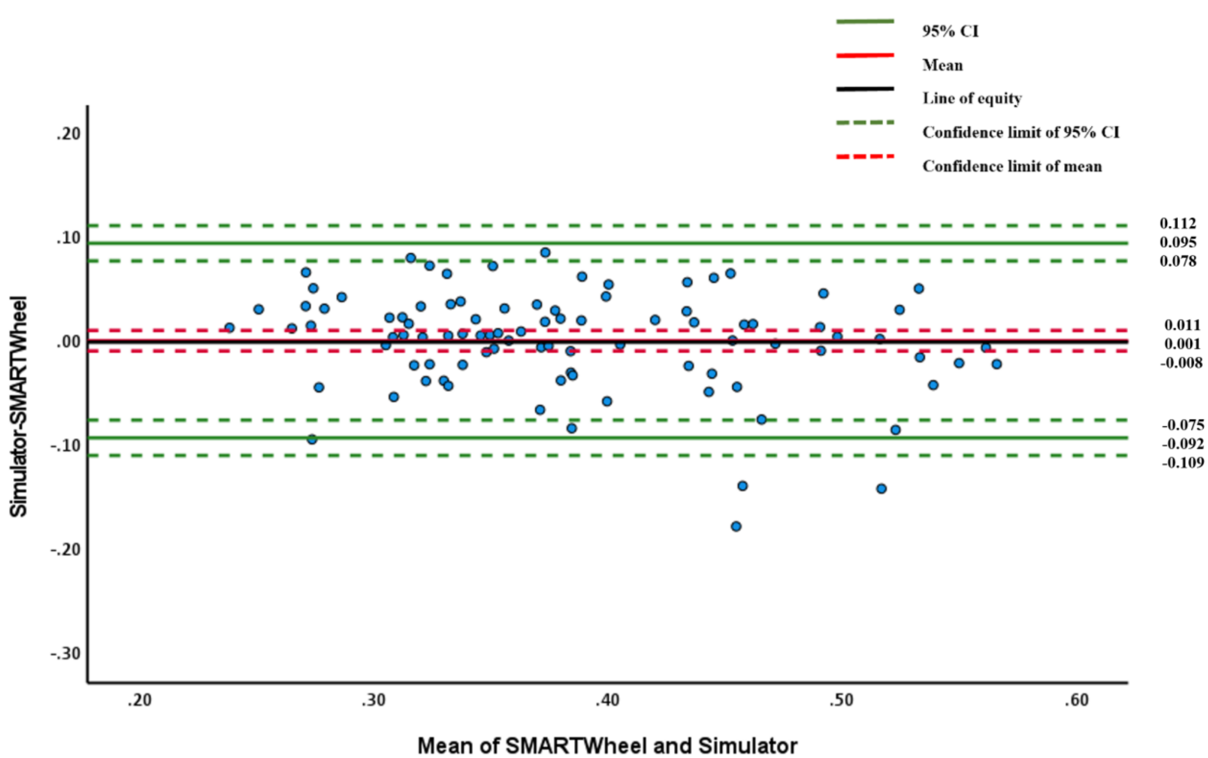


Figure: BA plot to assess accuracy of calibrated push time (sec) of semicircular pattern

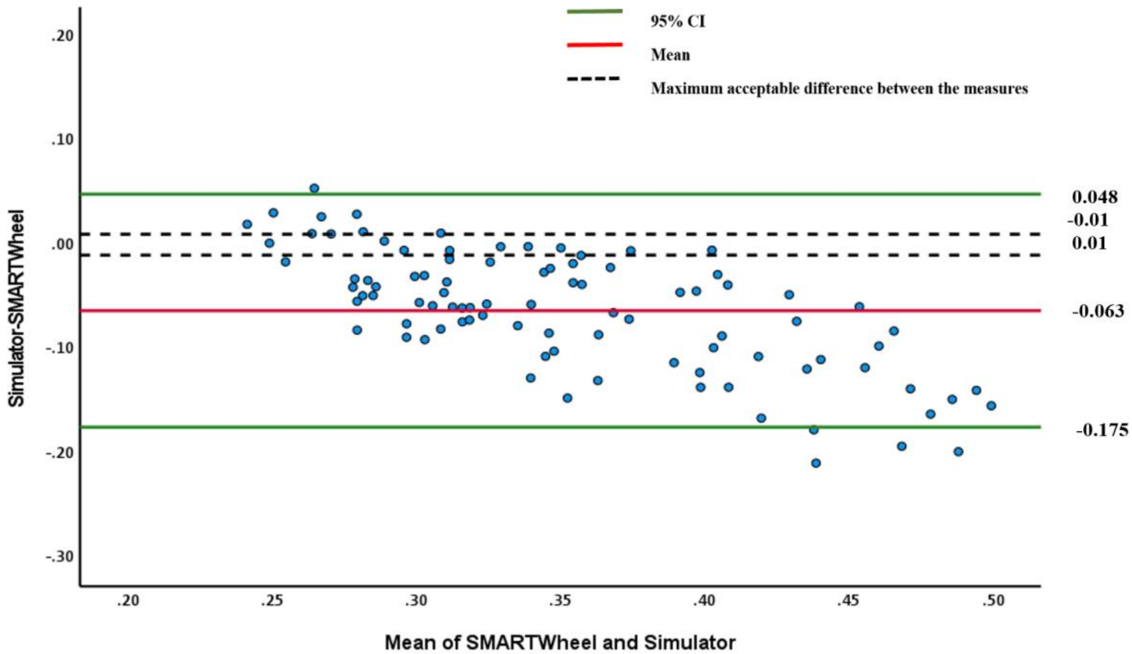


Figure: BA plot to assess precision of push time (sec) of semicircular pattern

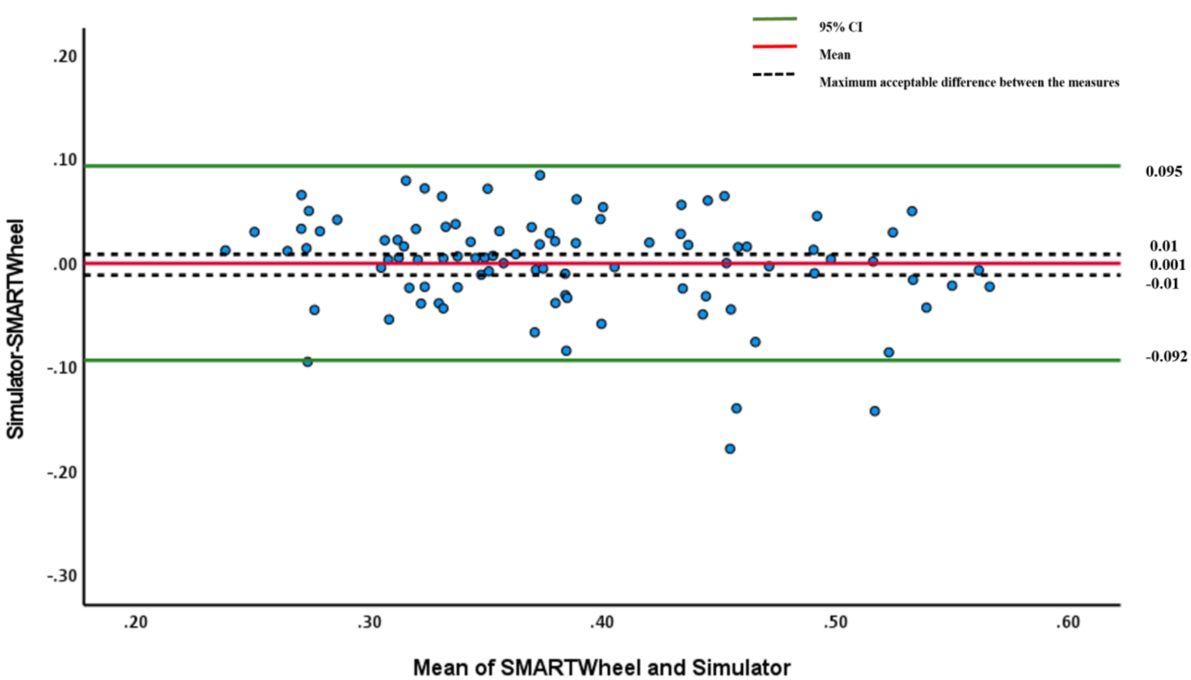


Figure: BA plot to assess precision of calibrated push time (sec) of semicircular pattern

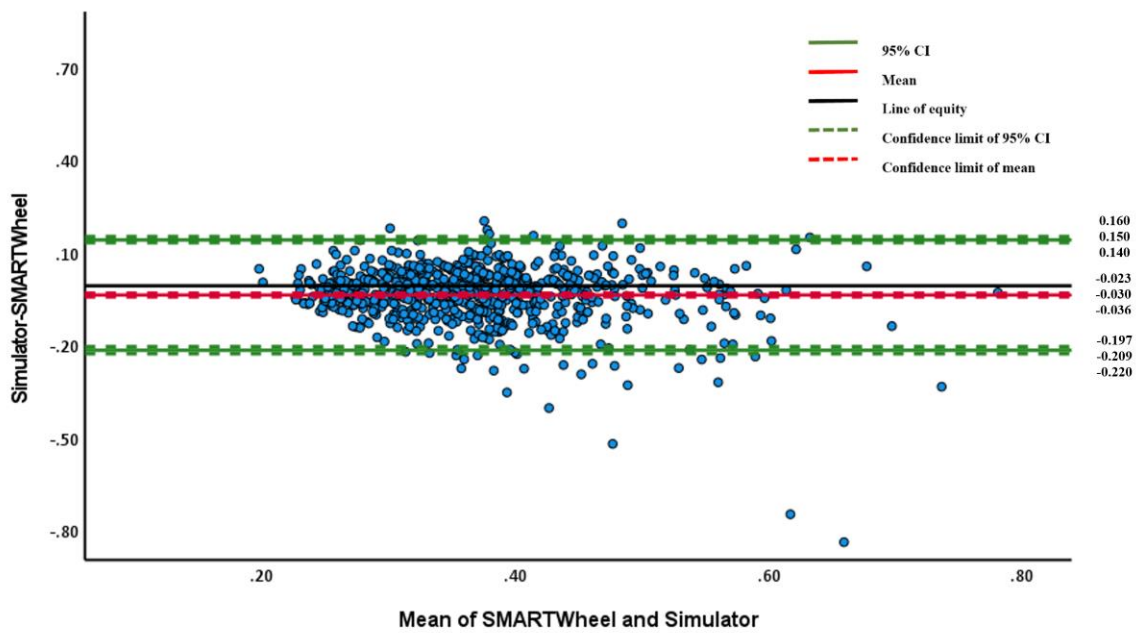


Figure: BA plot to assess accuracy of push time (sec) for ecological scenario

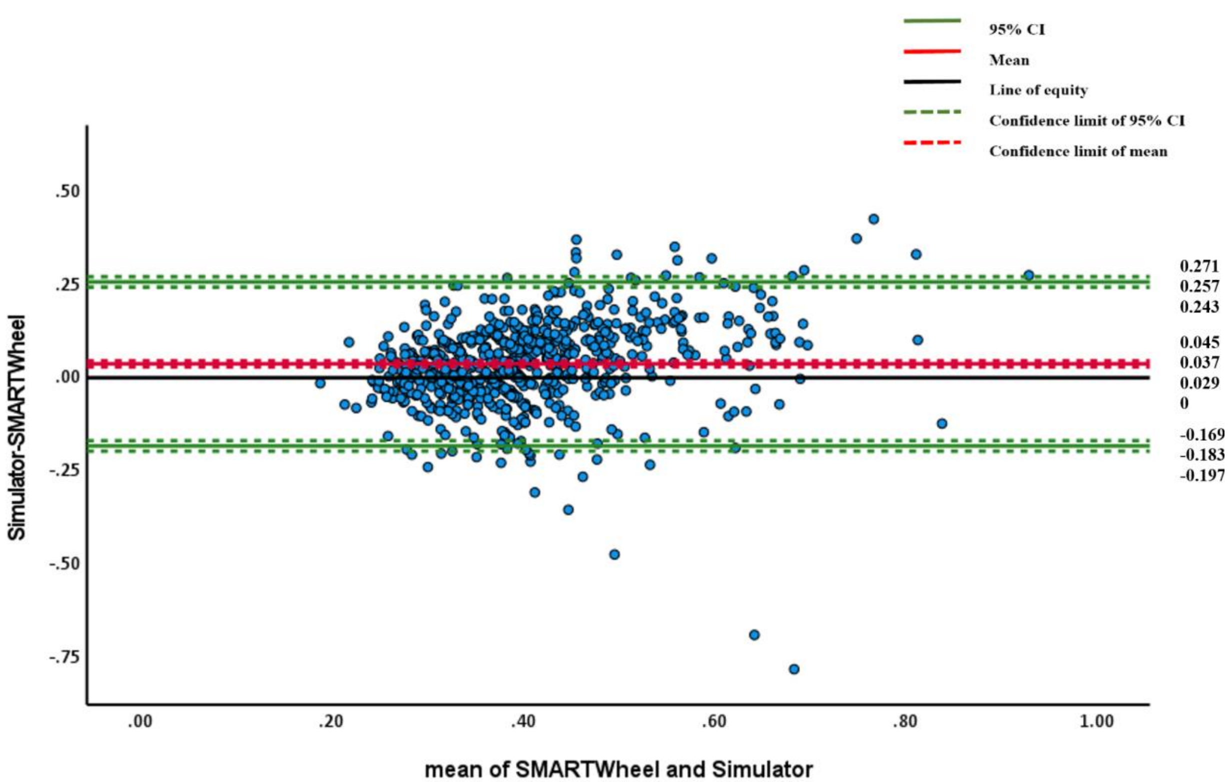


Figure: BA plot to assess accuracy of calibrated push time (sec) for ecological scenario

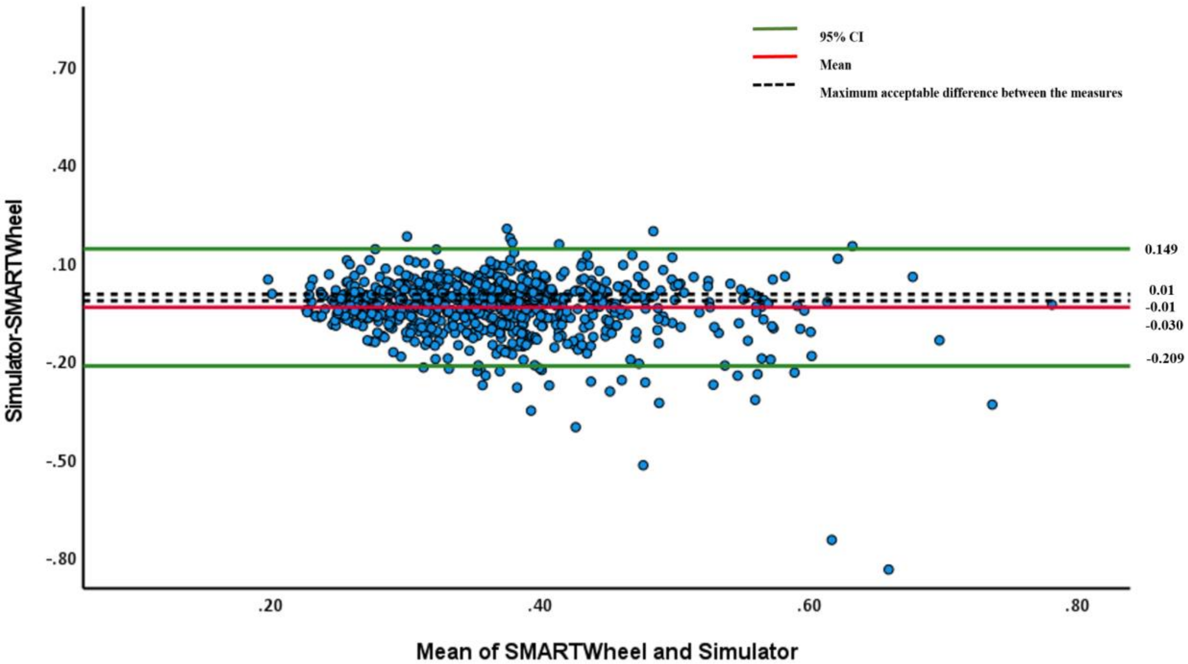


Figure: BA plot to assess precision of push time (sec) for ecological scenario

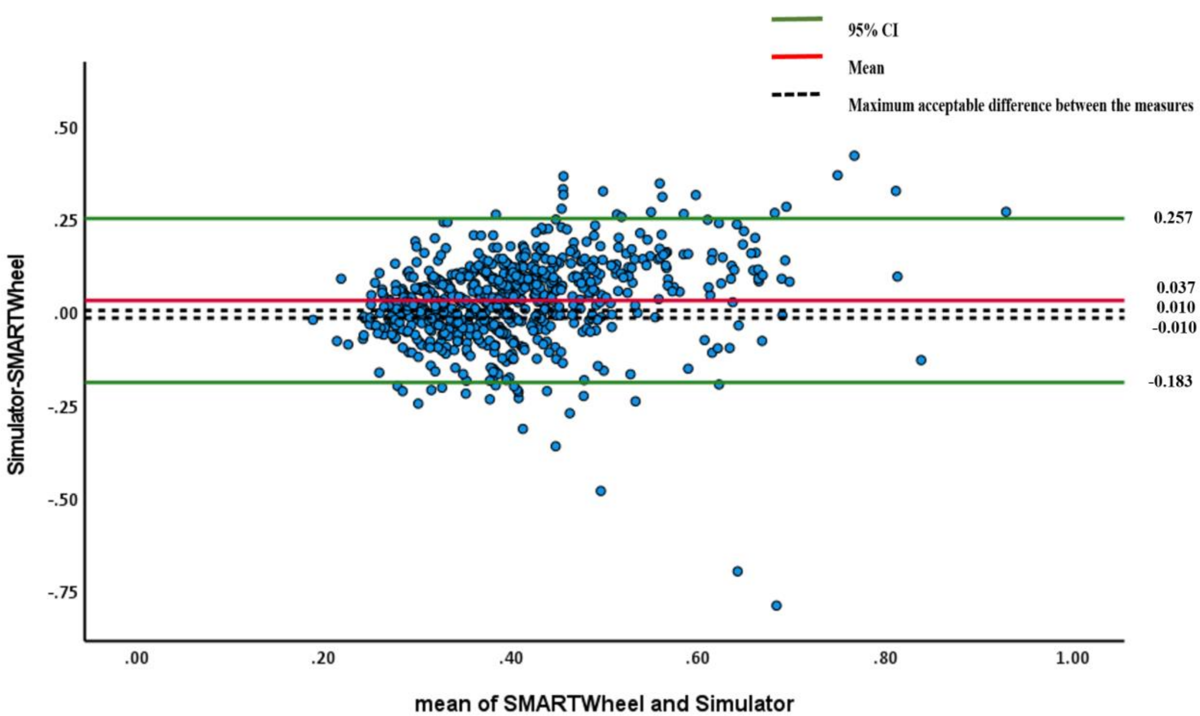


Figure: BA plot to assess precision of calibrated push time (sec) for ecological scenario

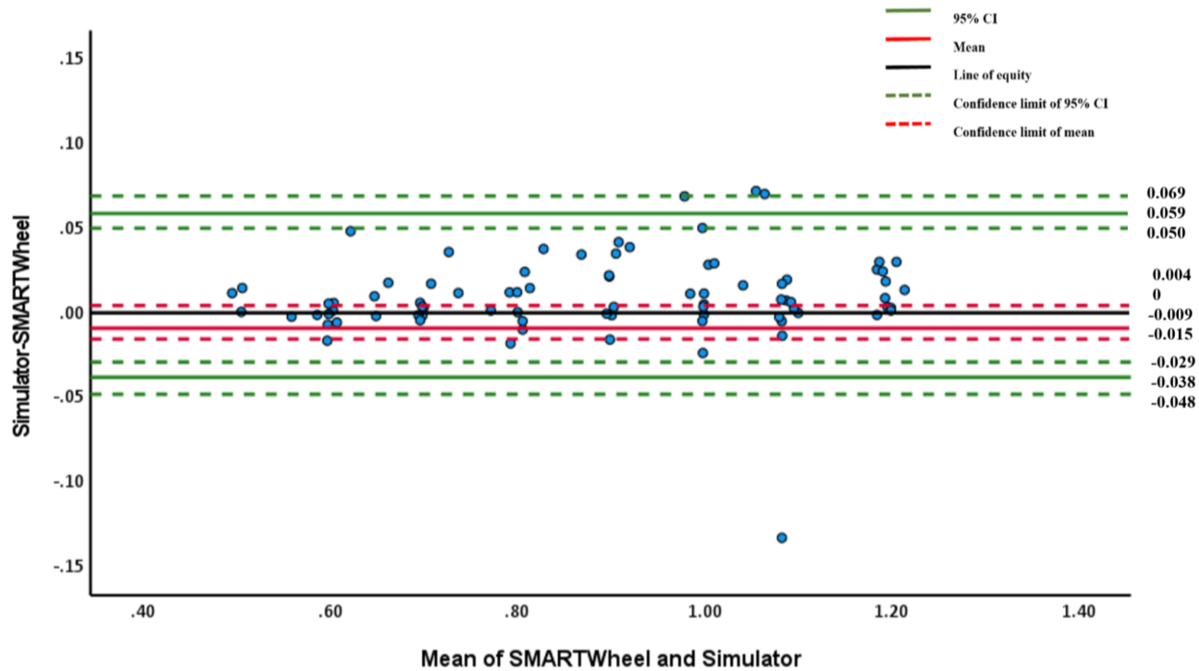


Figure: BA plot to assess accuracy of cycle time (sec) of arching pattern

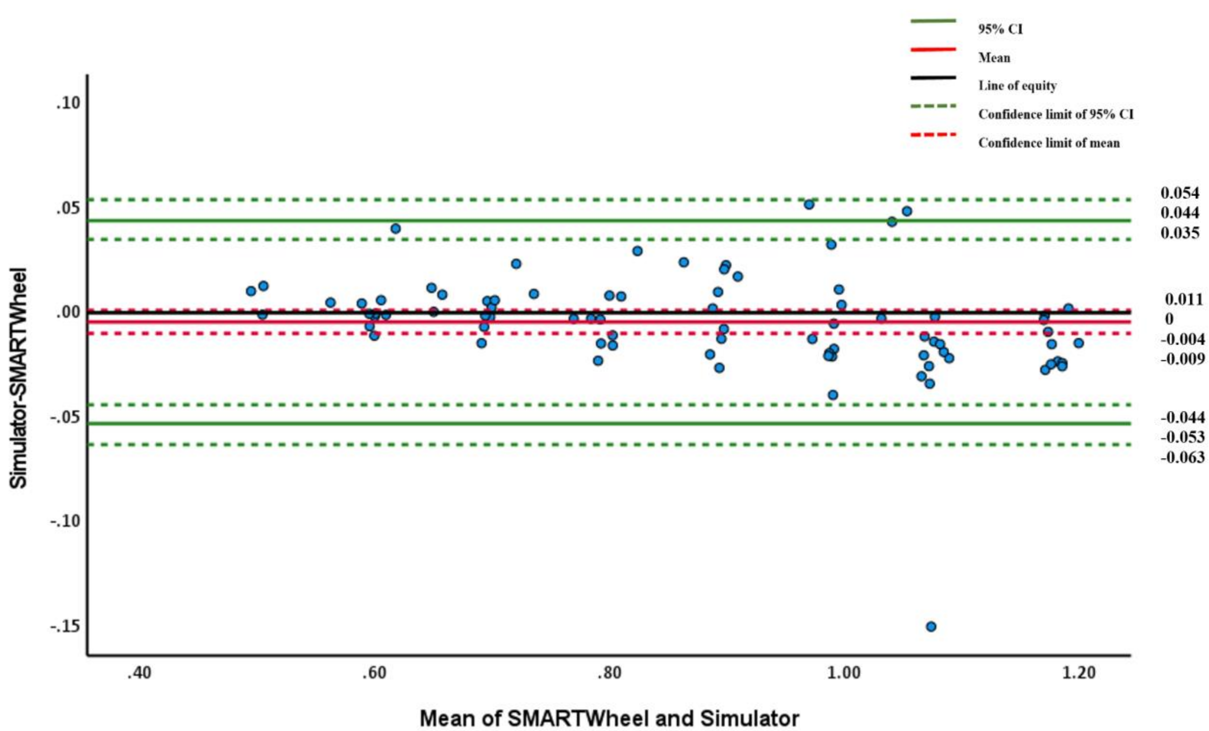


Figure: BA plot to assess accuracy of calibrated cycle time (sec) of arching pattern

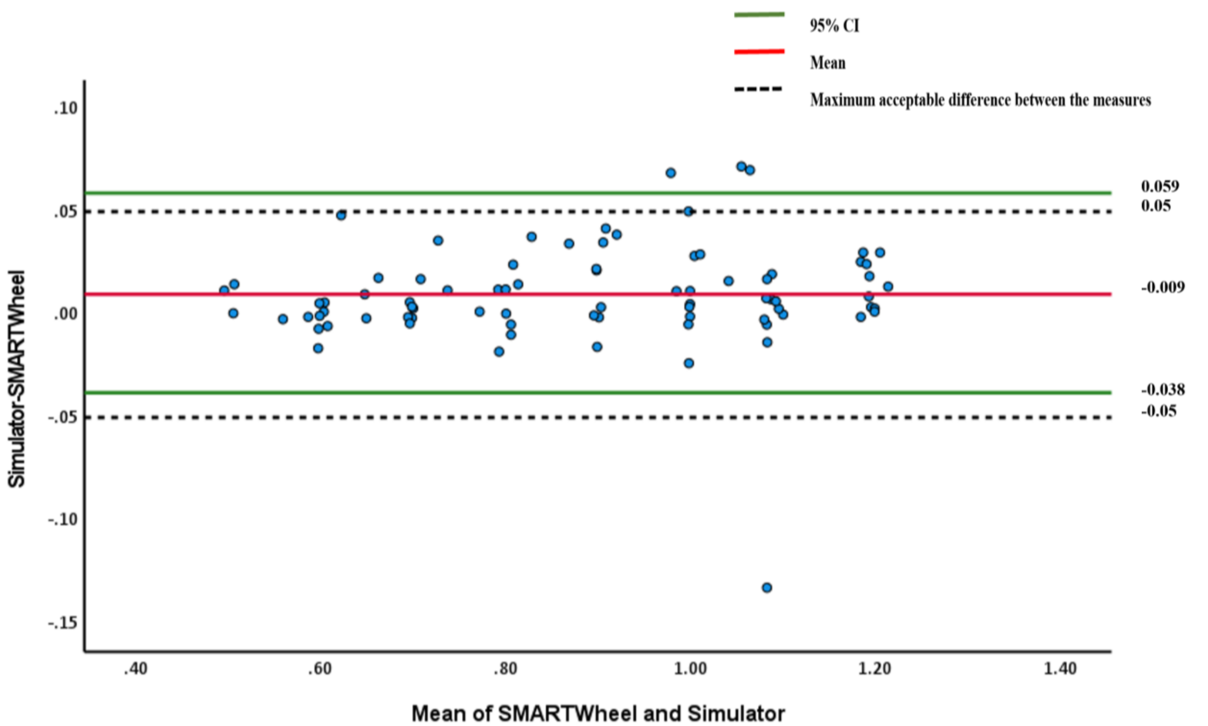


Figure: BA plot to assess precision of cycle time (sec) of arching pattern

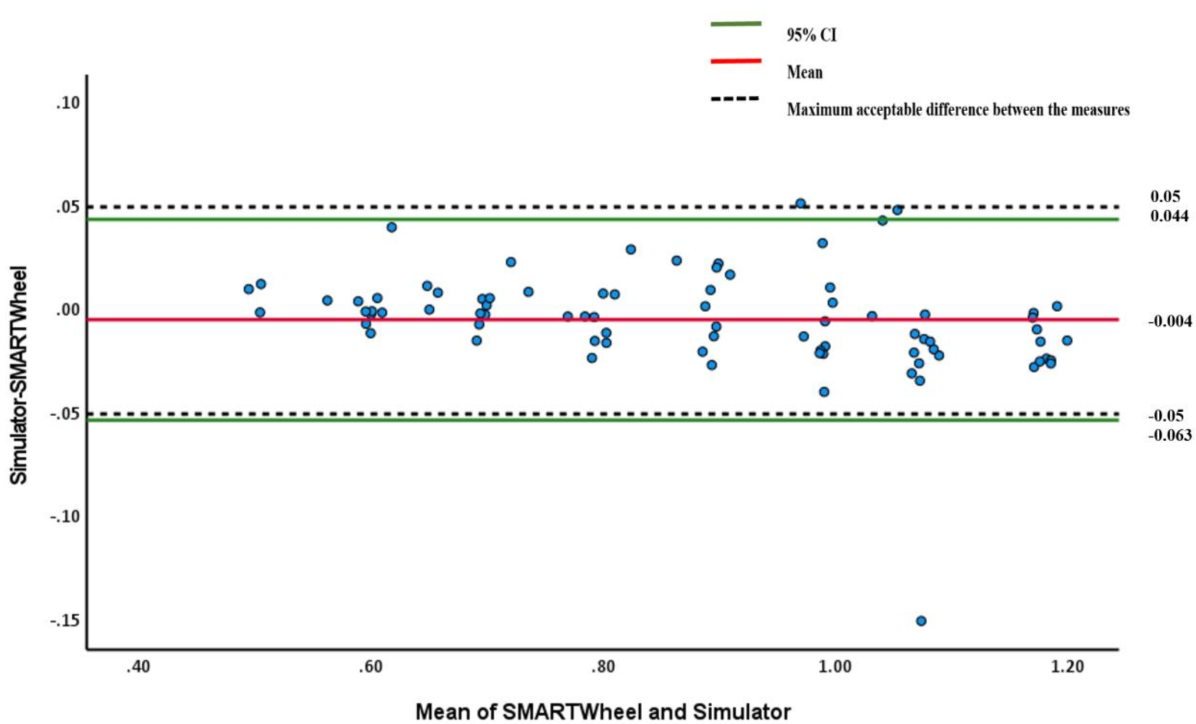


Figure: BA plot to assess precision of calibrated cycle time (sec) of arching pattern

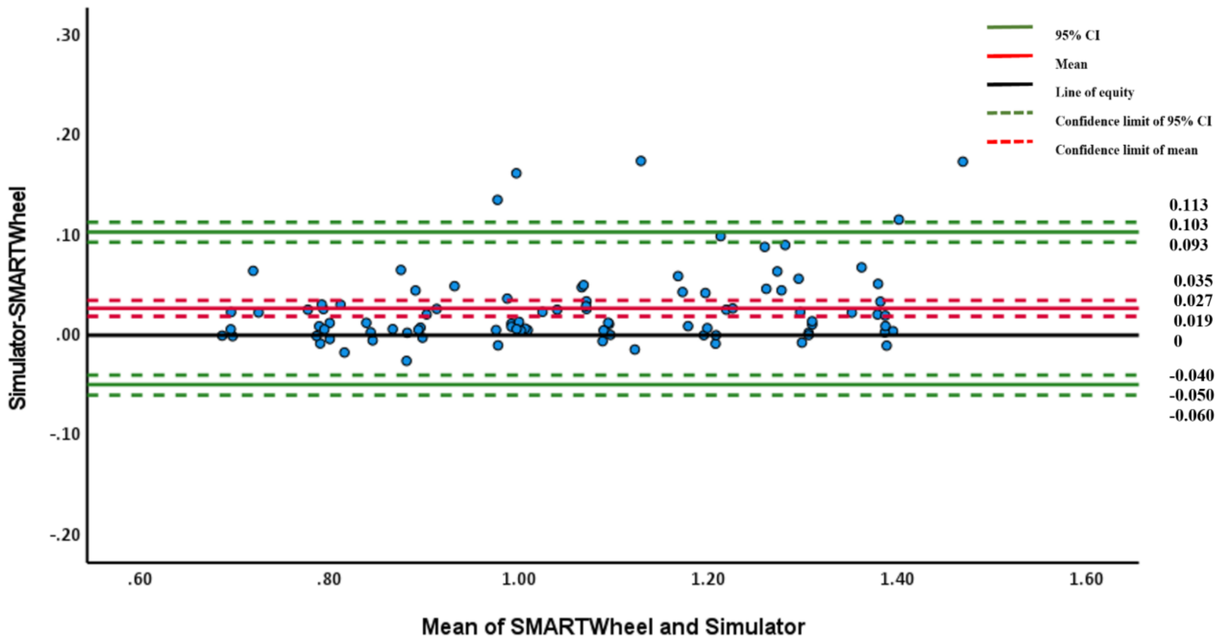


Figure: BA plot to assess accuracy of cycle time (sec) of semicircular pattern

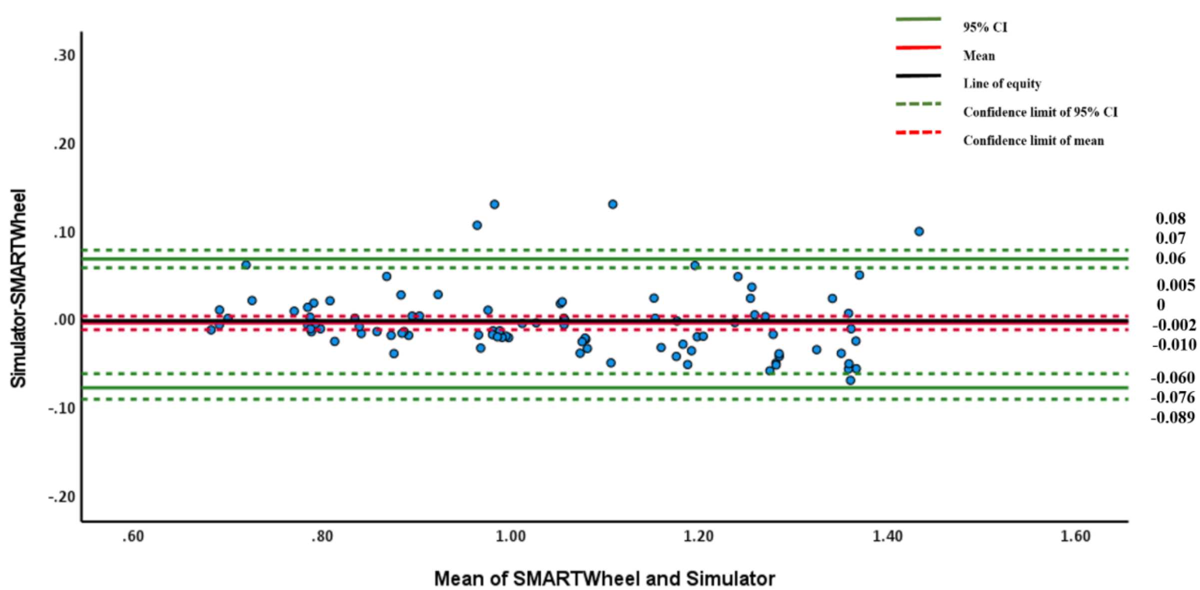


Figure: BA plot to assess accuracy calibrated of cycle time (sec) of semicircular pattern

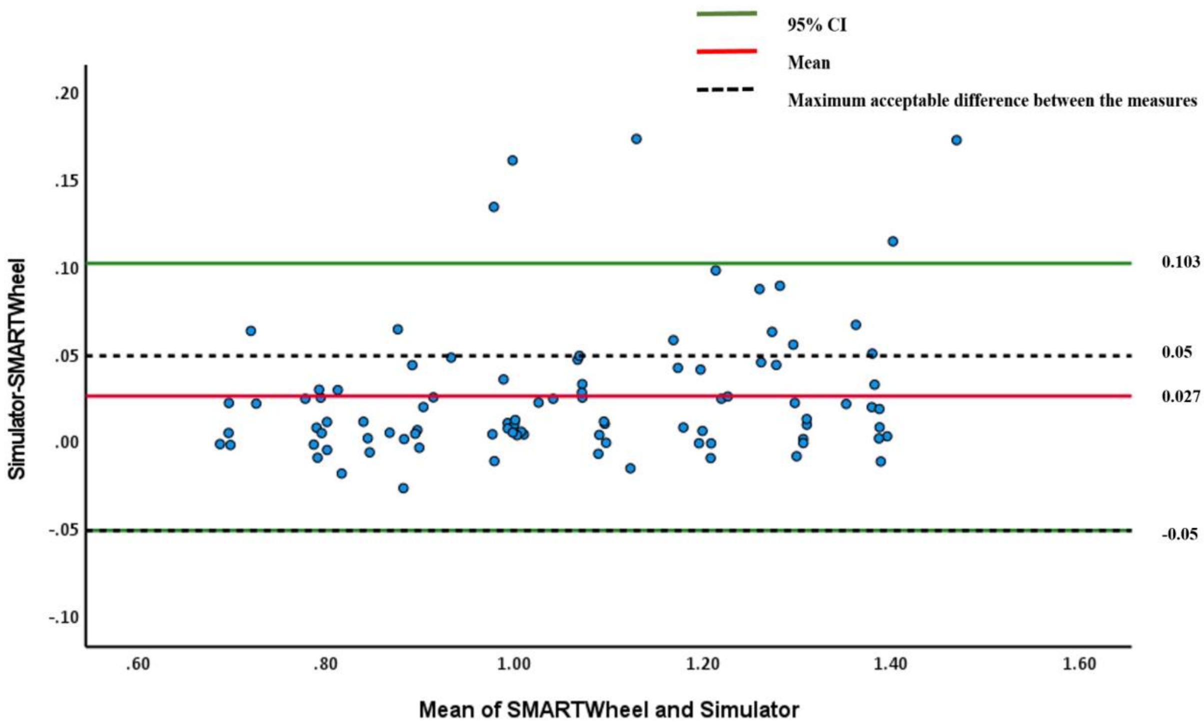


Figure: BA plot to assess precision of cycle time (sec) of semicircular pattern

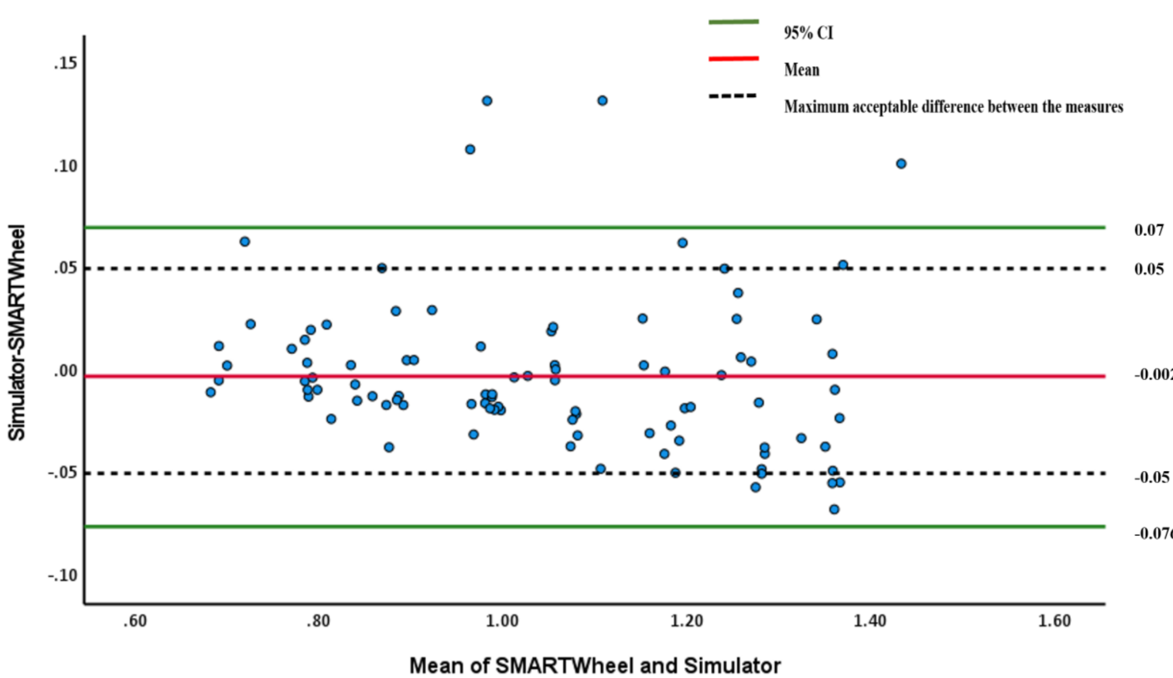


Figure: BA plot to assess precision of calibrated cycle time (sec) of semicircular pattern

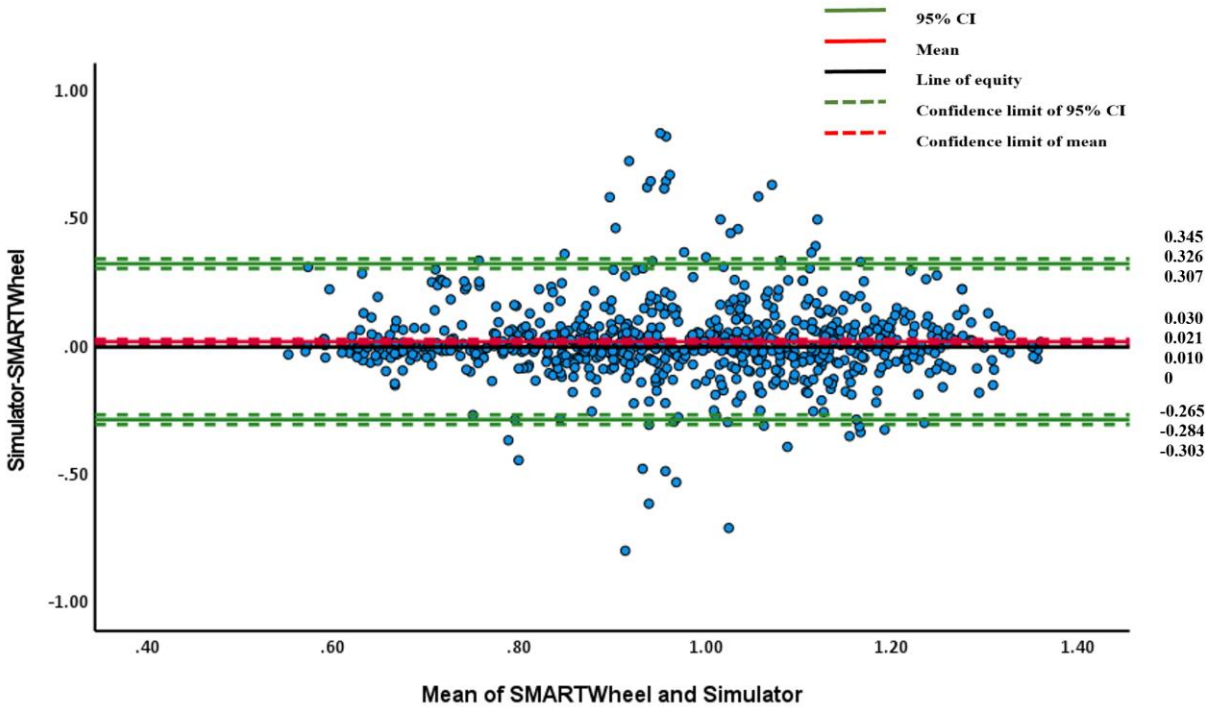


Figure: BA plot to assess accuracy of cycle time (sec) for ecological scenario

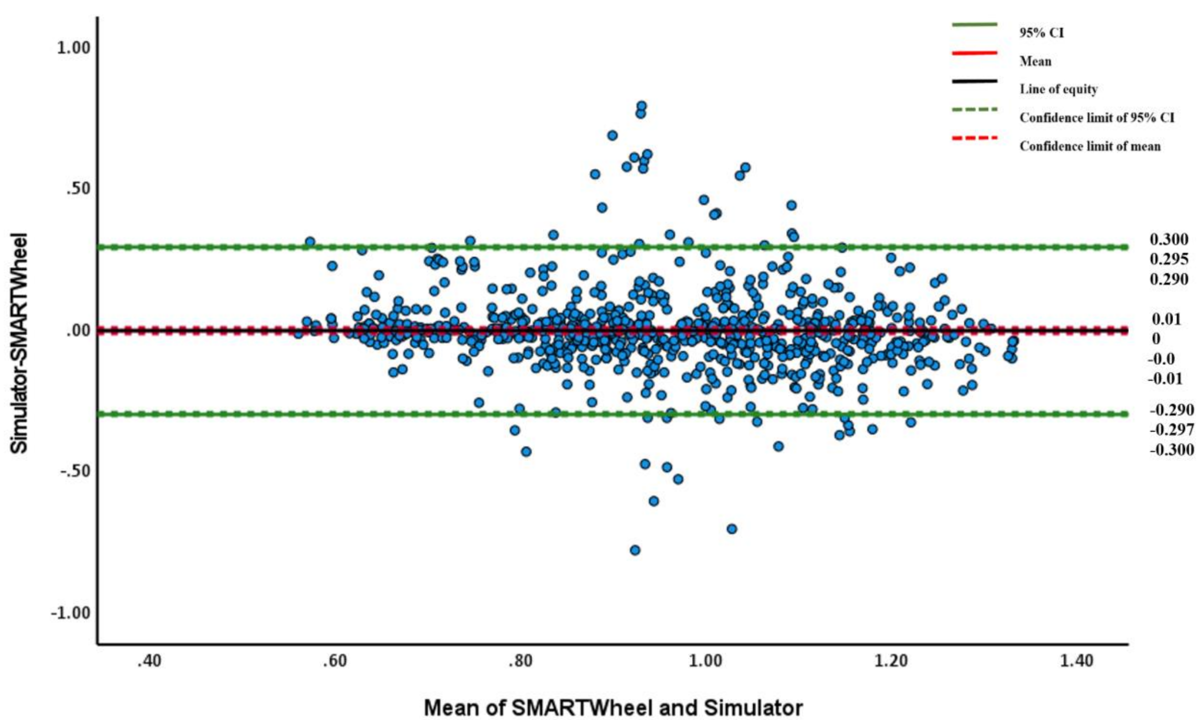


Figure: BA plot to assess accuracy of calibrated cycle time (sec) for ecological scenario

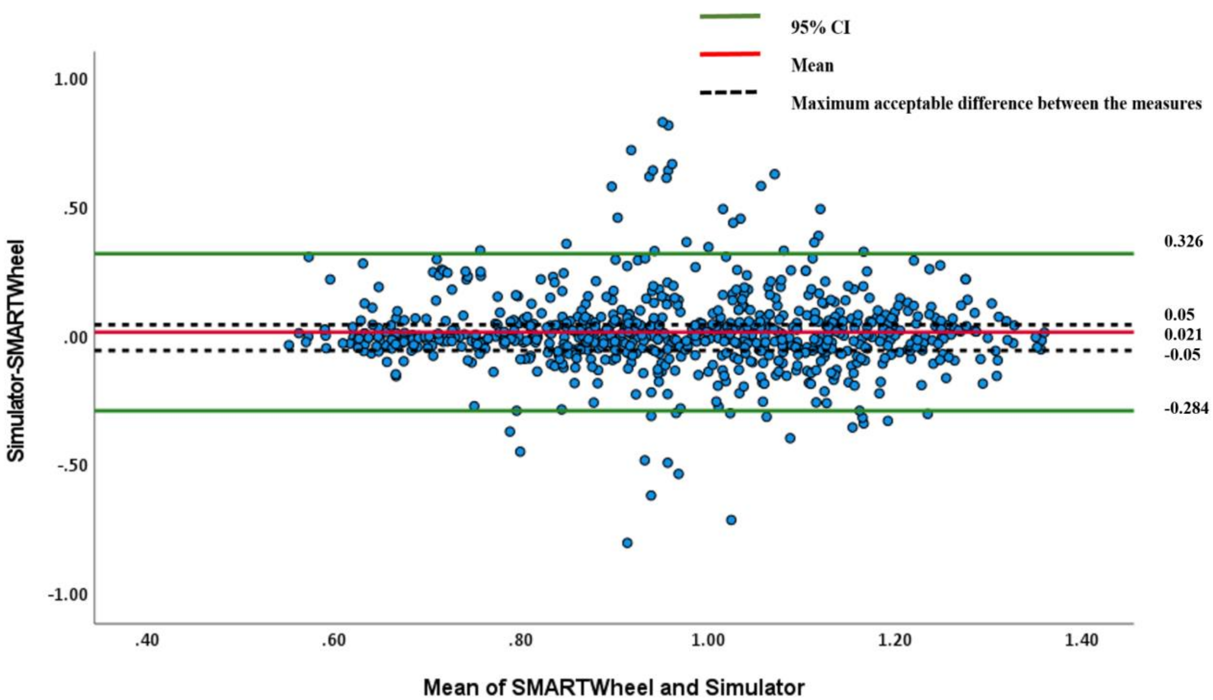


Figure: BA plot to assess precision of cycle time (sec) for ecological scenario

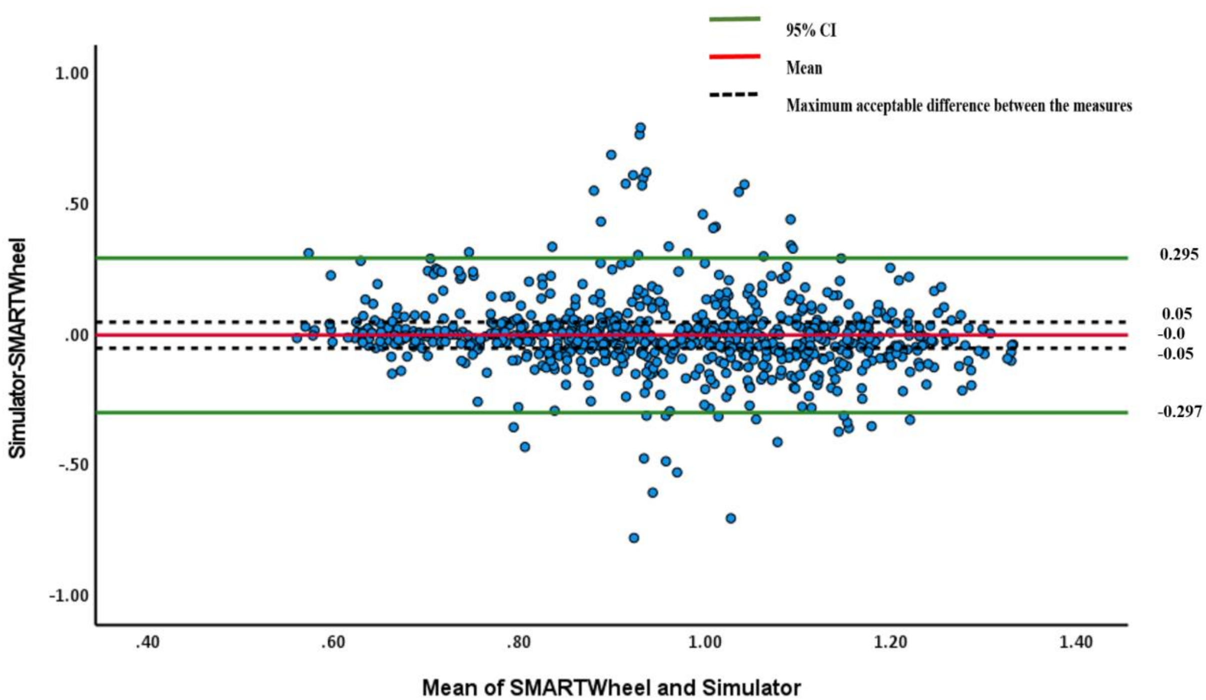


Figure: BA plot to assess precision of calibrated cycle time (sec) for ecological scenario

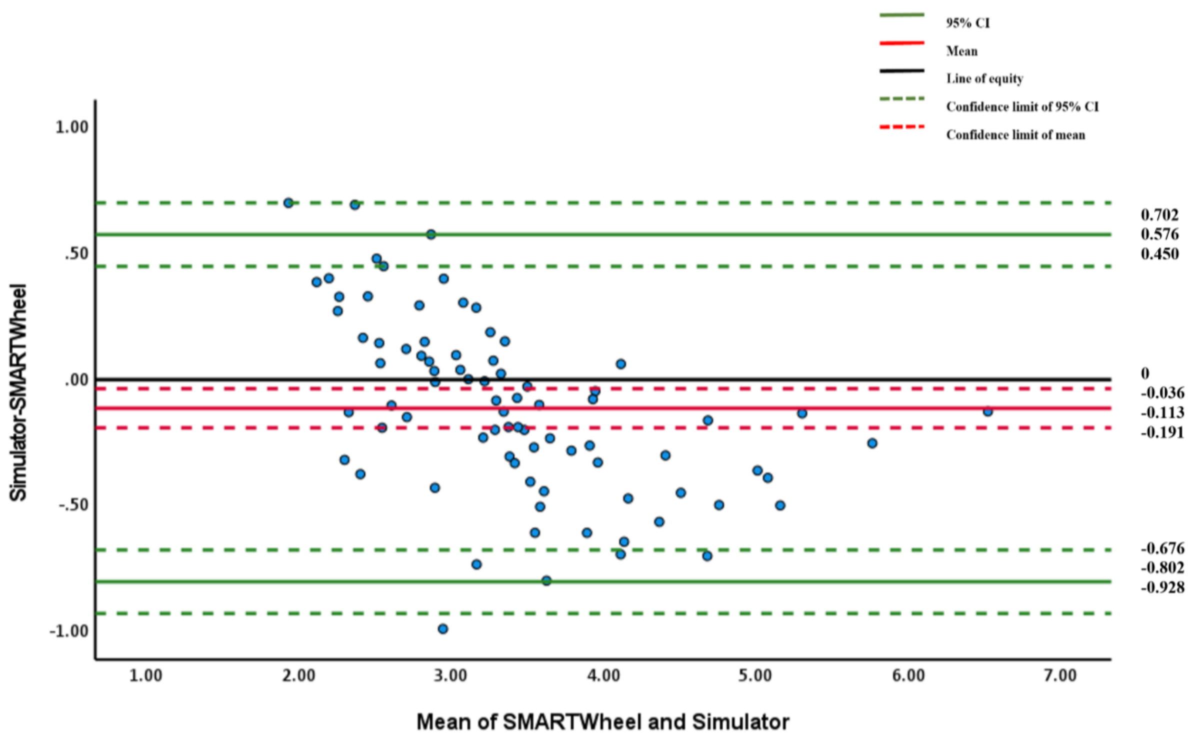


Figure: BA plot to assess accuracy of calibrated velocity (rad/sec) for arching pattern

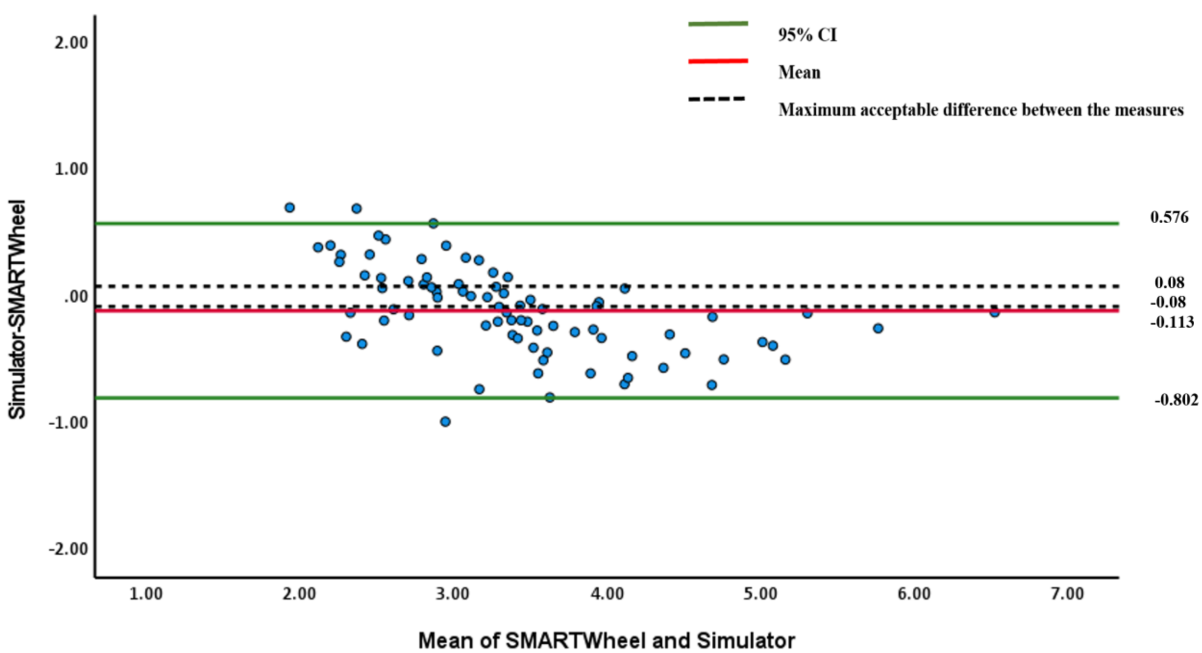


Figure: BA plot to assess precision of calibrated velocity (rad/sec) for arching pattern

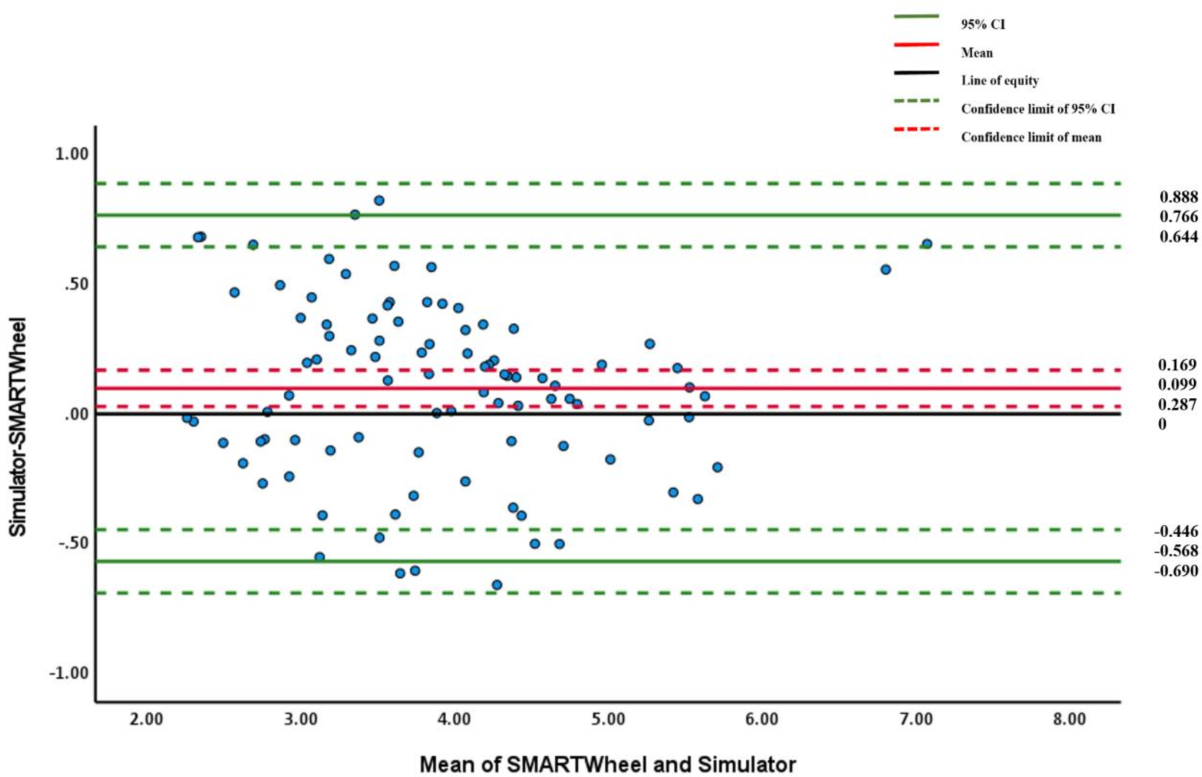


Figure: BA plot to assess accuracy of calibrated velocity (rad/sec) for arching pattern

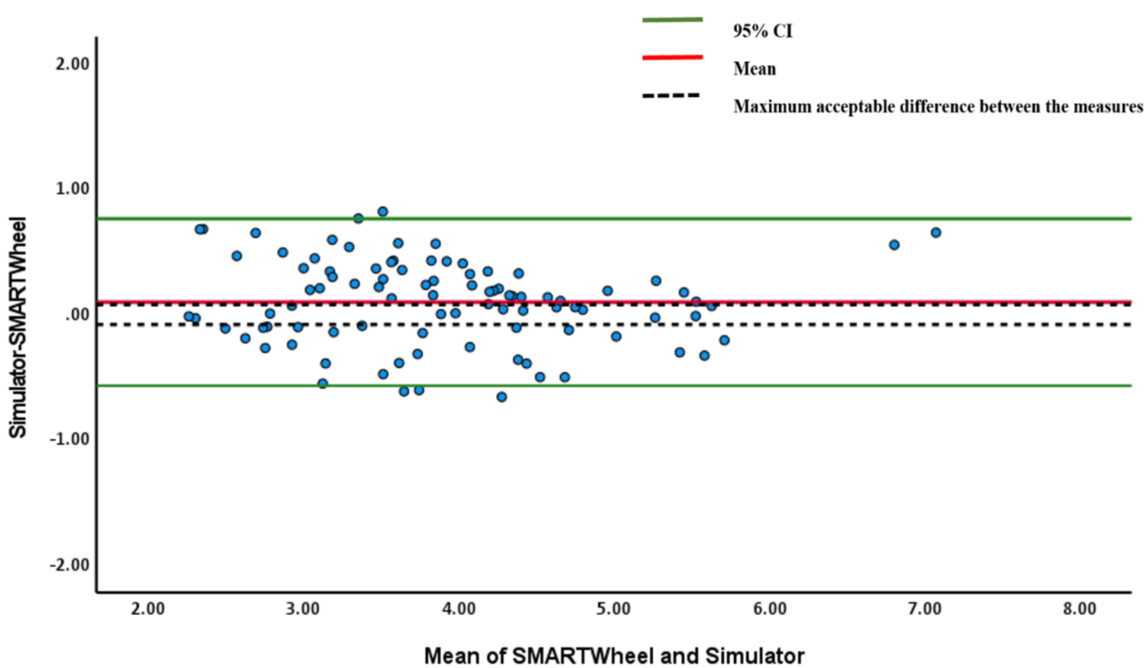


Figure: BA plot to assess precision of calibrated velocity (rad/sec) for arching pattern

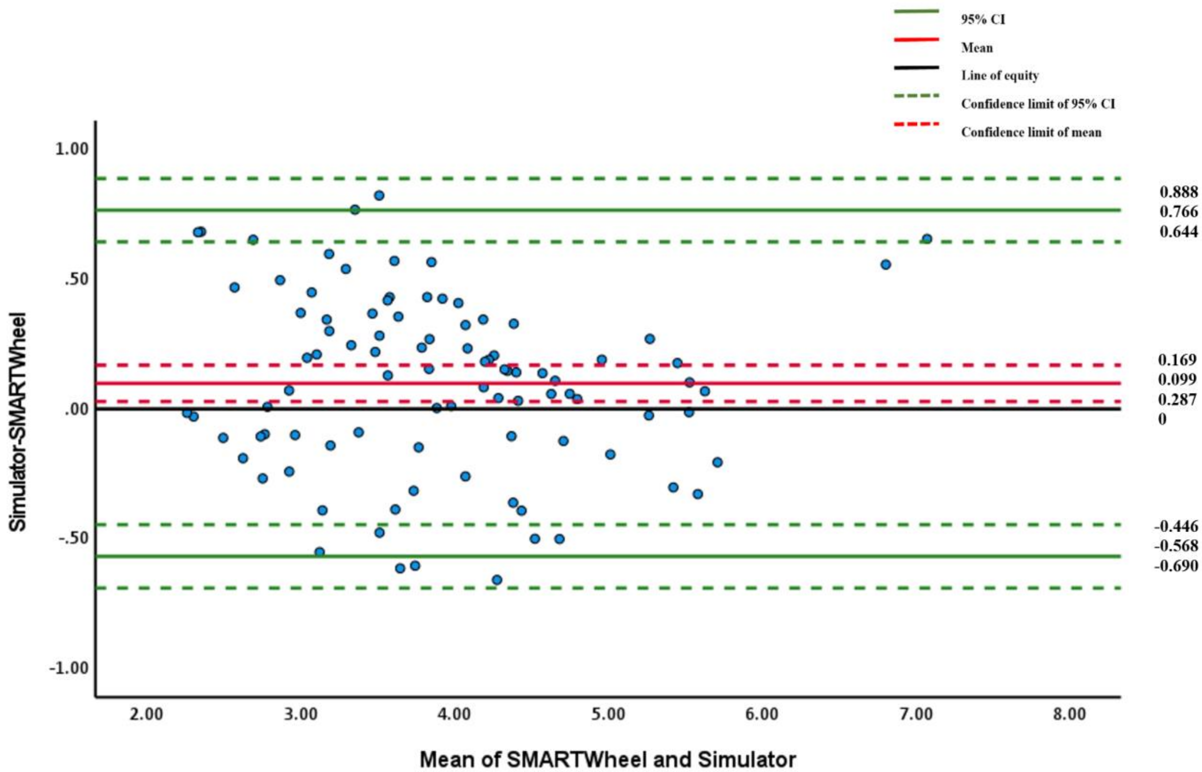

Figure: BA plot to assess accuracy of calibrated velocity (rad/sec) for semicircular pattern

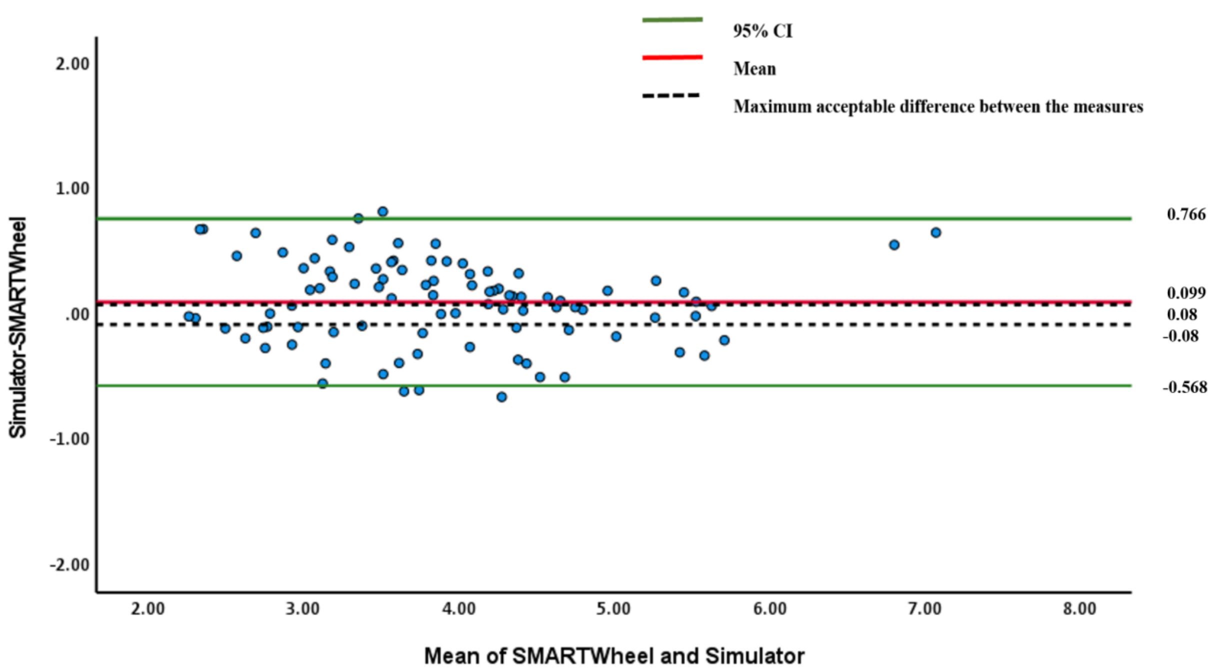

Figure: BA plot to assess precision of calibrated velocity (rad/sec) for semicircular pattern

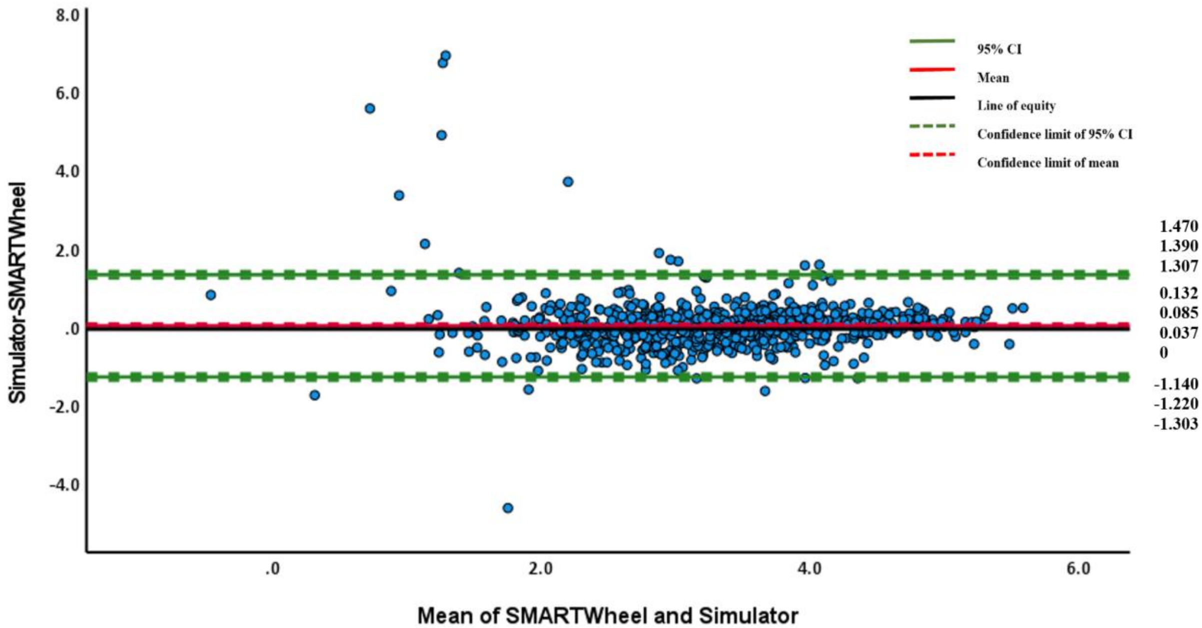


Figure: BA plot to assess accuracy of calibrated velocity (rad/sec) for ecological pattern

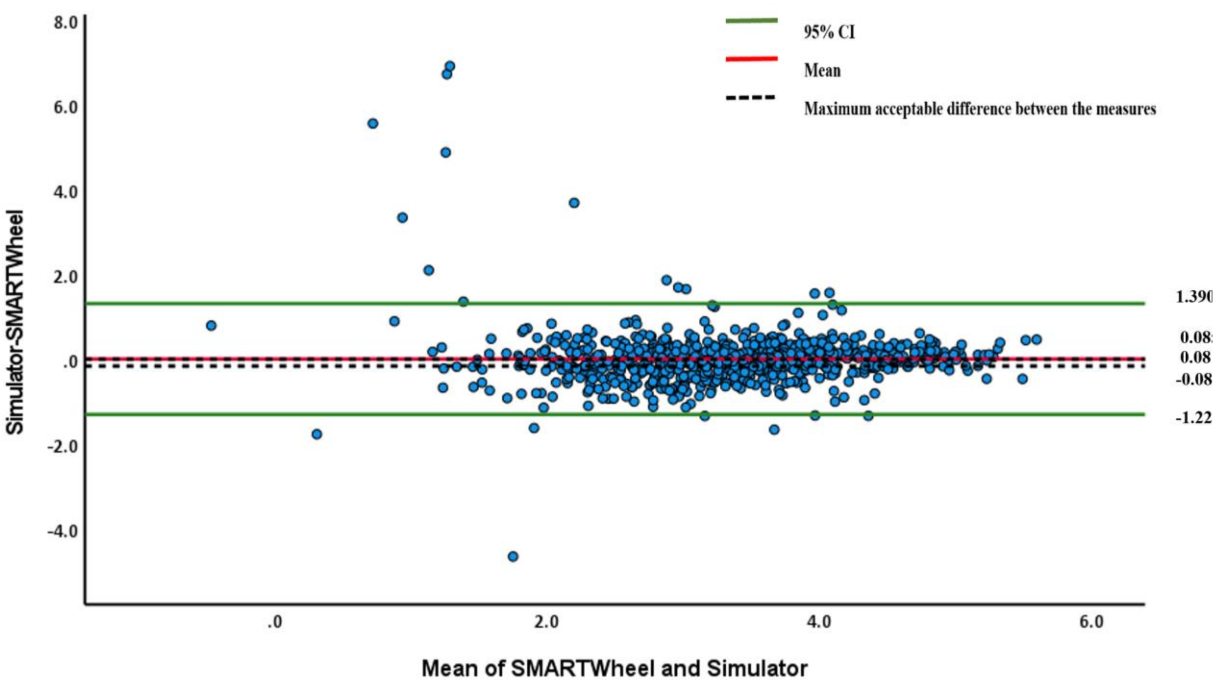


Figure: BA plot to assess precision of calibrated velocity (rad/sec) for ecological pattern

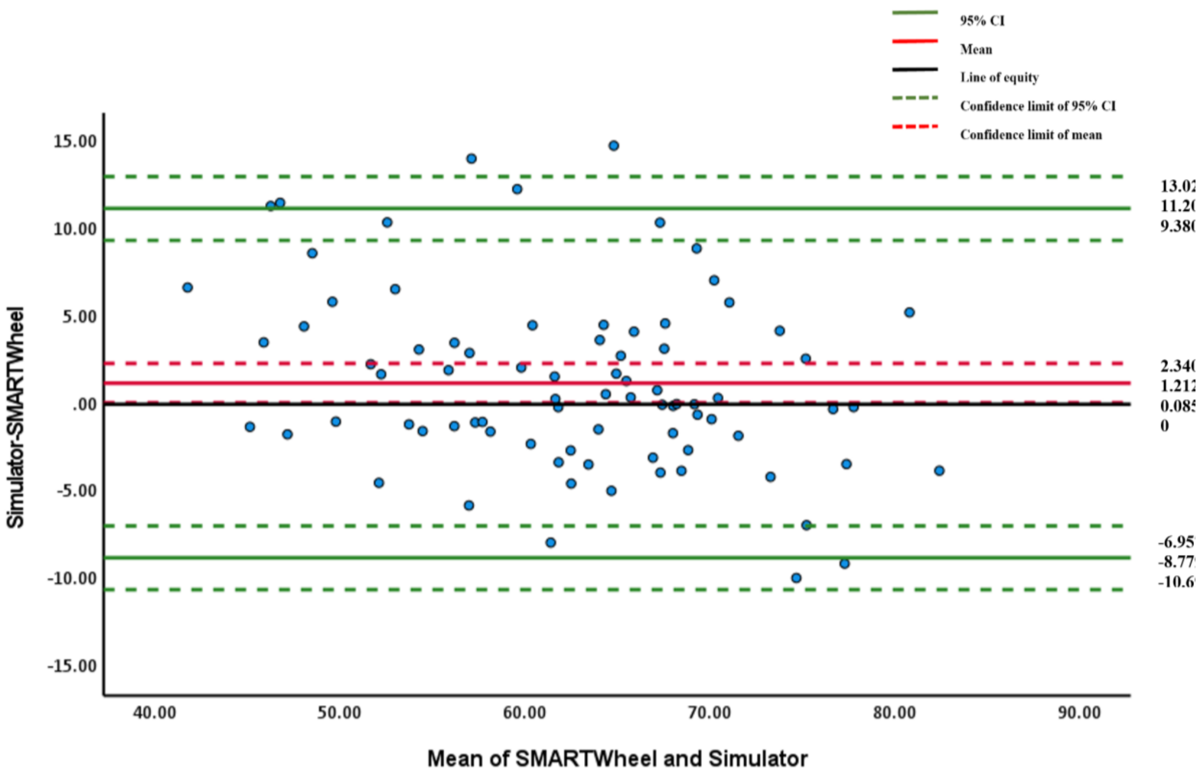


Figure: BA plot to assess accuracy of calibrated contact angle (°) for arching pattern

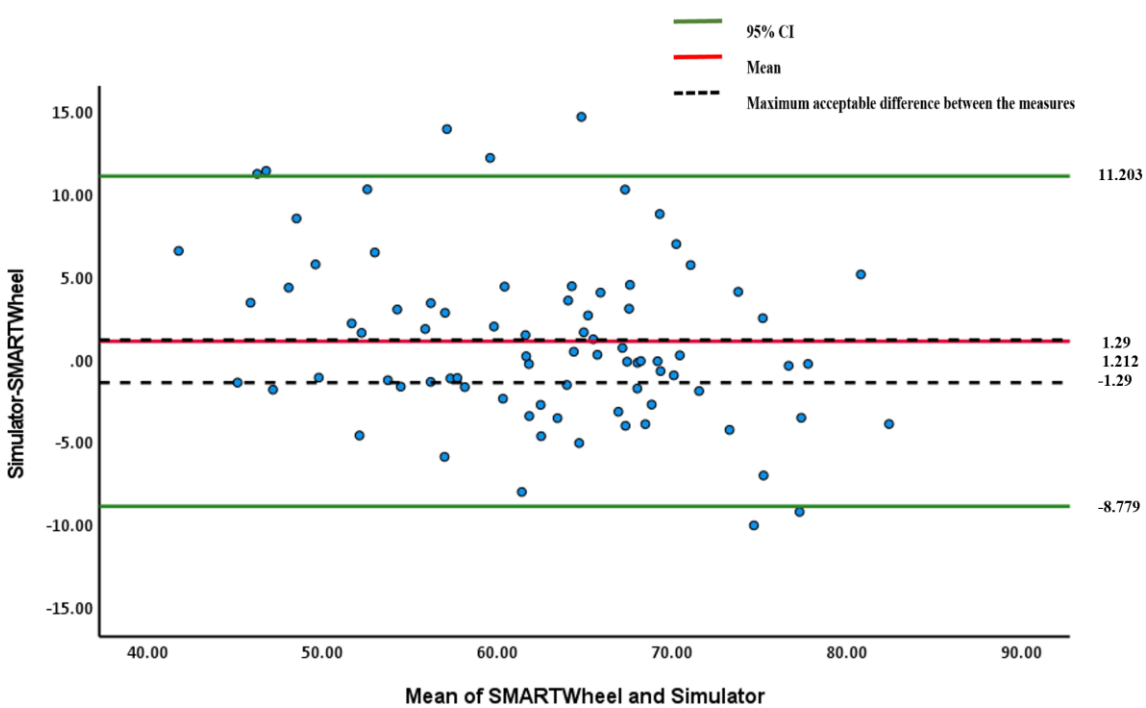


Figure: BA plot to assess precision of calibrated contact angle (°) for arching pattern

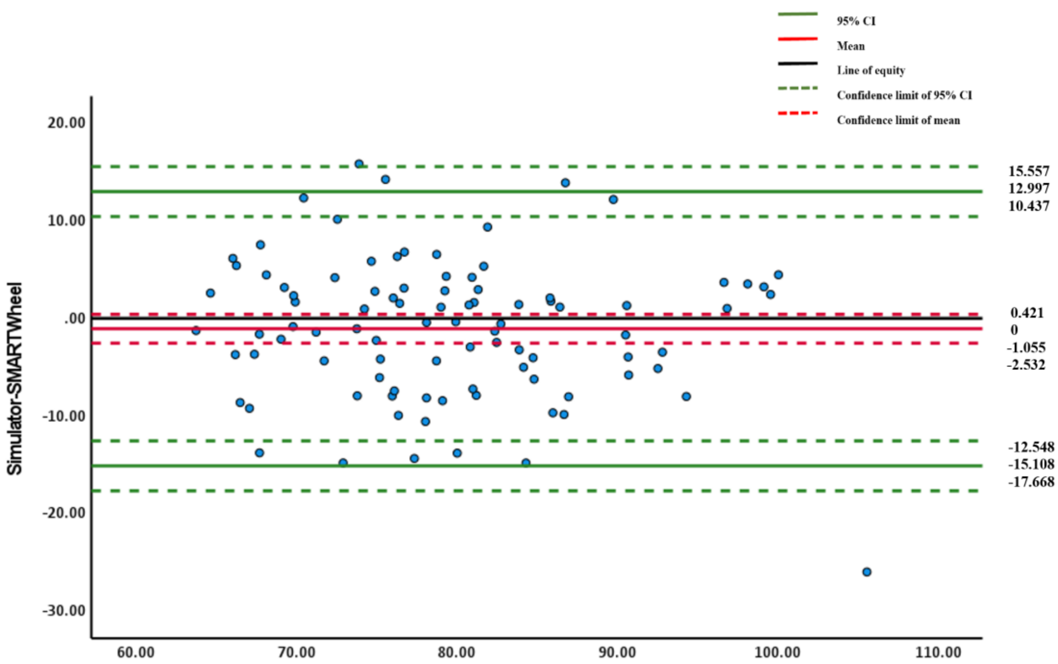


Figure: BA plot to assess accuracy of calibrated contact angle (°) for semi-circular pattern

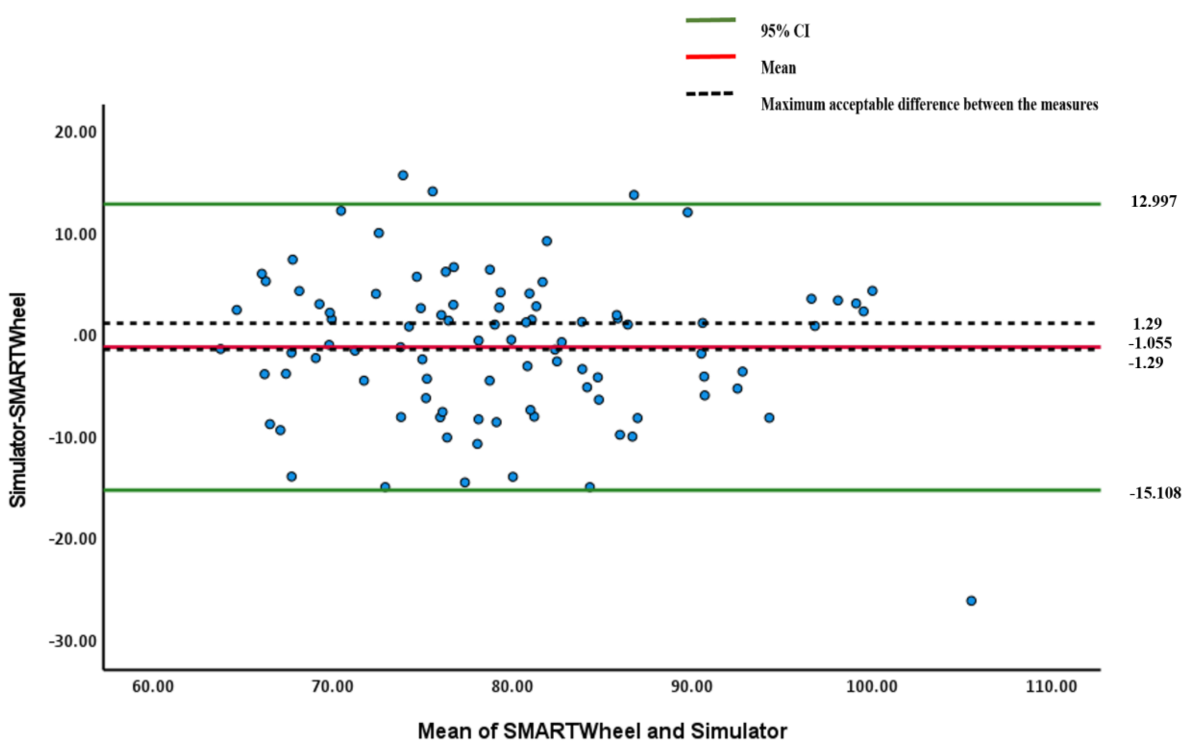


Figure: BA plot to assess precision of calibrated contact angle (°) for semi-circular pattern

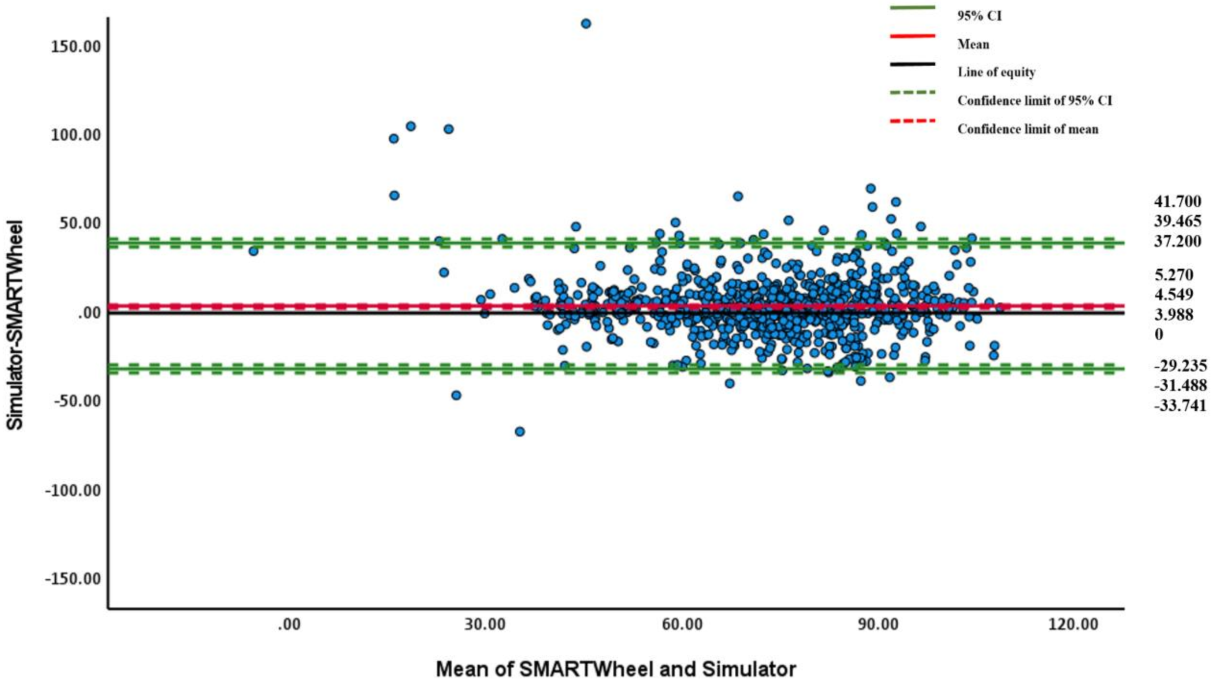


Figure: BA plot to assess accuracy of calibrated contact angle (°) for ecological scenario

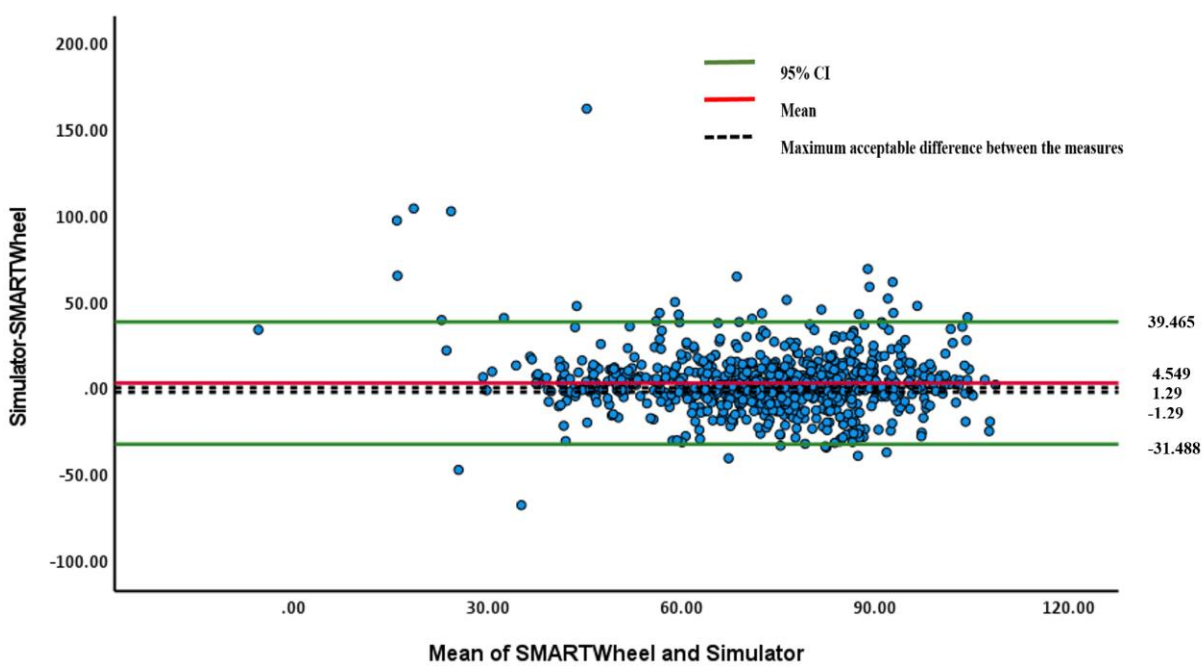


Figure: BA plot to assess precision of calibrated contact angle (°) for ecological scenario